

**Strain/Stress profile
investigation of crystals
mounted in an optical
instrument via FEM
simulation**

Matheus Amarante Machado

2023

[CODEN:LUTMDN/\(TMMV-5354\)/1-113/2023](#)



LUND
UNIVERSITY

LTH

**FACULTY OF
ENGINEERING**

MASTER THESIS

DIVISION OF PRODUCTION AND MATERIALS ENGINEERING

LUND UNIVERSITY

Supervisor: Aylin Ahadi
Co Supervisor: Amin Mirzai
Examiner: Jinming Zhou

Author: Matheus Amarante Machado
Lund, Sweden 2023

Avdelningen för Industriell Produktion
Lunds Tekniska Högskola

Lunds universitet

Box 118

221 00 Lund

Sverige

Division of Production and Materials Engineering

LTH, Faculty of Engineering

Lund University

Box 118

SE-221 00 Lund

Sweden

Printed in Sweden

Media-Tryck

Lund University

Foreword

This degree project has been carried out in the Division of Engineering of Lund University. It was supervised by Professor Aylin Ahadi at the Division of mechanics, co-supervised by Amin Mirzai at the Division of mechanics, and examined by Professor Jinming Zhou at the Division of mechanics. I first and foremost wish to express our gratitudes to Aylin and Amin for assisting me in various ways during this project and for sharing their knowledge and thank you for your patience, as well I thank Jinming for taking on the role as examiner.

I would also like to thank all of the faculty members in the division of Engineering at Lund University for their outstanding efforts in shaping my academics and for everything they have done over the last two years. I would also like to thank my family, my girlfriend and my friends that helped me endure all the challenges in the last 2 years, their help was crucial to the conclusion of this work.

Lund 2023-06-12

Matheus Amarante Machado

Abstract

This work is one of a series of related papers that were made in Lund University. They were done to analyze in a multi scalar way the Yttrium Orthosilicate crystals (YSO), analyzing the variation of material properties stemmed from the mounting, composition and other parameters in the optical properties of Yttrium Orthosilicate crystals.

This paper specifically focused on investigating the effect of the photoelasticity on the characteristics of the crystal, modeling the Strain/Stress effect on optical properties of pure and doped crystals due to variations in the mounting via FEM simulation.

In this work all the process is done with a combination of softwares firstly Abaqus and then Matlab. It starts with the creation and development of a finite element model with adequate material properties and boundary conditions as in the references. To achieve an optical model the simulations were done with various geometries, material orientations, loads and load cases. From these procedures in Abaqus an output for the stress was generated and post processed in Matlab to generate the photoelasticity output. Both the stress and photoelasticity results are presented through this paper.

With this combined procedure this paper was able to present an optimized way to model the variation in optical properties of the crystal in its pure form and doped with Eu. Presenting indications of the effect of the variation in load type, load modulus and crystal orientation being able to present a comparison between them and suggesting future works to increase the knowledge on the topic and optimize the modeling even more.

Keywords: Modeling, Abaqus, Y₂SiO₅, Finite Element Modeling, Strain, Stress, Yttrium Orthosilicate.

Modeling Photoelasticity in YSO by FEM

Popular Science Summary

This work is one of a series of related papers that were made in Lund University. They were done to analyze in a multi scalar way the Yttrium Orthosilicate crystals (YSO) in its pure form and the one doped with Eu. This paper focus on the modeling of the photoelastic effect on the crystal, via finite element method. In this work all the process is done with a combination of software firstly Abaqus and then Matlab.

To know how this behavior can be modeled is important because its applications are in extreme environment, cryogenic state of the art lasers resonators in example. These conditions make it very hard and expensive to do testing for each variation and do measurements.

Therefore, a development of an optical model for the simulations were done. In this primary work few variables of the system were analyzed as load modulus, orientation of the crystal, load direction/cases, geometries of the workpiece.

Firstly, a model as done in Abaqus to generate an output for the stresses and them it was post processed in Matlab to generate the photoelasticity output. Both the stresses and photoelasticity results are presented through this paper. With these combined procedures and data this paper was able to present an optimized way to model the variation in optical properties. In that way presenting indications of the effect of the variation in load type, load modulus and crystal orientation being able to present a comparison between them.

Table of Content

1. Introduction	1
1.1. Problem description	1
1.2. Objective	3
1.3. Limitations	4
1.4. Disposition of Report	4
2. Literature Review	7
2.1. Properties of Yttrium Orthosilicate	7
2.2. Existing models for similar situations	10
2.2.1. Similar material modeling : Micro scale	10
2.2.2. Similar material modeling : Nano scale	10
2.2.3. Similar mounting modeling	10
3. Methodology	11
3.1. Research Strategy	12
3.2. Selection of Software	12
3.2.1. FEM Software	12
3.2.2. Post-Processing Software	12
3.3. Geometry / Drawing in Abaqus	12
3.3.1. First Geometry: Cube	14
3.3.2. Second Geometry: Symmetrical Geometry	15
3.4. Meshing & Element type	16
3.4.1. Element type	16
3.4.2. Mesh size selection	17
3.5. Material Definition	18
3.5.1. Properties used in Abaqus	18
3.5.2. Photoelasticity	21
3.6. Assembly	21

3.7.	Steps	22
3.8.	Boundary Conditions and Load	23
3.8.1.	Full Body - Load Case X	25
3.8.2.	Full Body - Load Case Y	26
3.8.3.	Full Body - Load Case XY	27
3.8.4.	Symmetry Geometry - Load case X	29
3.8.5.	Symmetry Geometry - Load case Y	32
3.8.6.	Symmetry Geometry - Load case XY	34
3.9.	Obtaining Stresses	37
3.10.	Post-Processing	38
4.	Results of simulation & Discussions	41
4.1.	Results for Material Orientations Comparison	41
4.2.	Results for Mesh Size Comparison	47
4.2.1.	Full Body Model	47
4.2.2.	Symmetrical Model	49
4.3.	Results for Plane Choice Comparison	51
4.4.	Load Pattern Comparison	54
4.5.	Variation in Refractive Index Comparison	57
4.5.1.	Different load modulus	71
4.5.2.	Different load type	71
4.5.3.	Different material orientation	71
5.	Conclusions and Suggestion of further works	73
	References	75
	Appendix A – List of Nomenclature Abbreviations and Acronyms	79
	Appendix B - Matlab Code	80

1. Introduction

1.1. Problem description

Yttrium Orthosilicate is an optical crystal that is mostly used in laser applications, it can be used in its pure form or doped with various rare earth dopants such as Ce, Eu, or Lu. One such application is in the field of laser stabilization where the transition levels of the rare earth impurity is used as a reference cavity to tune the stability of the input laser as described in Thrope (2011). As explained by Bitarafan et al. (2017) those frequencies for resonance are deeply influenced by the path the length in the cavity, the light waves have to constructively interfere in each trip to generate a strong and coherent beam of light. This mechanism has the potential to optimize the signal-to-noise ratio enhancing the overall quality and accuracy of the laser's performance as mentioned by Dongmin et al. (2022).

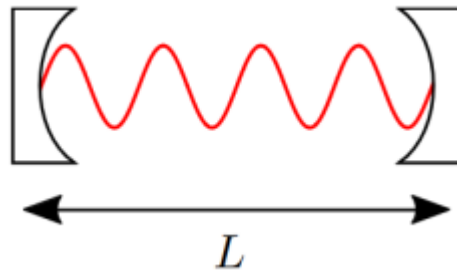


Figure 1: Schematic view of optical cavity, Mirzai (yet to be published).

As explained by Konijnenberg et al. (2021) the behavior of the resonance is given by the mathematical expression :

$$m * \lambda = 2 * n * L \quad \text{Equation 1}$$

where m the mode number (number of round trips in the cavity) is an integer, λ is the wavelength, L is the physical length of the cavity and n is the refractive index.

However, there are many ways to change the path length, either the change of the physical length of the cavity can be modified or the refractive index, this would mean a change in the other side of the equation to keep the equality. Therefore, a change in the wavelength would be seen due to the equation that correlates frequency, wavelength and speed of light

$$C = f * \lambda$$

Equation 2

Resulting in a change in wavelength while the speed of light remains constant, the frequency must also change. Hence a change in the optical path length of the cavity would result in a change of the resonant frequency of the cavity.

The crystals to be analyzed in this work are the pure and the Europium-doped with the properties measured by Mirzai (yet to be published). Since the crystal is a biaxial monoclinic crystal as explained by Li et al. (1992), meaning they have different optic axes.

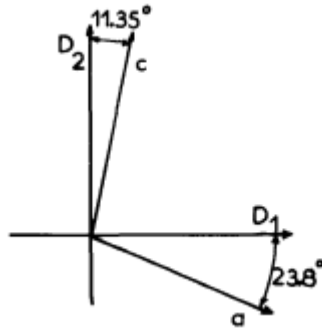


Figure 2: Optical axis in the pure crystal, Li et al. (1992).

These crystals have three different crystallographic axes, each with a different refractive index as explained in Nye (1985). In a biaxial crystal such as the monoclinic one, alpha, the lowest refractive index, designates a direction in the crystal known as the X-axis. Beta, the middle index, indicates a direction known as the Y-axis. Gamma, the highest index, denominates a direction known as the Z-axis.

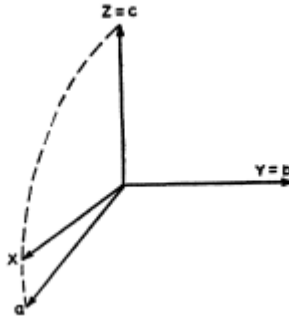


Figure 3: *Crystallographic Axes in Monoclinic Crystal Mason (1946).*

Therefore anisotropy is seen, the effect of this in the refractiveness is significant. The correct choice of position and orientation of the crystal can lead to different conclusions of the path length. The discovery of the optimal crystal orientation and path length to each application is a significant topic, since with them it would be possible to maximize the performance of the system.

Since these crystals are used in state-of-the-art areas and given these characteristics it becomes critical to fully understand them. This work is one of a series of related papers that were originated in Lund University to analyze in a multi scalar way the crystals, analyzing the effect of variation in the mounting, composition and other parameters in the optical properties of Yttrium Orthosilicate crystals.

This paper specifically focuses on investigating the effect of the photoelasticity on the characteristics of the crystal, modeling the Strain/Stress effect on optical properties of pure and doped crystals due to variations in the mounting via FEM simulation. The photoelastic effect offers a way to illustrate the interconnection of the light and stress in terms of intensity and polarization properties of light scattering.

1.2. . Objective

This paper aims to model the photoelastic behavior of the Yttrium Orthosilicate crystal in its pure form and the doped with Eu, investigating the effect of the photoelasticity on the characteristics of the crystal, modeling the Strain/Stress effect on optical properties of pure and doped crystals due to variations in the mounting via FEM simulation. Therefore, getting the effect of the variation in load type, load modulus and crystal orientation and presenting a comparison between them.

1.3. Limitations

There were certain limitations of this work, the ones to be seen first are the platform used, the languages of the articles that were analyzed in the research and the key words used in the search mechanism.

The websites and publishers used for the research were Google Scholar, ScienceDirect, Springer, MPDI, Scopus, Web of Science and the content analyzed was published in English and the main key words used were Abaqus, CAE, FEM, FE, Y2SiO5, Yttrium monosilicate, Yttrium Orthosilicate, Photoelasticity, Properties, Modeling. This could lead to a lack of information that is yet to be published in English or was being indicated by other key words beside the ones used.

Another limitation that may lead to imprecisions on this work is that the data being used comes from experiments done by researches of the university to determine the micro properties used in the model. As Luo et al. (2014) mention “experimental samples contain defects”, these experiments can have a bias or a defect that may be identified later on. Therefore, this data has to be carefully taken as the reality of the material.

There are limitations with the relation of time, software precision and computational power. Abaqus is a software that the more meshes and more nodes there are in the model the more time or an increase in computational power there is. Since there was a limitation of time to do all the simulations and to write this thesis and the computers of the university have a limited license and specific computational power a tradeoff of time and more precision was done.

1.4. Disposition of Report

The disposition of the report is based on the instructions in Bui (2013), the report begins with details about the thesis’s context, the explanation of the need to do this research in that area, the goals of the work, and foreseen limitations of it.

Following that a literature review of how other materials were modeled in similar situations and the material specificities are presented. The methodology is then introduced, which includes the data gathering with experimental data considered in the simulation and how it is obtained, the procedure used to model, the software used, the boundary conditions and loads used in the simulations, and post- processing of the data.

Afterwards, the results of simulations are described in tables, graphs and figures in the following section, which contains relevant details from the simulations with brief comments to the corresponding images. In the discussion portion, the majority of the findings are compared to experimental values and their similarities and differences highlighted. In the conclusion and suggestion of the further work section, the most significant findings and observations are summarized and ideas of further work to fill the gaps that still remain in the mastery of that knowledge are presented.

2. Literature Review

The aim of this section is to introduce the most important characteristics of the material and the modeling. Firstly, the specificities of the yttrium orthosilicate are highlighted and then a short description of the way similar problems were modeled are presented.

2.1. Properties of Yttrium Orthosilicate

There were many previous works that characterized the properties of the orthosilicate of yttrium in its pure and doped form. Literature shows that Yttrium Orthosilicate has good chemical and thermal stability as in Saha et al. (2005), its mechanical and thermal properties were extensively analyzed by Sun et al. (2008) and Sun et al. (2009).

For its doped form Mirzai et al. (2021) mention that “the doping process occurs through a substitution in the host crystal, that is, Eu^{3+} ions replace Y^{3+} ions”. This can be better illustrated by the images below for how the doping happens and how a standard crystal is. This change in the constitution also changes the properties of the materials; these doped properties were analyzed by Mirzai et al. (2021).

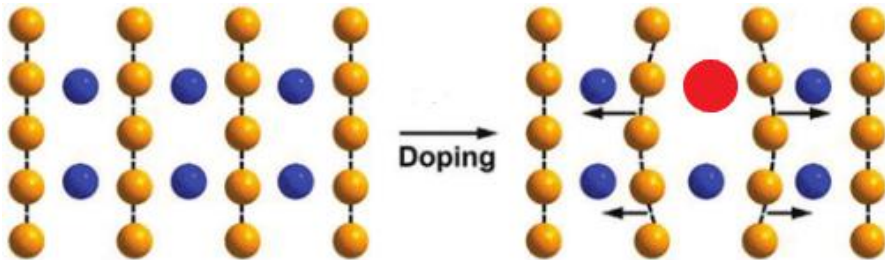


Figure 4: Doping , Fu et al. (2020) [modified].

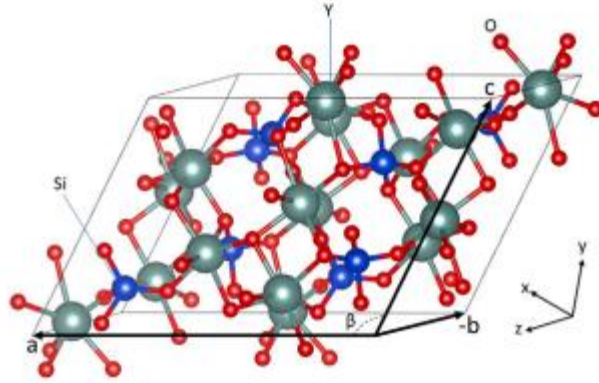


Figure 5: Schematic of a YSO standard unit cell, Mirzai et al. (2021).

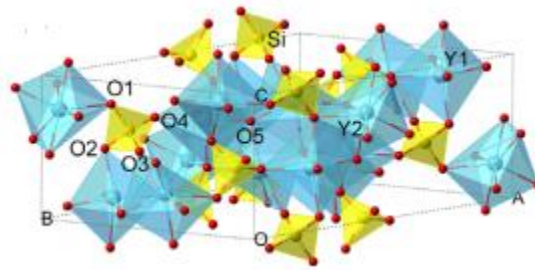


Figure 6: Crystal structures Y_2SiO_5 , Luo et al. (2014).

Both materials, the pure and doped crystals are anisotropic as mentioned in Mirzai et al. (2021) and Li et al. (1992) and Nye (1985). The anisotropic properties of the material refer to the dependence of direction for measurement. The effects of anisotropy are of deep importance as mentioned by Fung (1967), many authors refer to the need to have the knowledge on the materials behavior under the application of load, their response and the presence of one or more directions.

However, its properties vary from dopant concentration, the data base for material properties chosen for this research was the pure and the 1% Eu doping as in Mirzai et al. (2021) and Mirzai (yet to be published) paper with the piezo-optic constants, photoelastic constants and the stiffness matrix. This choice was due to having all data inside of the university and the access to the author himself as one of the supervisors of this work.

$$C = \begin{bmatrix} 212,21 & 62,78 & 78,65 & 0 & 11,64 & 0 \\ - & 197 & 49,50 & 0 & -13,56 & 0 \\ - & - & 173,21 & 0 & -21,07 & 0 \\ - & - & - & 61,42 & 0 & 10,08 \\ - & - & - & - & 48,41 & 0 \\ - & - & - & - & - & 69,25 \end{bmatrix}$$

Figure 7: Elastic Constants for Pure Crystal in GPa, Mirzai et al. (2021).

$$C = \begin{bmatrix} 209,35 & 60,1702 & 77,5923 & 0 & 11,4759 & 0 \\ - & 190,8224 & 47,3987 & 0 & -13,622 & 0 \\ - & - & 173,1555 & 0 & -20,994 & 0 \\ - & - & - & 61,2167 & 0 & 10,0385 \\ - & - & - & - & 47,7039 & 0 \\ - & - & - & - & - & 69,2415 \end{bmatrix}$$

Figure 8: Elastic Constants for Doped Crystal in GPa, Mirzai et al. (2021).

$$\begin{bmatrix} -0,0603 & 0,0880 & 0,1184 & 0 & -0,1223 & 0 \\ 0,0164 & 0,0551 & 0,0557 & 0 & -0,0131 & 0 \\ 0,0337 & 0,0725 & 0,0313 & 0 & 0,0365 & 0 \\ 0 & 0 & 0 & -0,0353 & 0 & -0,0037 \\ -0,0504 & -0,0073 & 0,0459 & 0 & -0,0594 & 0 \\ 0 & 0 & 0 & 0,0117 & 0 & -0,1476 \end{bmatrix}$$

Figure 9: PE constants times $e-11$ for Dielectric Impermeability for Pure Crystal , Mirzai (yet to be published).

$$\begin{bmatrix} -0,0634 & 0,1921 & 0,1390 & 0 & -0,1231 & 0 \\ 0,0195 & 0,1581 & 0,0815 & 0 & -0,0131 & 0 \\ 0,0478 & 0,1611 & 0,0440 & 0 & 0,0489 & 0 \\ 0 & 0 & 0 & 0,0032 & 0 & -0,0268 \\ -0,0442 & -0,0281 & 0,0269 & 0 & -0,0572 & 0 \\ 0 & 0 & 0 & 0,0025 & 0 & -0,1526 \end{bmatrix}$$

Figure 10: PE constants times $e-11$ for Dielectric Impermeability for Doped Crystal , Mirzai (yet to be published).

Table 1: *Refractive Index before stress, Mirzai (yet to be published)*

Material	N0X	N0Y	N0Z
YSO - Pure	1,7577	1,7621	1,7789
Eu:YSO	1,7691	1,7692	1,7892

Table 2: *Density, Mirzai et al. (2021)*

Material	ρ (g/cm³)
YSO - Pure	4,3142
Eu:YSO	4,4228

2.2. Existing models for similar situations

Since it's a new material in a new field of application not much referencing could be found related to the topic. The most prominent one was Prakash et al. (2021) which was a related paper from the group of researchers inside Lund University. Other ones were inspirations to certain choices in the work but too distant to be considered fully useful, they are present in the following sections as similar material modeling and similar mounting modeling.

2.2.1. Similar material modeling : Micro scale

Prakash et al. (2021) modeled Yttrium Orthosilicate in Abaqus as well. In their work they modeled the machining process and vibration of the mounting system. There are a few studies for the Yttrium Orthosilicate in different applications as for coating in Sun et al. (2008) and He et al. (2023)

2.2.2. Similar material modeling : Nano scale

Craiciu et al. (2019) modeled the Yttrium Orthosilicate with Eu doping for the cavity mode in the triangular nanobeam resonator to model the quantum storage.

2.2.3. Similar mounting modeling

The work of Prakash and Girigimmalayanapalya (2021) does a similar mounting system but analyzes it in regards to vibration.

3. Methodology

As Shih (2014) mentioned in a simulation it's better to start with a more basic model and then after its fulfillment proceed to more specific and refined models. Prakash et al. (2021) illustrated the step by step guide of a finite element method on the image below that was used as a base for this work.

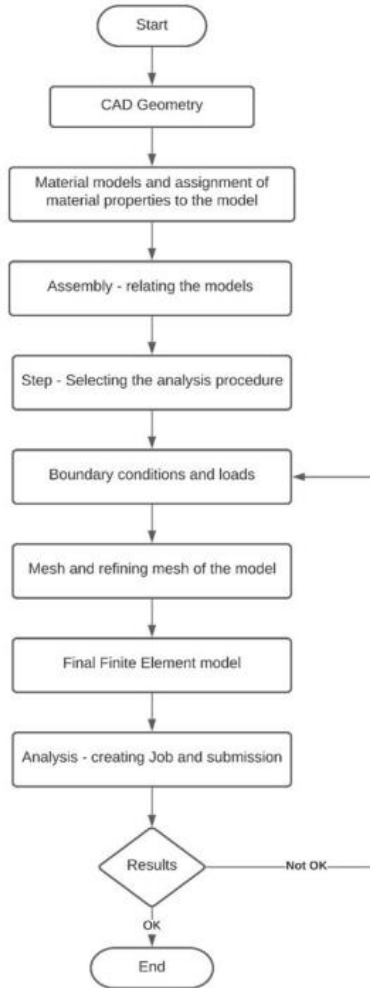


Figure 11: Working procedure used to develop the FE model, Prakash et al. (2021).

3.1. Research Strategy

The selection of key words for the literature review/bibliographical research was done using the concept presented in Creswell and Poth (2016) “ good strategy is to use the words or phrases that are commonly used in the current literature related to the specific topic”

3.2. Selection of Software

3.2.1. FEM Software

The software selected was Abaqus from Dassault Systemes S.A. This choice was made due to a number of factors, firstly its availability in the university with a full license and no need to utilize resources acquiring license for another.

Gardner et al. (2005), Börgesson (1996) also comments the advantages and disadvantages of Abaqus, as pros they highlight its two libraries for implicit and explicit solutions and the very high level of detail on many steps like meshing, defining material properties, etc that can be done on it and as cons the learning curve and the big set-up time for the parameters of the simulation.

The software is one of the most common used FEM softwares in the world being used since the late 1970 as illustrated in Chang and Wang (1983), it has been successfully used in the application of modeling orthosilicate of Yttrium in Prakash and Girigimmalayanapalya (2021).

3.2.2. Post-Processing Software

Since the Abaqus software has not yet a function for giving the photoelasticity a post-processing software had to be used. The software chosen was Matlab since it's a very mature software with a big community of users and many manuals and tutorials as Matlab (2012).

3.3. Geometry / Drawing in Abaqus

Parts are the elements that make up an Abaqus/CAE model. Each component is created, modified, and manipulated using the Part module. For this case there were 2 possible geometries to be studied: a cube or a cylinder, as the below images show



Figure 12: Cylinder of Yttrium Orthosilicate, ScientificMaterials (2023).



Figure 13: Cube of Yttrium Orthosilicate, Mirzai (yet to be published).

The geometry studied was a Cube since the crystal was a cube of dimensions 5x4x1mm in Mirzai (2021) experiments. First there were done two variations of it, one as a full cube and the other as a quarter of a cube with the symmetry on two of its faces.

This is done due to the possibility to reduce computational time with the use of symmetry and as Kumbasar (2022) mentioned, for stress and forces the symmetrical model tends to have a similar result to the full body. An

intermediary analysis of the computational time was done and the symmetrical model presented a significant increase in the processing time and for the final analysis it was to choose geometry.

3.3.1. First Geometry: Cube

The first geometry studied was a cube of dimensions 5x4x1 mm. The modeling space was set to 3D deformable, and the base function was set to solid extrusion when creating the part. The cube has a length of 1 mm, a width of 5 mm and height of 4 mm. These dimensions are the same as the one in the experiment.

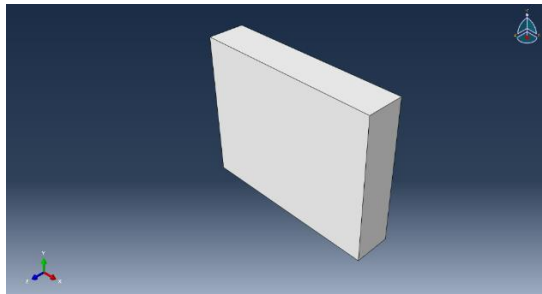


Figure 14: FullBody Isometric view.

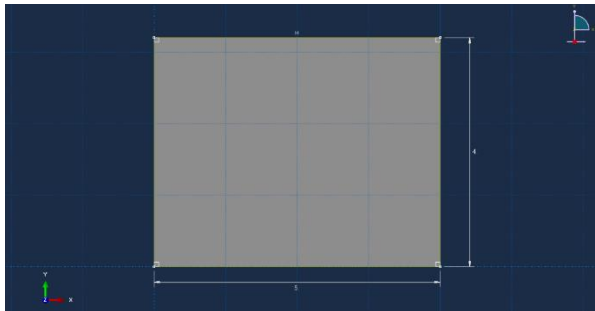


Figure 15: FullBody XY View.

3.3.2. Second Geometry: Symmetrical Geometry

The second geometry studied was the symmetrical cube of dimensions 2.5x 2 x 1 mm. The modeling space was set to 3D deformable, and the base function was set to solid extrusion when creating the part. The cube has a length of 1 mm, a width of 2.5 mm and height of 2 mm. These dimensions are the halves of the one in the experiment.

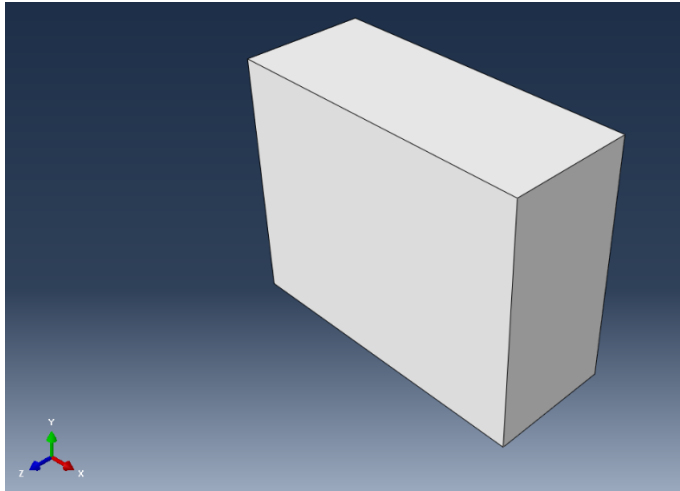


Figure 16: Symmetrical Geometry Isometric view.

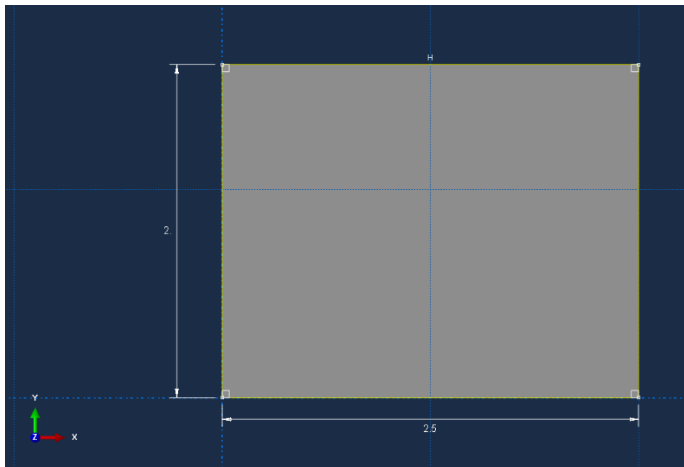


Figure 17: Symmetrical Geometry XY View.

3.4. Meshing & Element type

The next module to be done is the definition of element type and the meshing. The type of the element to be used and its size and division on the model are determined in this section, the selection of those characteristics of the simulation are of deep influence on the result of simulation.

3.4.1. Element type

The follow up of that is to assign the element type, it has variations inside of it, like the element library to be used, the family to be chosen and the geometric order (depending on the choice).

The option for the element library varies in 2 options, standard (implicit) and explicit, the implicit model is incremental as well as iterative but, explicit is only incremental. As Sun et al. (2000) explain, the implicit model tends to use more computational power and has the best performance in the scenario of quasi-static problem while explicit tends to perform better in the fast cases. Prior et al. (1994) mention that the implicit model has disadvantages when the size of it is too large.

Khennane (2013) and Prakash and Girigimmalayanapalya (2021) mentions that “Abaqus/Standard is used to simulate static and low-speed dynamic events while Abaqus/Explicit is used to simulate highly nonlinear and high-speed dynamic events”.

The family is a in deep variety of options, some families have their differences related to geometric shape of them as the image from Hibbitt et al. (2011)

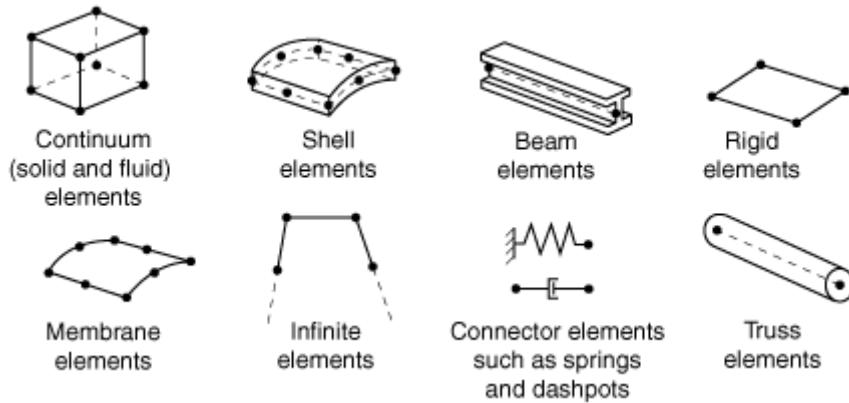


Figure 18: Types of Families, Hibbitt et al. (2011).

There is also variation from the geometric order, that can be from linear and quadratic and are represented as the image below



Figure 19: Types of Geometric Order, Linear, Quadratic and Modified Second Order, Hibbitt et al. (2011)

Feather et al (2021) and Giannakeas et al. (2020) mentioned the importance of the converging speed versus number of nodes, indicating a C3D8 as a suitable element for similar applications. Therefore a 3D element was chosen since the simulation is of a 3D problem, the element library was standard, the family was 3D Stress and the elements were a continuous and linear C3D8 and the other options were set as default since it's the most standard way of doing

3.4.2. Mesh size selection

The meshing is a very important part of the process of modeling where the division of the part into many smaller elements is made. As Dutt (2015) mentioned that the increase in the number of meshes in the model generates

a bigger need of computational power but also if those meshes are put in the right place their increase can lead to more precision.

The main goal here is to reach an optimum mesh size and minimize the error in the modeling, the best is a very much debated topic in literature as mentioned in Bugada et al. (1993). Prakash et al. (2021) mentioned about the lack of significant increase in precision after a certain level of fineness and in their work which is one of the most similar to this they use mesh size 0.05mm.

However, in this work there was also a limitation from the License of Abaqus software which was the Academic Teaching License that has a limit of 100.000 nodes. This result in a limitation in the modeling in finer meshes. Another limitation was time and since more than 216 cases were going to be analyzed and simulated the need to have a feasible simulation time in each simulation to run all was crucial.

With these limitations in mind an investigation for the optimal mesh size that would give precision and which computational power it demanded was made. It is presented in the section 4.2 of this work.

3.5. Material Definition

3.5.1. Properties used in Abaqus

The definition of the material properties is a crucial step in the modeling procedure. The correct use of it can result in a smaller error between reality and the model as Horgan et al. (2018). The properties as mentioned before were taken from the experimental data conducted by Mirzai (2021) and Mirzai (yet to be published).

As Gosh et al. (2006) mentioned that the properties are sensitive to the crystal structure, meaning that an analysis of the material orientation has to be made. The material orientation plays an important role in the simulation as mentioned in Liu et al. (2008). Since the material is anisotropic the standard procedure as commented by Börgesson (1996) of an input of Young's modulus and Poisson number should not be used.

As the Abaqus User Manual (2009) mentions is to enter the 21 independent elastic stiffness parameters to define an anisotropic material. Since the primary data comes from a stiffness matrix C these values need to be converted to the D parameters for the Abaqus input, this is done using the

matrix of conversion of units from Voigt to Mandel notation as Kitamura et al. (2009) and Mandel (1965)

$$\Delta \epsilon_{ij}^{-1} = p_{ijkl} * e_{kl} \quad \text{Equation 3}$$

$$p_{ijkl} = \begin{bmatrix} p_{11} & p_{12} & p_{13} & 0 & 0 & p_{16} \\ p_{21} & p_{22} & p_{23} & 0 & 0 & p_{26} \\ p_{31} & p_{32} & p_{33} & 0 & 0 & p_{36} \\ 0 & 0 & 0 & p_{44} & p_{45} & 0 \\ 0 & 0 & 0 & p_{44} & p_{45} & 0 \\ p_{61} & p_{62} & p_{63} & 0 & 0 & p_{66} \end{bmatrix} \begin{bmatrix} xx = 1 \\ yy = 2 \\ zz = 3 \\ yz = 4 \\ xz = 5 \\ xy = 6 \end{bmatrix}$$

Figure 20: matrix of conversion, Kitamura et al. (2009)

A possible way to vary the orientation one should select the orientation of those properties in the system with the command “assign material orientation in Abaqus. Using it is possible to rotate the main direction of the properties in a rotating axis or by stacking direction, as shown in the image below:

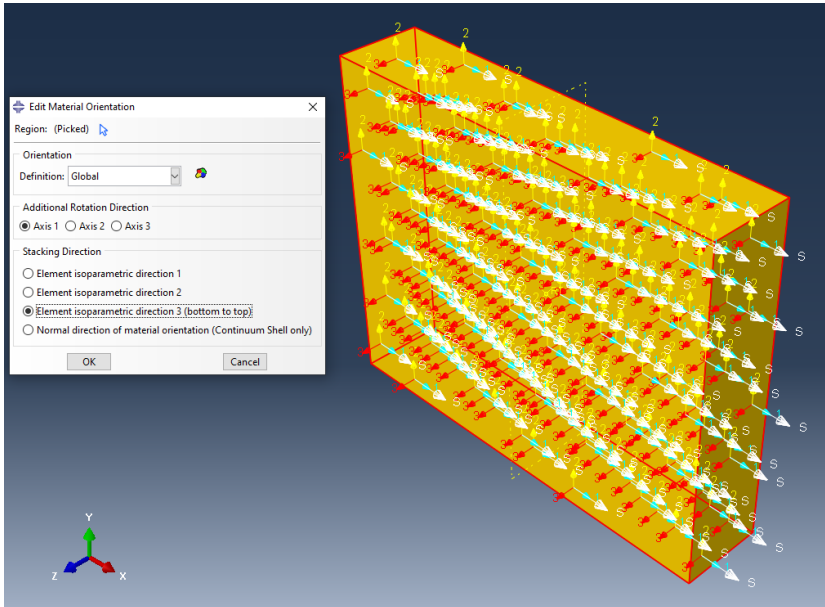


Figure 21: Edit material orientation standardized by Abaqus

The other possibility is to define an anisotropic material in the elastic behavior and do the filling of the anisotropic stiffness matrix in the correct order. This can be seen in the image below:

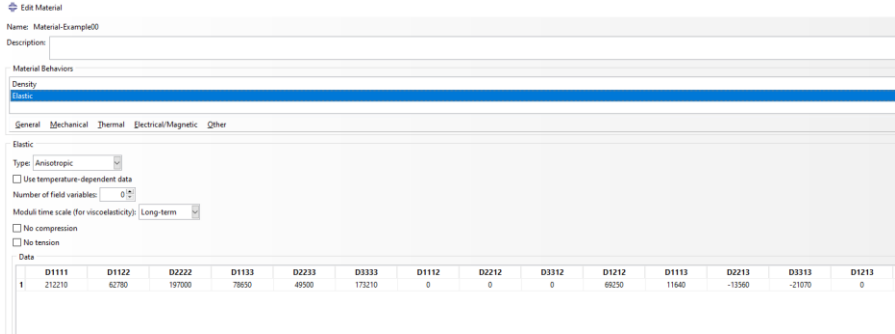


Figure 22: Filling of the stiffness matrix

To reach all the possible variations of orientation the permutation of the values in the stiffness matrix can be done instead of changing the standard material orientation. This would result in five material orientations in this work called A, B, C, D, E.

In this work the second possibility was chosen since it was an easier to do checkups. The result for each material orientation of the conversion of stiffness matrix C to the corresponding values in the D parameters are represented in the following tables:

MatA	MatOriA	Value	Mat B	MatOriB	MatOriE	MatOriE2	Mat C	MatOriC	Mat D	MatOriD
d1111	c11	212.21	d2222	c22	d3333	c33	D2222	C22	D1111	C11
d1122	c12	62.78	d2233	c23	d3322	c32	D2211	C21	D1133	C13
d1133	c13	78.65	d2211	c21	d3311	c31	D2233	C23	D1122	C12
d1113	c15	11.64	d2221	c26	d3331	c35	D2223	C24	D1112	C16
d2222	c22	197	d3333	c33	d2222	c22	D1111	C11	D3333	C33
d2233	c23	49.5	d3311	c31	d2211	c21	D1133	C13	D3322	C32
d2213	c25	-13.56	d3321	c36	d2231	c25	D1123	C14	D3312	C36
d3333	c33	173.21	d1111	c11	d1111	c11	D3333	C33	D2222	C22
d3313	c35	-21.07	d1121	c16	d1131	c15	D3323	C34	D2212	C24
d2323	c44	61.42	d3131	c66	d2121	c66	D1313	C55	D3232	C44
d1223	c46	10.08	d2331	c45	d3221	c46	D2113	C65	D1332	C54
d1313	c55	48.41	d2121	c66	d3131	c55	D2323	C44	D1212	C66
d1212	c66	69.25	d2323	c44	d3232	c44	D2121	C66	D1313	C55

Figure 23: Permutation of the values in the stiffness matrix to make all the five material orientations in the Pure YSiO, Values in GPa , 10^3 to MPa

MatA	MatOriA	Value	Mat B	MatOriB	MatOriE	MatOriE2	Mat C	MatOriC	Mat D	MatOriD
d1111	c11	209.3528	d2222	c22	d3333	c33	D2222	C22	D1111	C11
d1122	c12	60.1702	d2233	c23	d3322	c32	D2211	C21	D1133	C13
d1133	c13	77.5923	d2211	c21	d3311	c31	D2233	C23	D1122	C12
d1113	c15	11.4759	d2221	c26	d3331	c35	D2223	C24	D1112	C16
d2222	c22	190.8224	d3333	c33	d2222	c22	D1111	C11	D3333	C33
d2233	c23	47.3987	d3311	c31	d2211	c21	D1133	C13	D3322	C32
d2213	c25	-13.622	d3321	c36	d2231	c25	D1123	C14	D3312	C36
d3333	c33	173.1555	d1111	c11	d1111	c11	D3333	C33	D2222	C22
d3313	c35	-20.994	d1121	c16	d1131	c15	D3323	C34	D2212	C24
d2323	c44	61.2167	d3131	c66	d2121	c66	D1313	C55	D3232	C44
d1223	c46	10.0385	d2331	c45	d3221	c46	D2113	C65	D1332	C54
d1313	c55	47.7039	d2121	c66	d3131	c55	D2323	C44	D1212	C66
d1212	c66	69.2415	d2323	c44	d3232	c44	D2121	C66	D1313	C55

Figure 24: Permutation of the values in the stiffness matrix to make all the five material orientations in the Doped YSiO, Values in GPa , 10^3 to MPa

With the definition of the material orientation done, it's necessary to compare a result of simulations of each to get the 3 that would represent the 3 crystallographic axis. In that case the ones were material orientation A, C, E.

3.5.2. Photoelasticity

Since Abaqus has not yet a photoelasticity analysis an adaptation had to be made. From the stresses generated in each simulation the stresses of each element were gathered and then post-processed in Matlab. In this post processing they were multiplied by the photoelastic constant measured by Mirzai (yet to be published).

3.6. Assembly

The workpiece is then added as itself in the assembly process in order to allow the following parts, an instance is created and the part is added to its center.

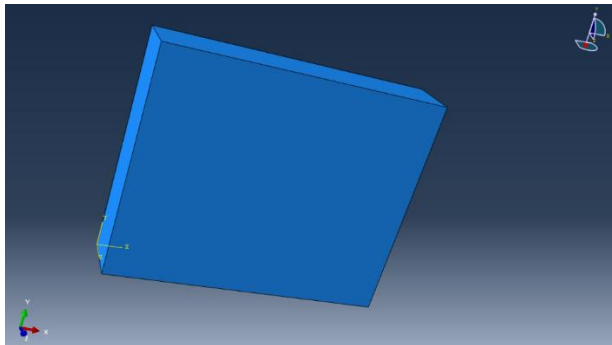


Figure 25: Assembly image

3.7. Steps

In the steps part its where the implicit or explicit time integration is selected and if a thermo-mechanic or just mechanical analysis should be done. As Prakash et al. (2021) mentioned “The splitting of the problem history into steps is a fundamental principle in Abaqus. Any suitable phase of the past can be a thermal transient, a creeping hold, a dynamic transient, and so on is referred to as a step. A step can be as simple as static analysis of a load shift from one magnitude to another in Abaqus/Standard.”

Regarding the choice of the nonlinear geometry (NLgeom) is explained in Hample et al. (2019), Steffen (2013) and Zamani (2017), where this analysis is mostly referred to the “large-displacement” approach. Therefore since the displacement and the deformation are going to be small the use of nonlinear geometry is not necessary as commented in and in Hample et al. (2019), Steffen (2013) and Zamani (2017).

Since the main goal of this work is to analyze the mounting process the procedure is set to Static, General and the NLgeom is set to OFF as shown in the images below:

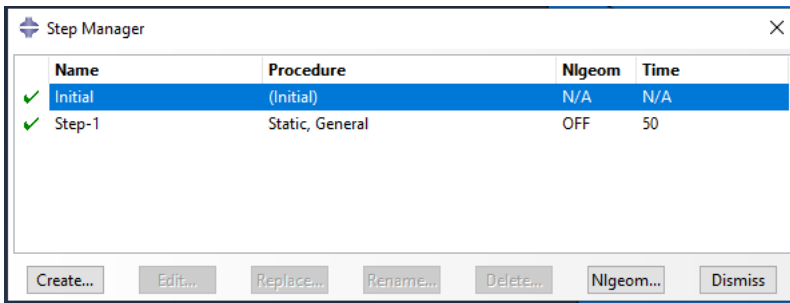


Figure 26: Setting Step Variables 1

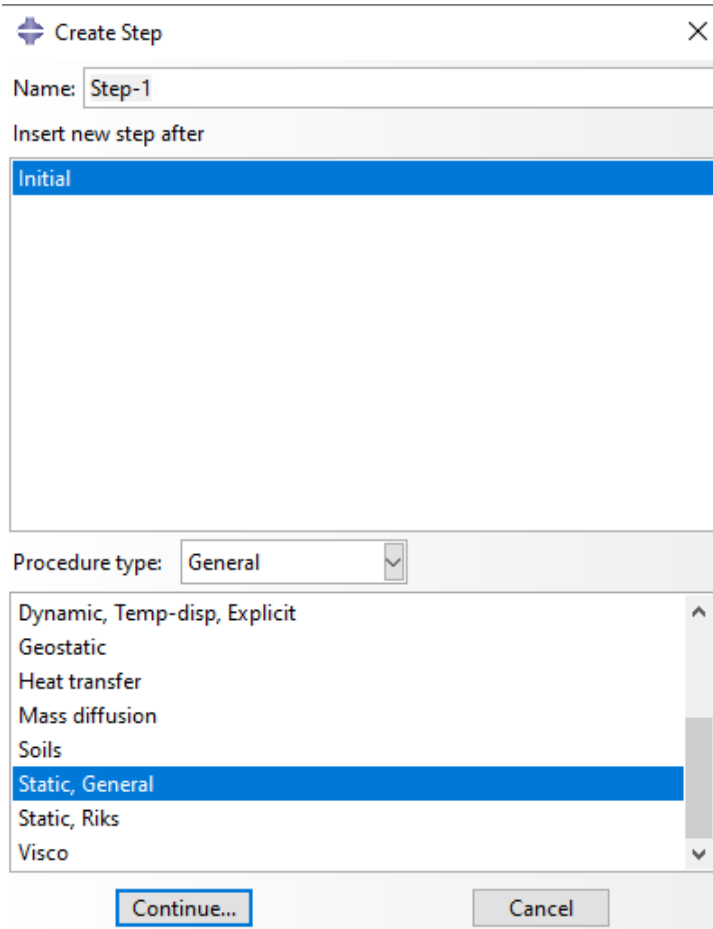


Figure 27: Setting Step Variables 2

3.8. Boundary Conditions and Load

The main idea in this part is to do the choice of the boundary conditions and the loads to be applied in a way that the model corresponds to the reality in the most precise way. As Okereke et al. (2018) “the solution of any FEM problem is highly dependent on the boundary conditions implemented”. The loads and boundary conditions applied are going to modify the tensions suffered by each node and their stress state generating different stresses that

can result in deformation or failure depending on their choice as image below shows:

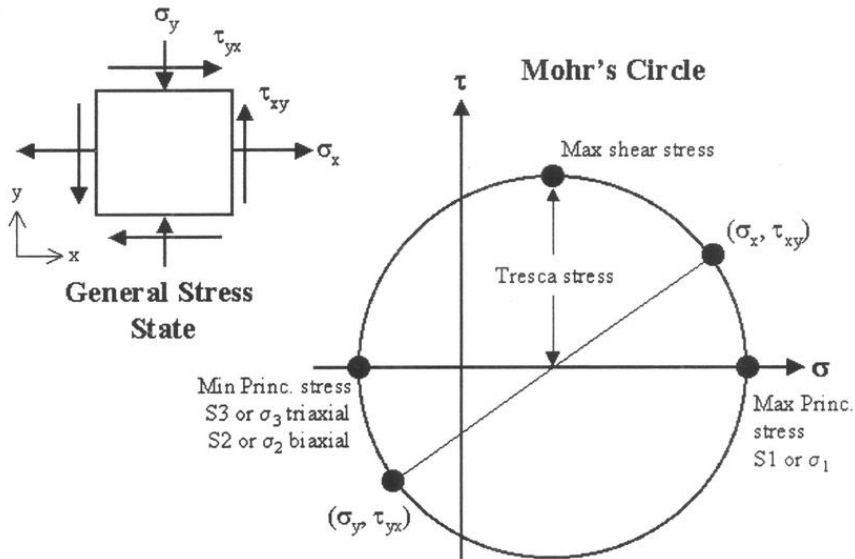


Figure 28: Image for stress state in each element, Tănăsoiu et al. (2010)

As Prakash et al. (2021) mentioned “Boundary conditions are applied to restrict the model’s movement from the forces or loads applied externally or due to self-driven load in the model”. The goal when setting the boundaries conditions was not to create an anomaly in one of the elements with way higher stresses than the other in a unrealistic way and also to limited the movements of the system to what is seen in a crystal used in this kind of applications as in Prakash et al. (2021), Bernhardi (2008). The boundary conditions selected specifically to each load case inspired by Bernhardi (2008) and Prakash et al. (2021).

In this work many simulations of the mounting system were studied, resulting at the end in 3 variations to see which would better represent the mounting system in real life. The variations were pressure load on X direction, pressure load on Y direction and pressure load on X and Y direction simultaneously. The modules varied from 100 KPa to 1500KPa since they started around the ones measured in Pavel et al. (1996) and also finished around the order of pressure in laser stabilization experiments as in the system in Mirzai (yet to be published). They are as the table below:

Table 3: *Table of analyzed load for each Load Case*

Load X	Load Y	Load XY
100	100	100
150	150	150
200	200	200
250	250	250
300	300	300
350	350	350
400	400	400
450	450	450
500	500	500
750	750	750
1000	1000	1000
1500	1500	1500

3.8.1. Full Body - Load Case X

In this model the surfaces in the X direction were loaded receiving the pressure load and were locked to moving in all directions except by the X one.

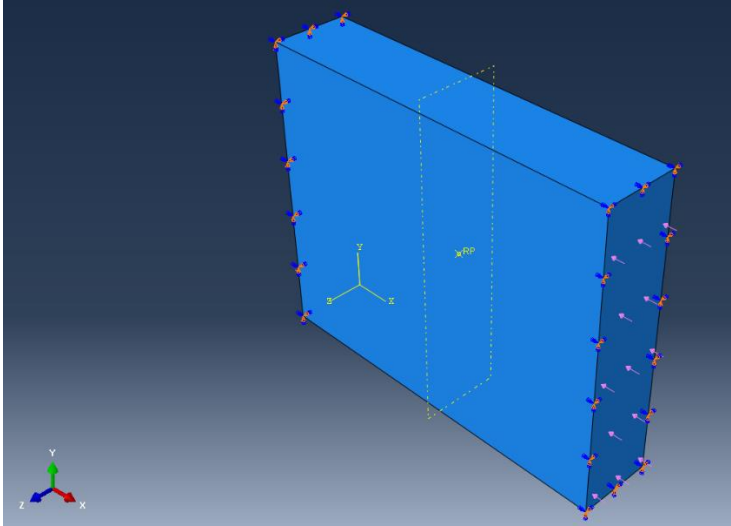


Figure 29: Load Case X

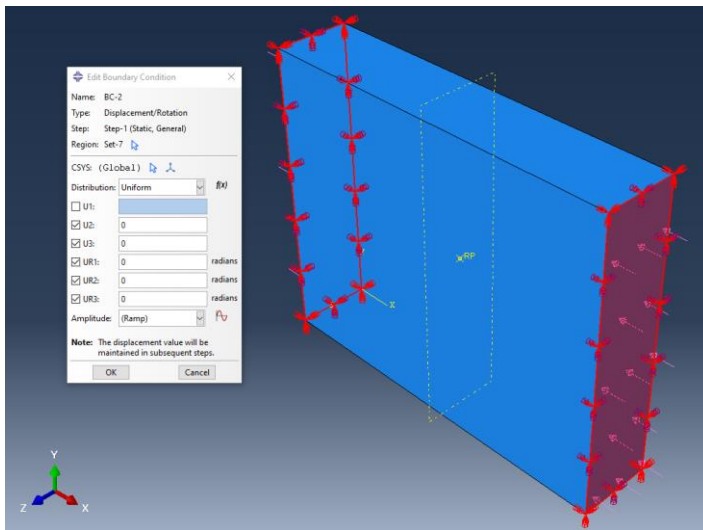


Figure 30: Boundary Conditions in Full Body Geometry Load Case X

3.8.2. Full Body - Load Case Y

In this model the surfaces in the Y direction were loaded receiving the pressure load and were locked to moving in all directions except by the Y one.

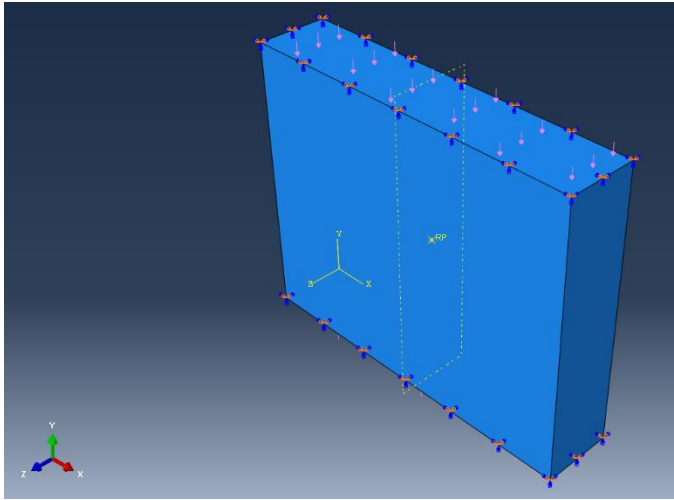


Figure 31: Load Case Y

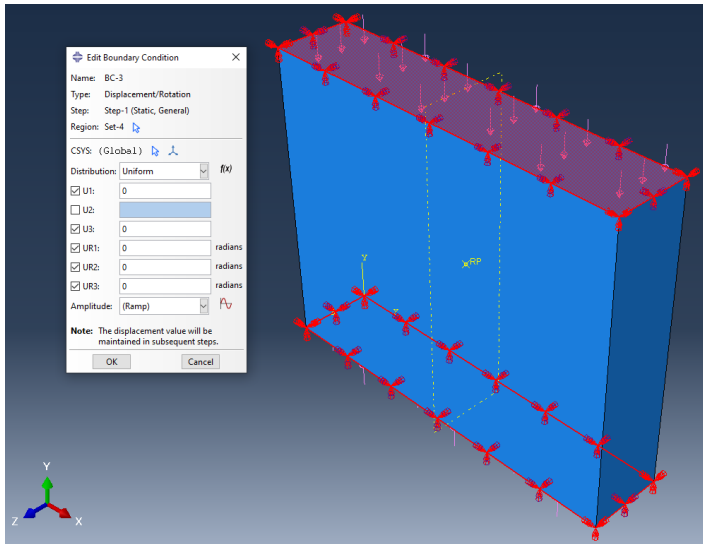


Figure 32: Boundary Conditions in Full Body Geometry Load Case Y

3.8.3. Full Body - Load Case XY

In this model the loaded surfaces X and Y received the pressure load and were locked to moving in all directions except by the X and the Y one.

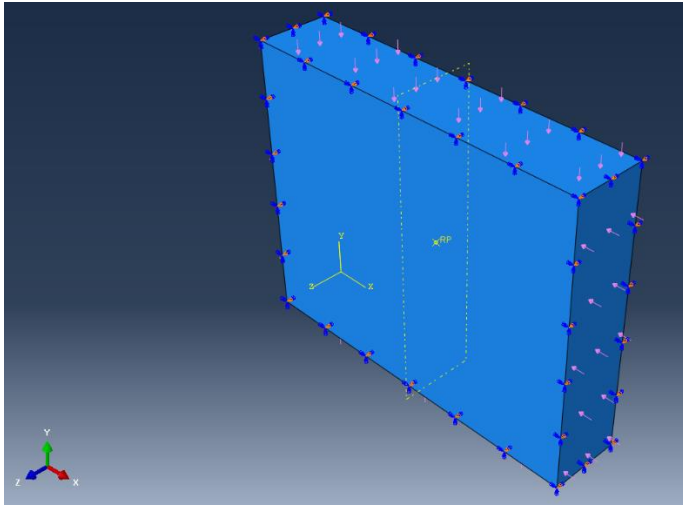


Figure 33: Load Case XY

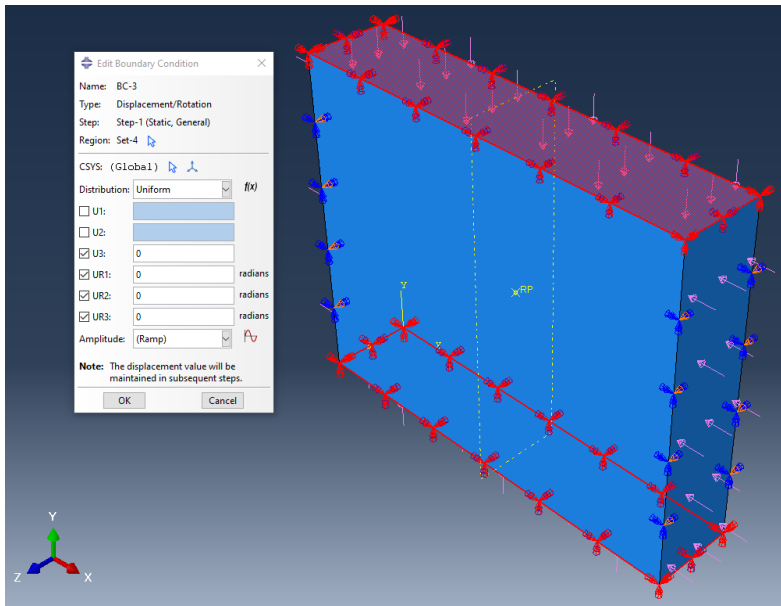


Figure 34: Boundary Conditions in Full Body Geometry Load Case XY

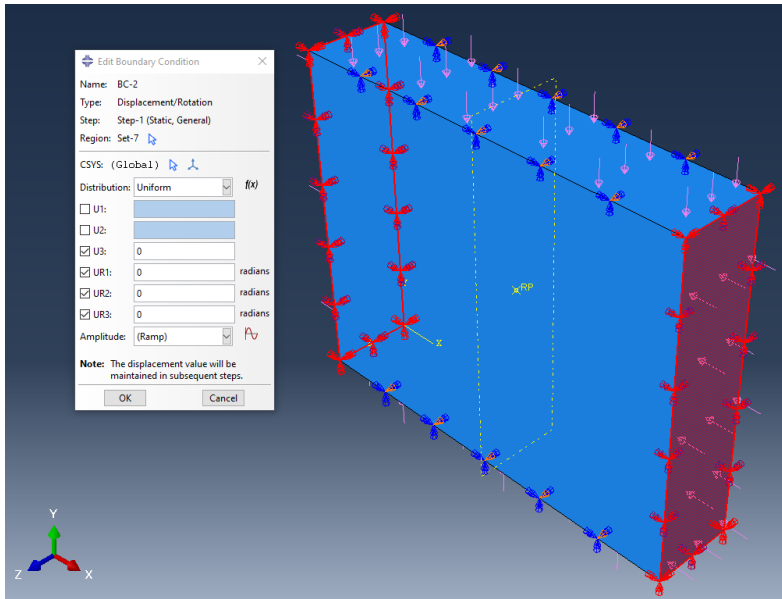


Figure 35: Boundary Conditions in Full Body Geometry Load Case XY

3.8.4. Symmetry Geometry - Load case X

In this model the two surfaces were defined and a symmetry XSYMM and YSYMM and the loaded surface perpendicular to X axis received the pressure load and was locked to moving in all directions except by the X one.

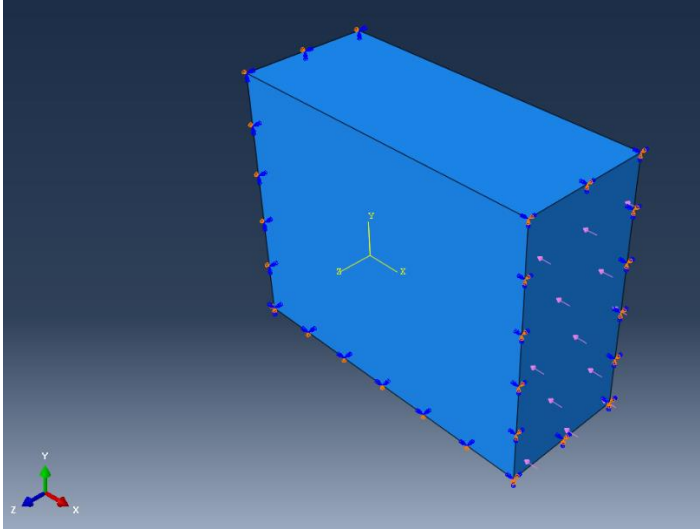


Figure 36: Symmetry Geometry Load Case X

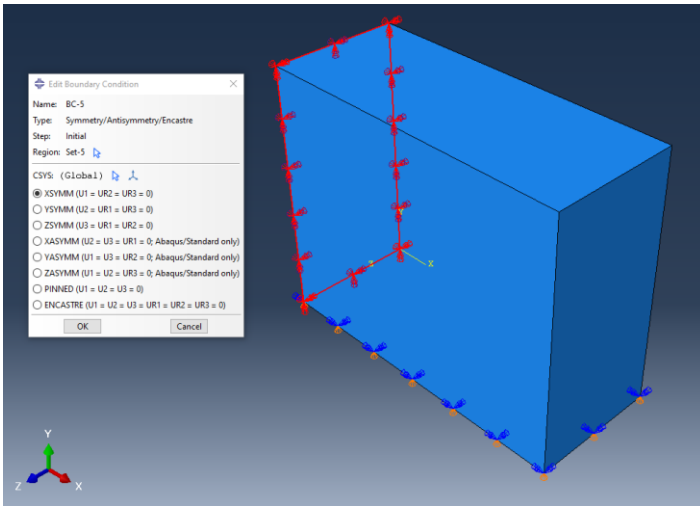


Figure 37: Symmetry Boundary Conditions in YZ Plane in Symmetry Geometry Load Case X

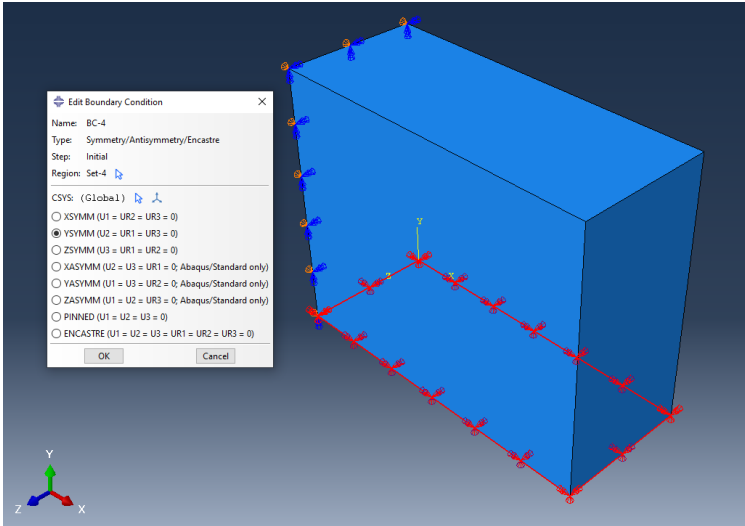


Figure 38: Symmetry Boundary Conditions in XZ Plane in Symmetry Geometry Load Case X

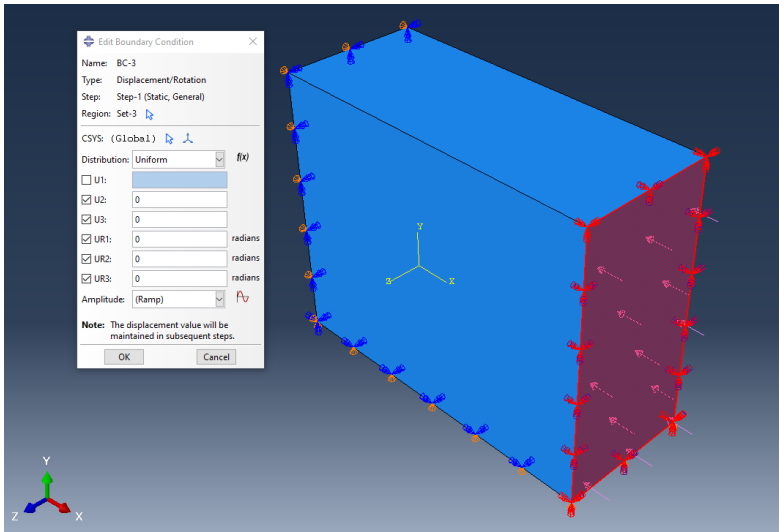


Figure 39: Boundary Conditions in Symmetry Geometry Load Case X

3.8.5. Symmetry Geometry - Load case Y

In this model two surfaces were defined and a symmetry XSYMM and YSYMM and the loaded surface perpendicular to Y axis received the pressure load and was locked to moving in all directions except by the Y one.

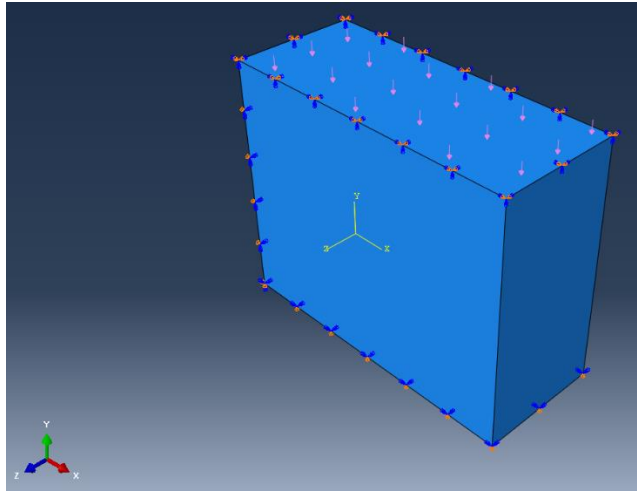


Figure 40: Symmetry Geometry Load Case Y

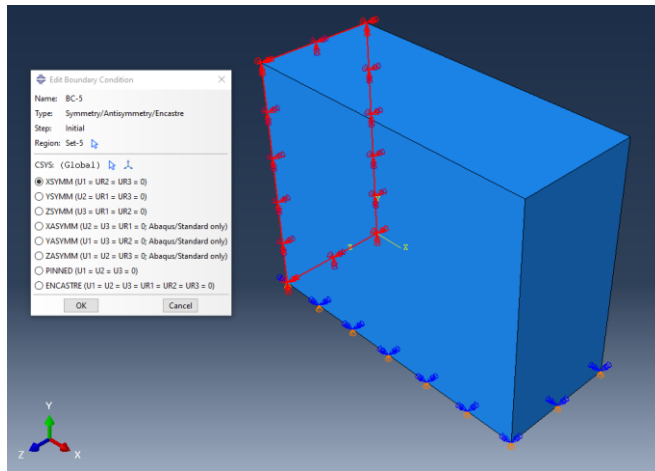


Figure 41: Symmetry Boundary Conditions in YZ Plane in Symmetry Geometry Load Case Y

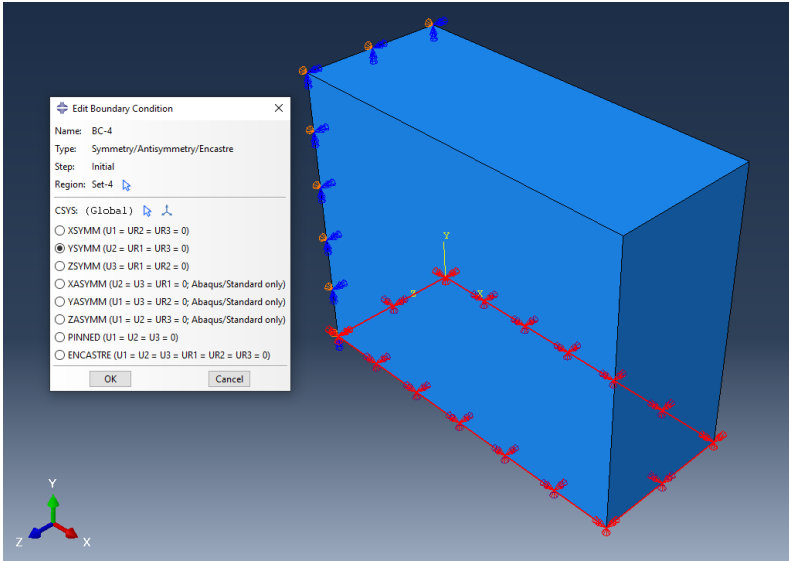


Figure 42: Symmetry Boundary Conditions in XZ Plane in Symmetry Geometry Load Case Y

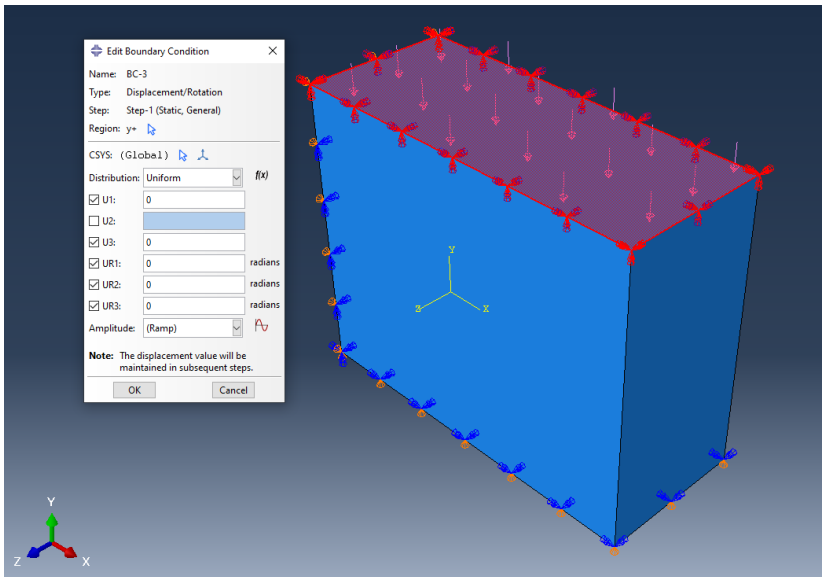


Figure 43: Boundary Conditions in Symmetry Geometry Load Case Y

3.8.6. Symmetry Geometry - Load case XY

In this model the two surfaces were defined and a symmetry XSYMM and YSYMM and the loaded surfaces X and Y received the pressure load and were locked to moving in all directions except by the X and the Y one.

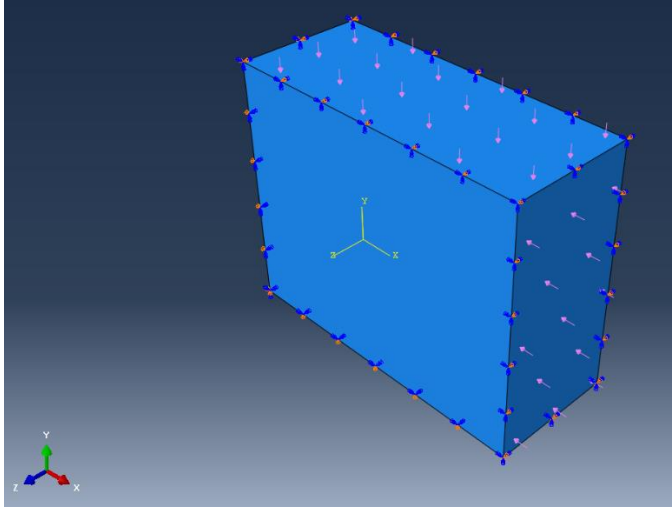


Figure 44: Symmetry Geometry Load Case XY

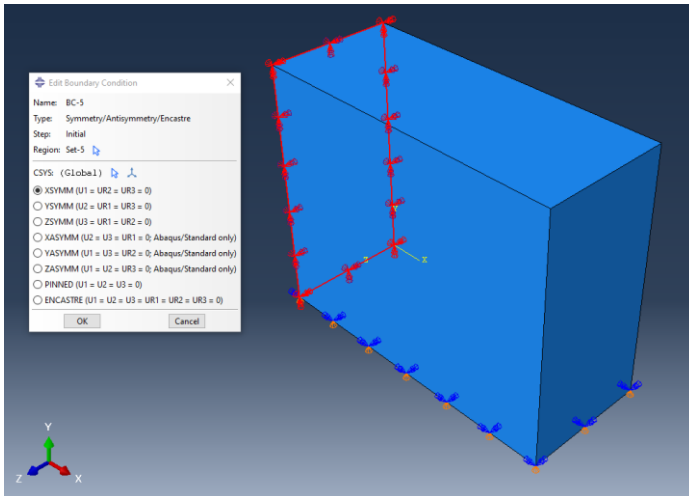


Figure 45: Symmetry Boundary Conditions in YZ Plane in Symmetry Geometry Load Case XY

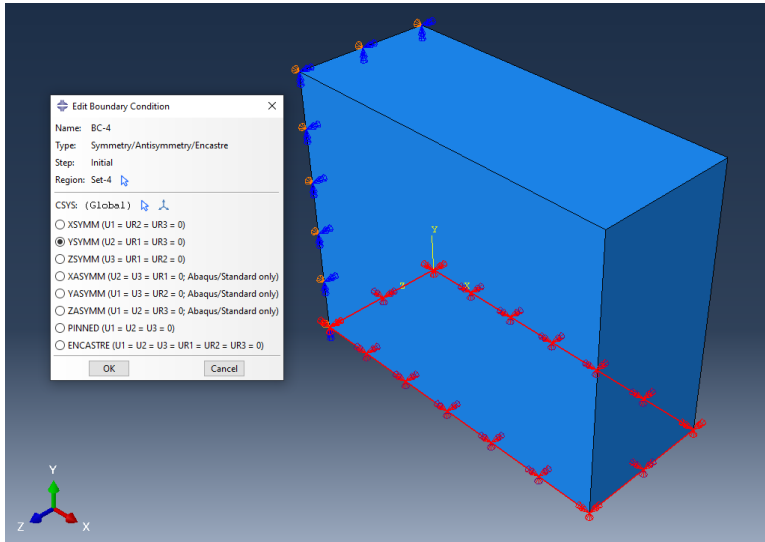


Figure 46: Symmetry Boundary Conditions in XZ Plane in Symmetry Geometry Load Case XY

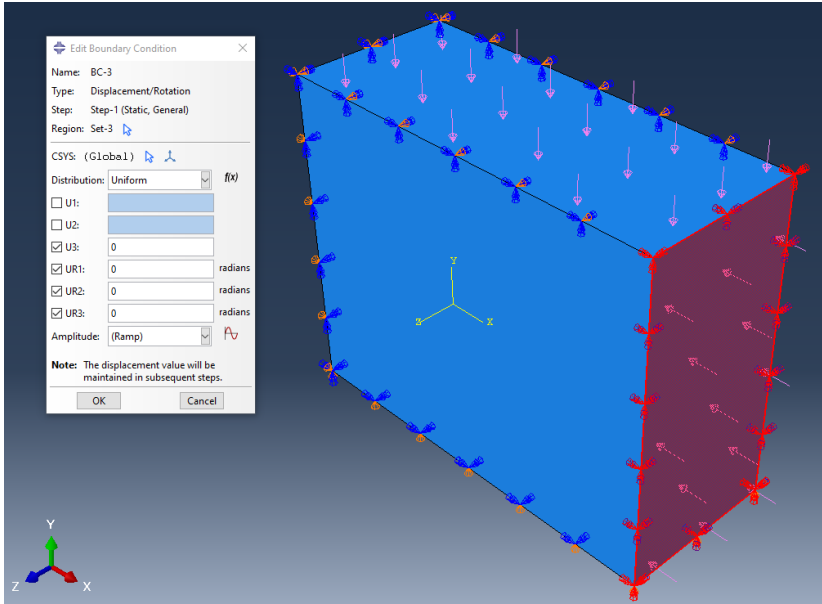


Figure 47: Boundary Conditions in Symmetry Geometry Load Case XY

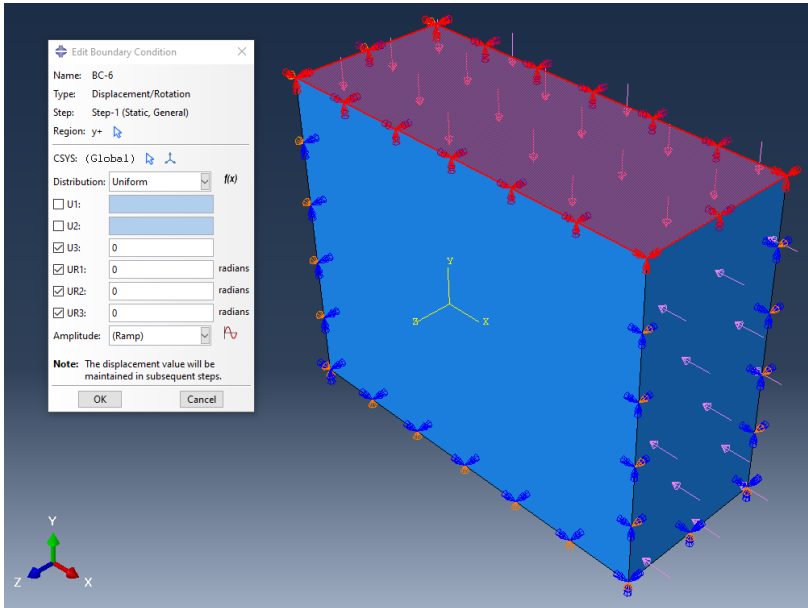


Figure 48: Boundary Conditions in Symmetry Geometry Load Case XY

3.9. Obtaining Stresses

In order to obtain a matrix of the stresses for each node that composes the elements of the model is extracted with the command report field output, as the Abaqus Analysis User Manual (2009) mentions. The choice to get all the stress is each node of each element is the position element nodal and the check in the respective stress to be analyzed are S.S11 S.S22 S.S33 S.S12 S.S13 S.S23. These six stresses represent the three normal stresses and three shear stresses. They are selected as the images below show:

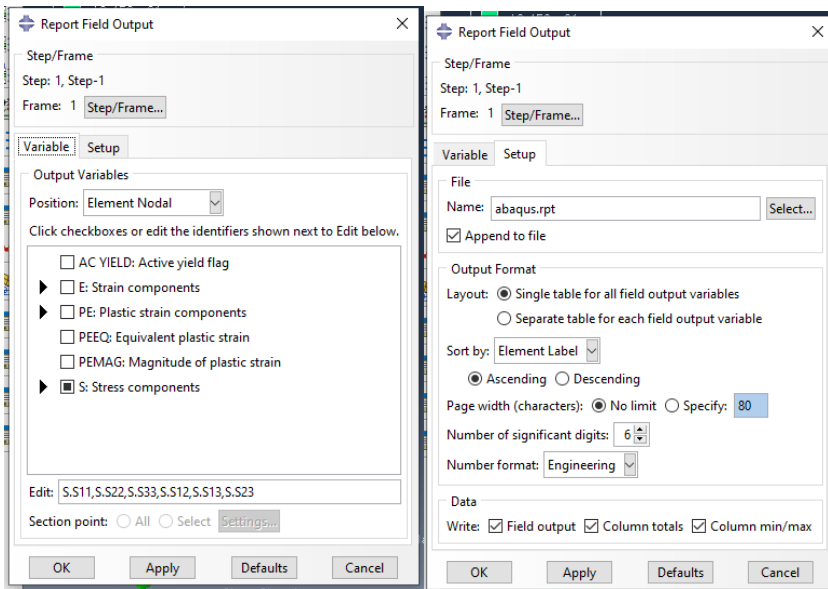


Figure 49: Image of the procedure to obtain the stresses 1

Figure 50: Image of the procedure to obtain the stresses 2

Element Label	Node Label	S.S11 @Loc 1	S.S22 @Loc 1	S.S33 @Loc 1	S.S12 @Loc 1	S.S13 @Loc 1	S.S23 @Loc 1
1	1	-854.482E-03	-76.4861E-03	-104.918E-03	-82.9576E-03	-63.3394E-03	-13.4096E-03
1	2	-902.177E-03	-115.648E-03	-113.691E-03	-112.950E-03	-67.9079E-03	-14.8769E-03
1	22	-920.142E-03	-85.2316E-03	-156.766E-03	-79.1083E-03	-64.3161E-03	-14.7401E-03
1	23	-971.220E-03	-134.073E-03	-171.135E-03	-106.550E-03	-68.6557E-03	-17.6523E-03
1	127	-796.933E-03	-28.9970E-03	-40.9948E-03	-44.5295E-03	-13.0375E-03	-9.66687E-03
1	128	-856.041E-03	-57.4059E-03	-49.0857E-03	-73.1836E-03	-17.7326E-03	-11.3796E-03
1	148	-873.456E-03	-37.4338E-03	-75.3931E-03	-40.8164E-03	-18.8401E-03	-10.9343E-03
1	149	-854.482E-03	-72.9470E-03	-104.918E-03	-68.0648E-03	-24.5263E-03	-14.0918E-03
2	2	-902.177E-03	-115.648E-03	-113.691E-03	-112.950E-03	-67.9079E-03	-14.8769E-03
2	3	-937.920E-03	-164.881E-03	-117.103E-03	-132.696E-03	-72.8623E-03	-12.9172E-03
2	23	-971.220E-03	-134.073E-03	-171.135E-03	-106.550E-03	-68.6557E-03	-17.6523E-03
2	24	-1.00929	-191.267E-03	-178.781E-03	-123.597E-03	-73.9017E-03	-16.7300E-03
2	128	-856.041E-03	-57.4059E-03	-49.0857E-03	-73.1836E-03	-17.7326E-03	-11.3796E-03
2	129	-913.799E-03	-105.247E-03	-54.0287E-03	-103.391E-03	-22.6338E-03	-9.92762E-03
2	149	-949.873E-03	-72.9470E-03	-122.463E-03	-68.0648E-03	-24.5263E-03	-14.0918E-03
2	150	-999.103E-03	-130.787E-03	-100.385E-03	-97.2138E-03	-30.6682E-03	-13.9139E-03
3	3	-937.920E-03	-164.881E-03	-117.103E-03	-132.696E-03	-72.8623E-03	-12.9172E-03
3	4	-933.399E-03	-182.074E-03	-114.252E-03	-115.607E-03	-73.7233E-03	-9.30999E-03
3	24	-1.00929	-191.267E-03	-178.781E-03	-123.597E-03	-73.9017E-03	-16.7300E-03
3	25	-1.00391	-209.648E-03	-174.426E-03	-107.158E-03	-75.4963E-03	-11.9838E-03
3	129	-913.799E-03	-105.247E-03	-54.0287E-03	-103.391E-03	-22.6338E-03	-9.92762E-03
3	130	-916.502E-03	-135.399E-03	-51.6703E-03	-98.8199E-03	-23.2609E-03	-6.11790E-03
3	150	-999.103E-03	-130.787E-03	-100.385E-03	-97.2138E-03	-30.6682E-03	-13.9139E-03
3	151	-1.00129	-163.806E-03	-96.8186E-03	-93.4142E-03	-31.5746E-03	-9.14340E-03
4	4	-933.399E-03	-182.074E-03	-114.252E-03	-115.607E-03	-73.7233E-03	-9.30999E-03
4	5	-936.680E-03	-193.557E-03	-115.115E-03	-98.6860E-03	-73.8445E-03	-7.77982E-03
4	25	-1.00391	-209.648E-03	-174.426E-03	-107.158E-03	-75.4963E-03	-11.9838E-03
4	26	-1.00731	-221.125E-03	-175.159E-03	-91.8971E-03	-75.5926E-03	-9.76789E-03
4	130	-916.502E-03	-135.399E-03	-51.6703E-03	-98.8199E-03	-23.2609E-03	-6.11790E-03
4	131	-919.954E-03	-153.965E-03	-51.8531E-03	-86.1741E-03	-23.3609E-03	-4.71046E-03
4	151	-1.00129	-163.806E-03	-96.8186E-03	-93.4142E-03	-31.5746E-03	-9.14340E-03

Figure 51: Image of the result file for stresses in each element of the 8 ones of each one of the 4000 elements

3.10. Post-Processing

As mentioned before the post processing took place in Matlab software, the code for all the procedures is at the end of this report in the coding appendix. This data is going to be processed in MatLab to only get the data from the specific plane aimed, with it its possible to get a matrix of the stress values for the stress in the plane.

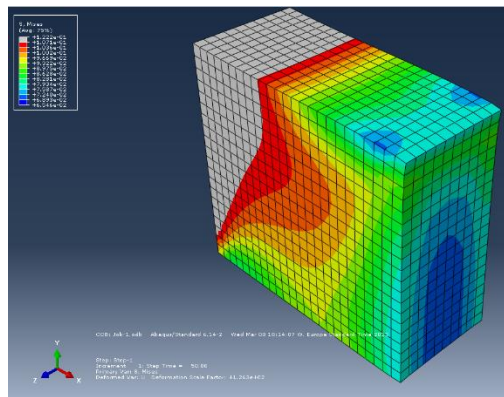


Figure 52: Images of simulation of stresses of a symmetrical geometry cube

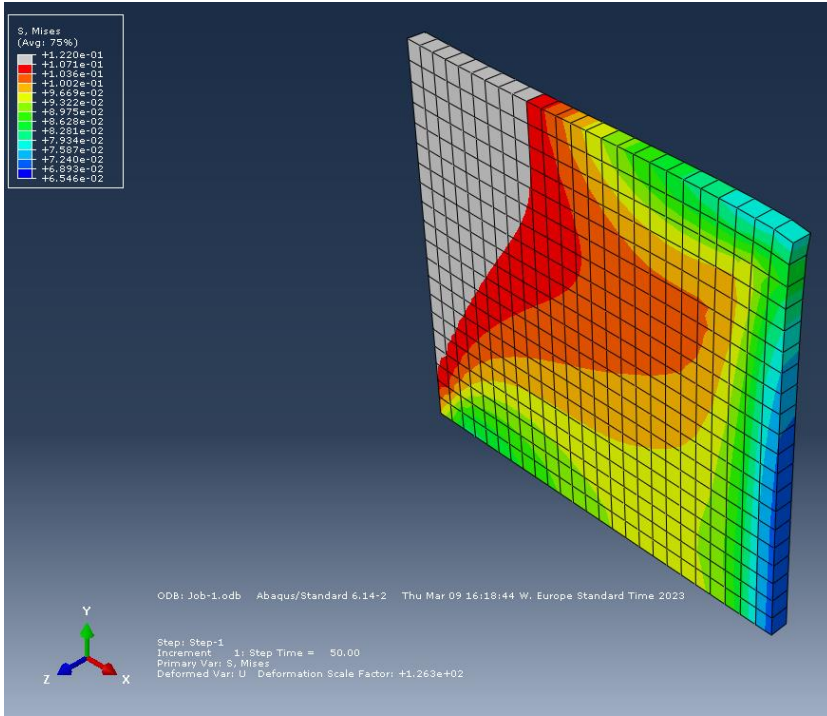


Figure 53: Images of simulation of stresses of middle plane of a cube

The code was created to transform the matrix of stress for each element got from Abaqus into a matrix of the variation of dielectric impermeability known as DeltaB. This process is done through the multiplication of the stress matrix for each node with the PEconstants for dielectric impermeability as the formula below:

$$\begin{bmatrix} \Delta B_1 \\ \Delta B_2 \\ \Delta B_3 \\ \Delta B_4 \\ \Delta B_5 \\ \Delta B_6 \end{bmatrix} = \begin{bmatrix} p_{11} & p_{12} & p_{13} & p_{14} & p_{15} & p_{16} \\ p_{21} & p_{22} & p_{23} & p_{24} & p_{25} & p_{26} \\ p_{31} & p_{32} & p_{33} & p_{34} & p_{35} & p_{36} \\ p_{41} & p_{42} & p_{43} & p_{44} & p_{45} & p_{46} \\ p_{51} & p_{52} & p_{53} & p_{54} & p_{55} & p_{56} \\ p_{61} & p_{62} & p_{63} & p_{64} & p_{65} & p_{66} \end{bmatrix} \begin{bmatrix} S_1 \\ S_2 \\ S_3 \\ S_4 \\ S_5 \\ S_6 \end{bmatrix}$$

Figure 54: Formula DeltaB matrix, Dielectric impermeability
Narasimhamurty (2012)

With this DeltaB matrix and the constant of refractive index before stress for each direction obtained by Mirzai (yet to be published) it is possible to calculate the refractive index after stress for each direction. This is done using the formula from Narasimhamurty (2012):

$$N_1 = \sqrt{\frac{1}{\Delta B + \frac{1}{N_0^2}}} \quad \text{Equation 2}$$

4. Results of simulation & Discussions

The below subsection indicates the results for a few of simulations that were done. The first one is the results for Material Orientation Comparison, secondly the results for Mesh Size Comparison, third Results for Plane Choice Comparison, fourth Load Pattern Comparison and finally Variations in Refractive Index Comparison. These are done in this order to reduce the amounts of simulations needed and therefore time taken to obtain results.

4.1. Results for Material Orientations Comparison

The below images represent the deformation and stress distributions on the different material orientations for the symmetrical model with load in the X axis in mesh size 0.1mm , load 100KPa.

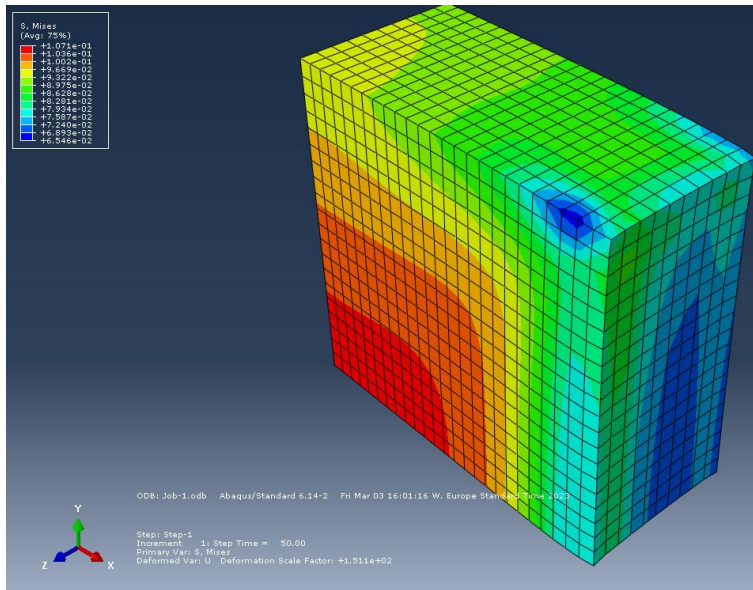


Figure 55: Stresses Material Orientation A

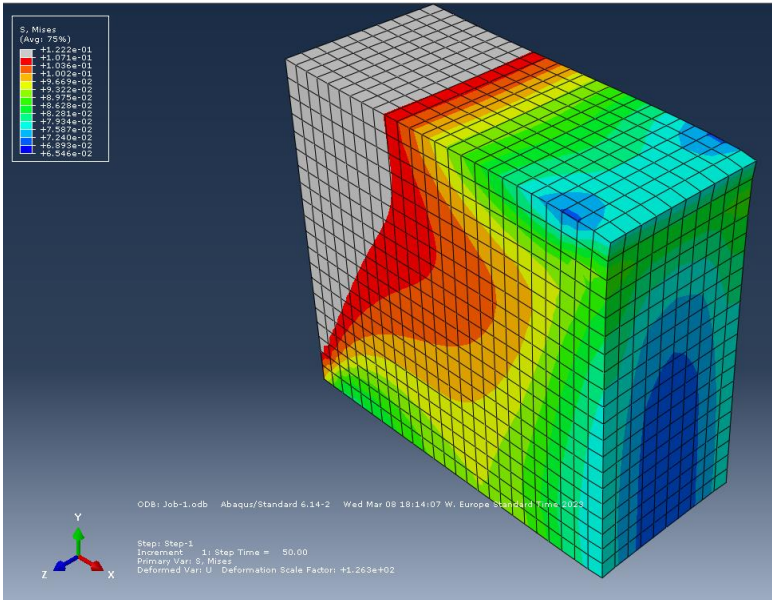


Figure 56: Stresses Material Orientation B

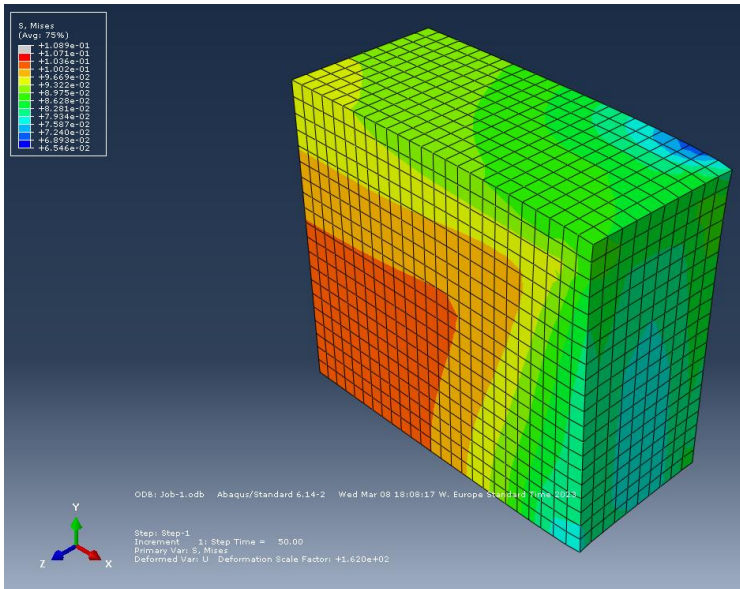


Figure 57: Stresses Material Orientation C

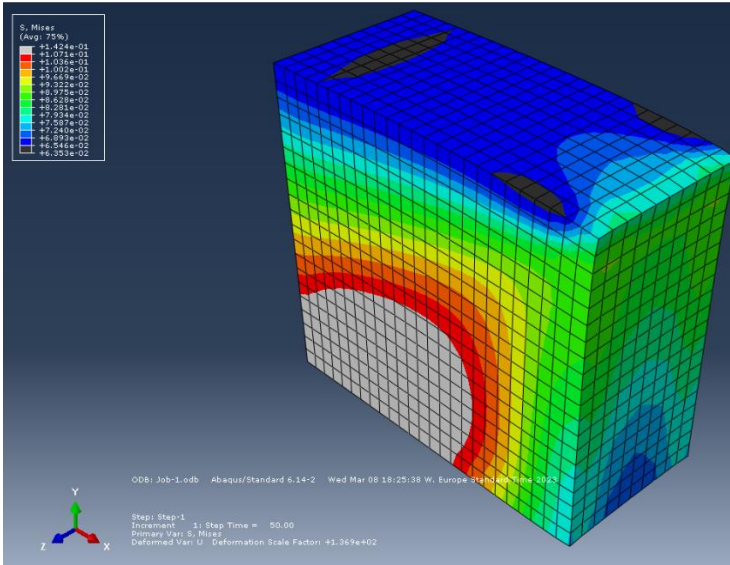


Figure 58: Stresses Material Orientation D

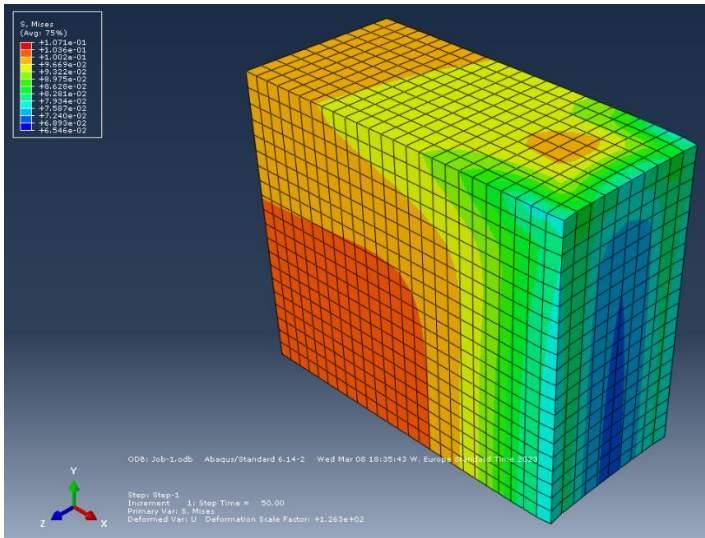


Figure 59: Stresses Material Orientation E

The below images represent the variation in the dielectric impermeability ΔB on the different material orientations for the symmetrical model with load in the X axis in mesh size 0.1mm , load 200KPa.

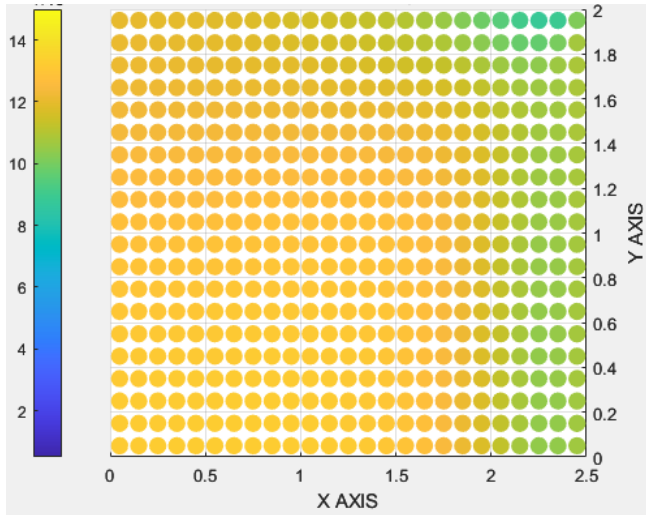


Figure 60: Dielectric impermeability Material Orientation A

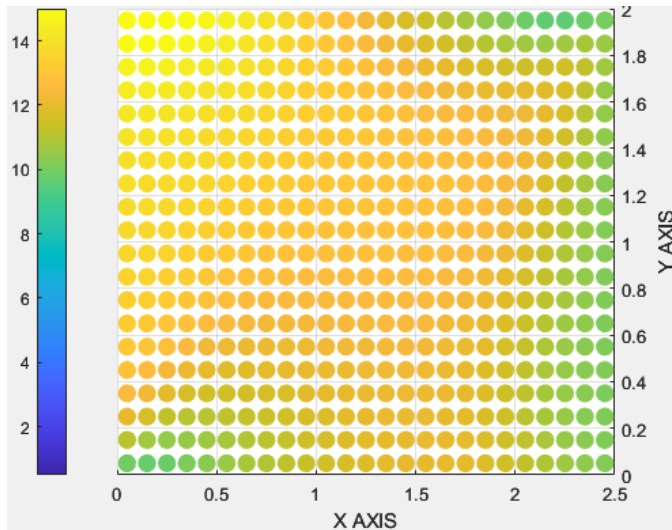


Figure 61: Dielectric impermeability Material Orientation B

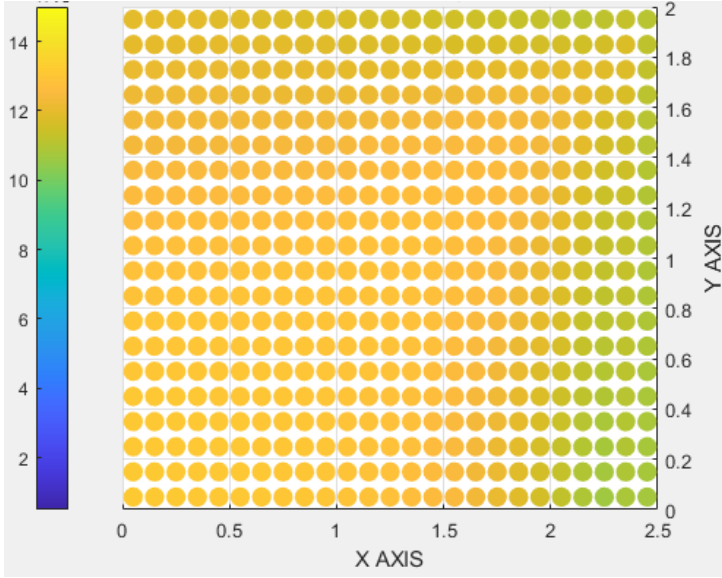


Figure 62: Dielectric impermeability Material Orientation C

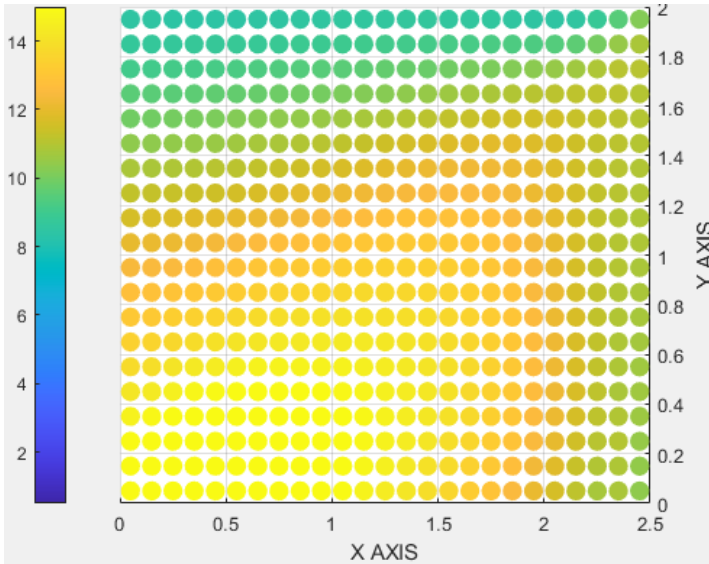


Figure 63: Dielectric impermeability Material Orientation D

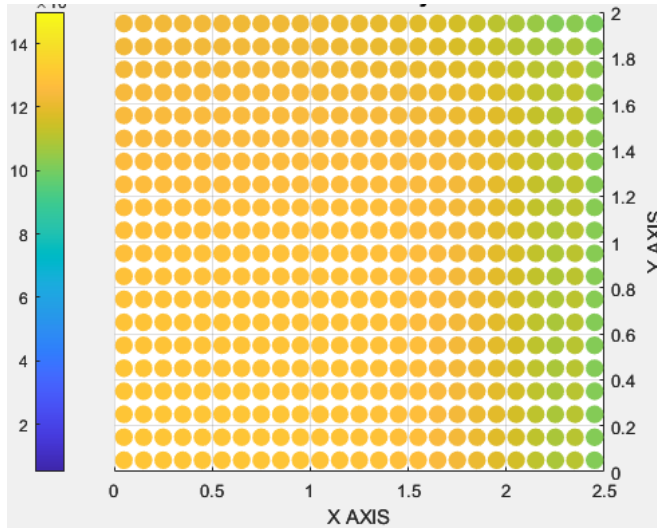


Figure 64: Dielectric impermeability Material Orientation E

Knowing these two results it is possible to set them side by side and identify which would correspond to which crystallographic orientation as the images below from Mirzai (yet to be published). The focus of this work was the simulation in the 3 main crystallographic axes.

Since it is a known fact that material orientation A is one of the main crystallographic axes due to D1111 being the same as C11 by a comparison it is possible to identify the other two. The results that exhibit a similar pattern of result to material A are the material C and E so it is possible to affirm that they are the other main crystallographic axes. So the focus of this work was in the Material Orientations A, C and E.

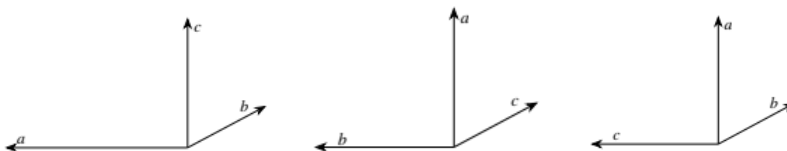


Figure 65: Crystallographic Axis X Material Orientation A

Figure 66: Crystallographic Axis X Material Orientation B

Figure 67: Crystallographic Axis X Material Orientation C

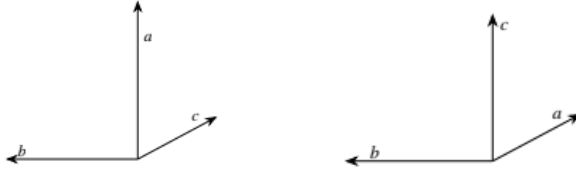


Figure 68: Crystallographic Axis X Material Orientation D

Figure 69: Crystallographic Axis X Material Orientation E

4.2. Results for Mesh Size Comparison

4.2.1. Full Body Model

The below images represent the deformation and stress distributions on the different mesh sizes for the full body model with load in the X axis in mesh size 0.1mm, load 100KPa.

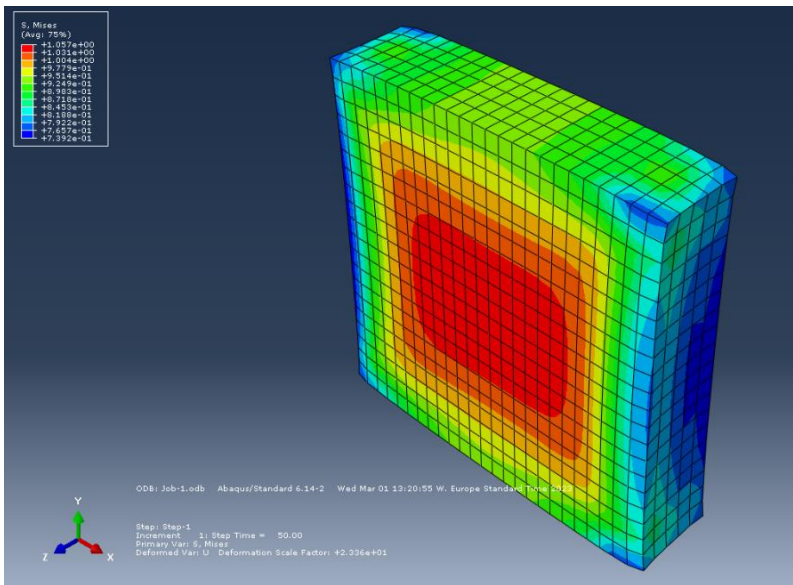


Figure 70: Plot Mesh Size 0,2 Full Body Geometry pressure X

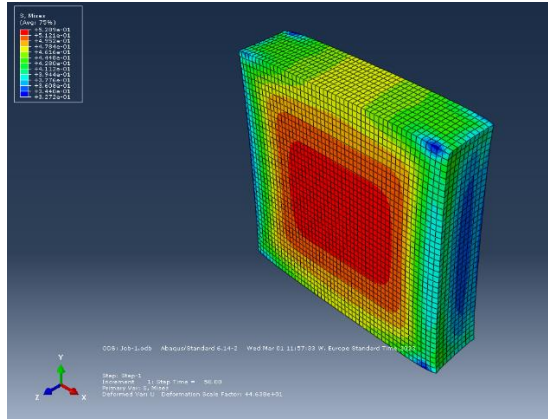


Figure 71: Plot Mesh Size 0.1 Full Body Geometry pressure X

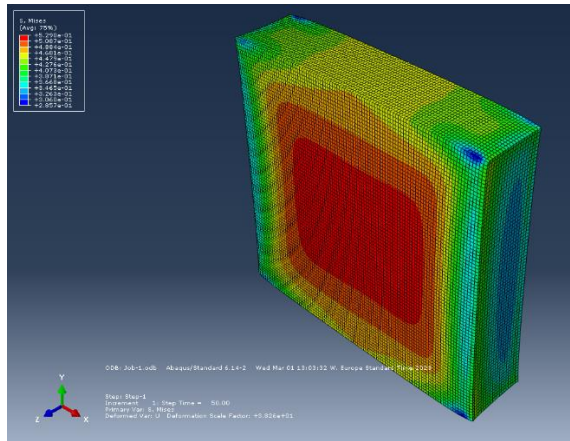


Figure 72: Plot Mesh Size 0,05 Full Body Geometry pressure X

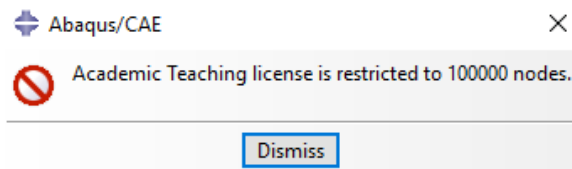


Figure 73: Mesh size 0,02 Full Body Geometry generates problems in processing

4.2.2. Symmetrical Model

The below images represent the deformation and stress distributions on the different mesh sizes for the symmetrical model with load in the X axis in mesh size 0.1mm, load 100KPa.

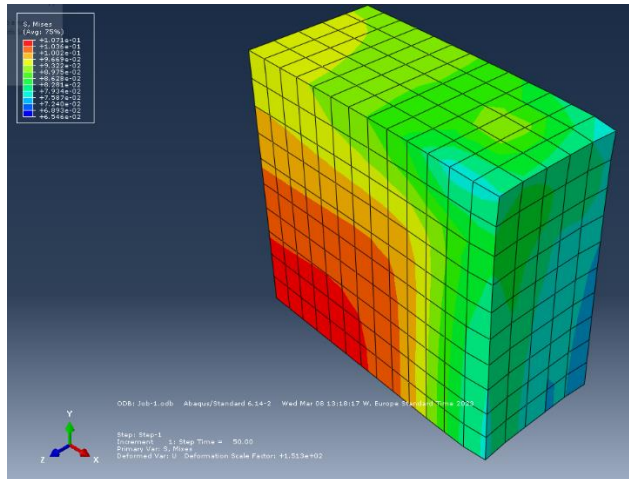


Figure 74: Plot Mesh Size 0,2 Symmetry Geometry pressure X

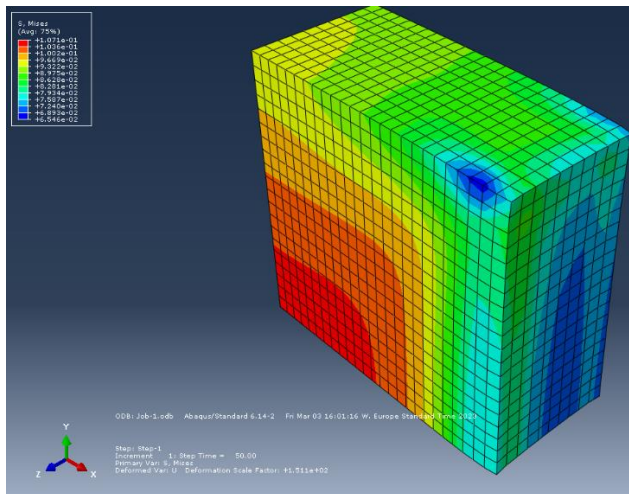


Figure 75: Plot Mesh Size 0.1 Symmetry Geometry pressure X

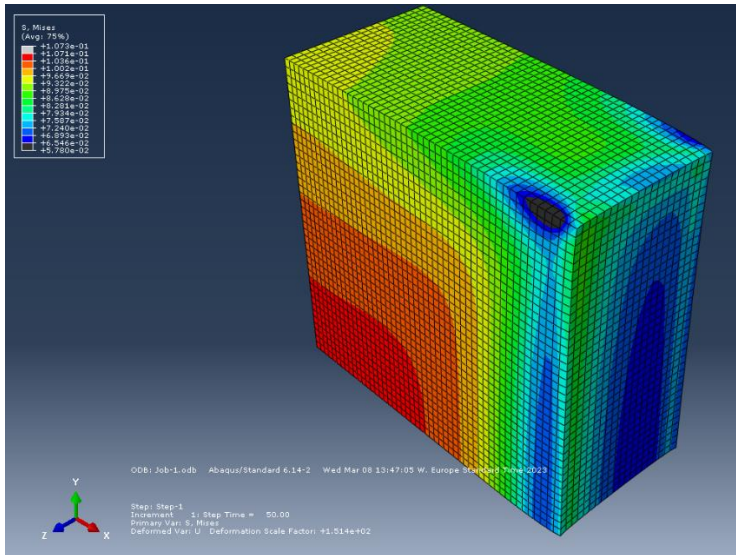


Figure 76: Plot Mesh Size 0,05 Symmetry Geometry pressure X

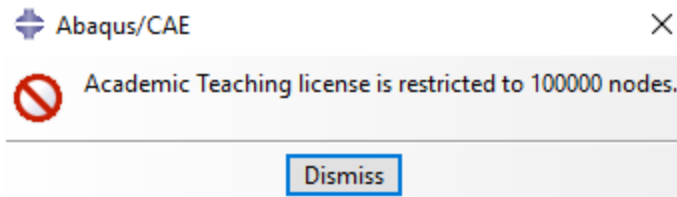


Figure 77: Mesh Size 0.02 Symmetry Geometry generates problems in processing

The images from both models show the increase in mesh fineness by eye since all of them are in the same scale. This perceptible increase in the precision of the model with finer mesh in addition to the limitation in the mesh size and the computational time taken (as table below) results that the best mesh size would be the 0.05mm.

As for the model to be chosen, the symmetry model presents a better computational time for an equivalent precision and therefore is the one to be taken as standard to the full analysis.

Table 4: Mesh Size x Geometry type x Time to process x Number of elements

Mesh Size	Type of Geometry	Number of Elements	Time to Process
0,2	Symetrical	650	15 seconds
0,1	Symetrical	5.000	15 seconds
0,05	Symetrical	40.000	3 minutes
0,02	Symetrical	625.000	30 minutes
0,2	FullBody	2.500	15 seconds
0,1	FullBody	20.000	25 seconds
0,05	FullBody	160.000	20 minutes
0,02	FullBody	1.000.000	5 hours

4.3. Results for Plane Choice Comparison

The below images represent the variation in the dielectric impermeability $\Delta\epsilon_B$ on the outer and middle plane in the models for 0.05mm mesh sizes. The goal was to analyze if the choice of the plane would influence the most the variance of the dielectric impermeability $\Delta\epsilon_B$.

The images below show for different material orientations and different loads that the biggest effect of variance on the $\Delta\epsilon_B$ is in the middle plane. This is confirmed for the first analyzes with 200KPa for material orientation A as well as 100 KPa for all the material orientations for pure crystals and doped ones. For that reason the plane chosen for the full analysis was the middle one.

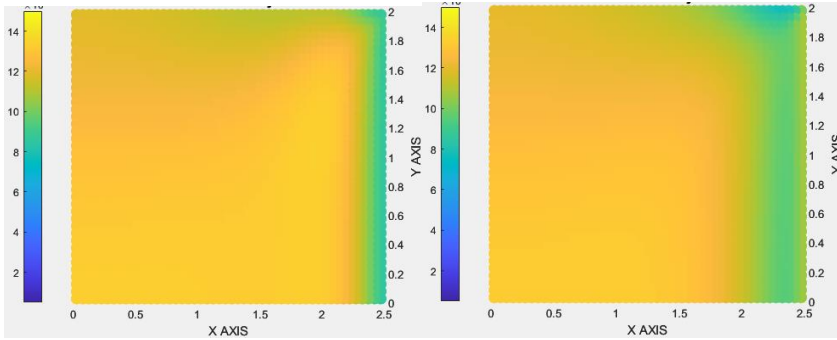


Figure 78: Dielectric Impermeability for different planes Material Orientation A Load Case X 200 KPa Pure Material, left Middle plane and right outer plane

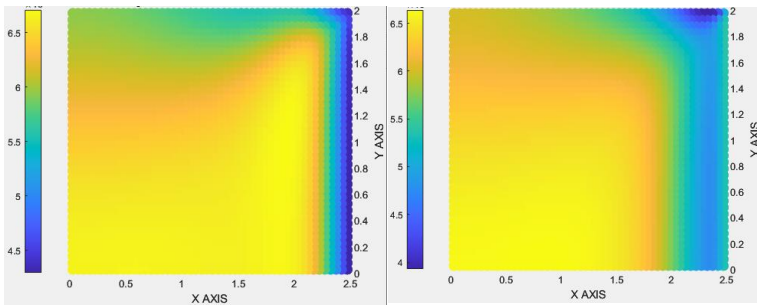


Figure 79: Dielectric Impermeability for different planes Material Orientation A Load Case X 100 KPa Pure Material, left Middle plane and right outer plane

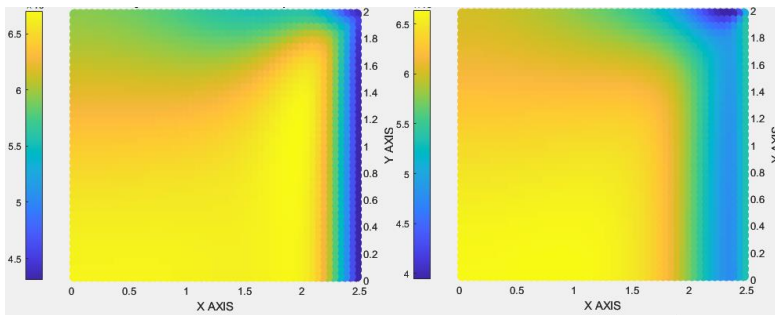


Figure 80: Dielectric Impermeability for different planes Material Orientation A Load Case X 100 KPa Doped Material, left Middle plane and right outer plane

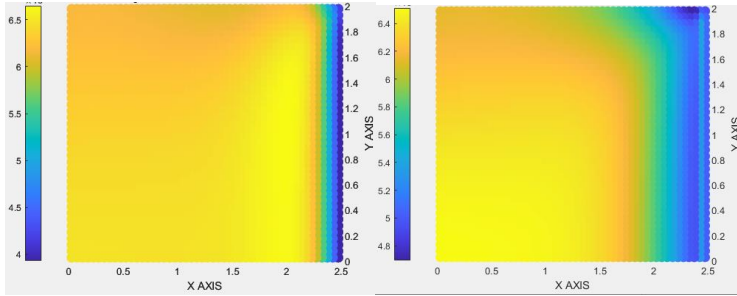


Figure 81: Dielectric Impermeability for different planes Material Orientation E Load Case X 100 KPa Pure Material, left Middle plane and right outer plane

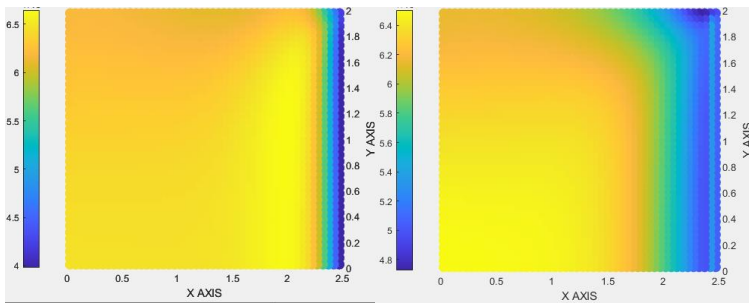


Figure 82: Dielectric Impermeability for different planes Material Orientation E Load Case X 100 KPa Doped Material, left Middle plane and right outer plane

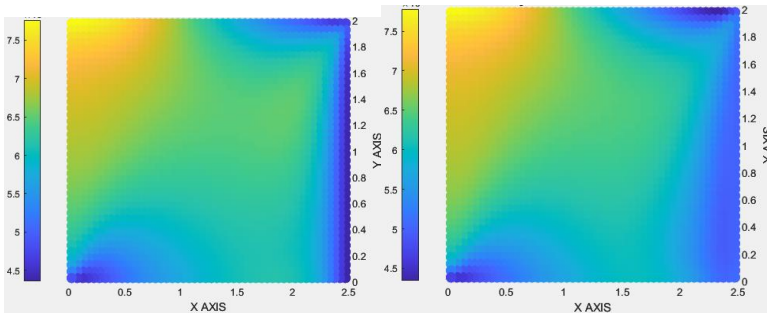


Figure 83: Dielectric Impermeability for different planes Material Orientation B Load Case X 100 KPa Pure Material, left Middle plane and right outer plane

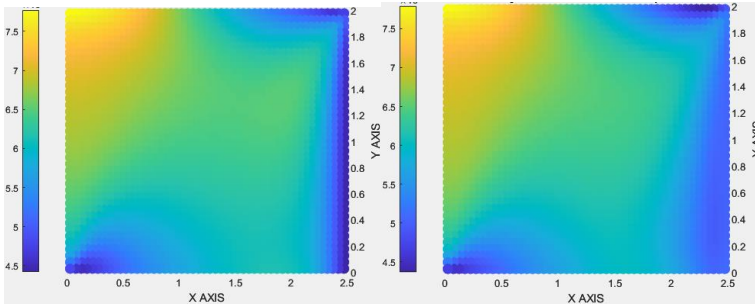


Figure 84: Dielectric Impermeability for different planes Material Orientation B Load Case X 100 KPa Doped Material, left Middle plane and right outer plane

4.4. Load Pattern Comparison

The below images represent the variation in the dielectric impermeability ΔB on the middle plane for models with 0.05mm mesh sizes with different load modulus. The goal was to analyze if the pattern of the places with the biggest variations of dielectric impermeability would change, checking if it would have variation due to the load or if it would be a constant.

The images below show that for different material orientations and different loadcases and different loads that there is no major effect of pattern of variance on the ΔB . This is confirmed for the first analysis with Material Orientation A where for all the load patterns of ΔB is the same for the secondary analysis with the loads 100KPa , 400KPa, 1500KPa for the Load cases X, Y and XY in material A and E.

For that reason it is expected that the change in the refractive index will be a continuous factor for all elements in relation to the load and it can be analyzed as a continuous function, since they are proportional as described in Narasimhamurty (2012).

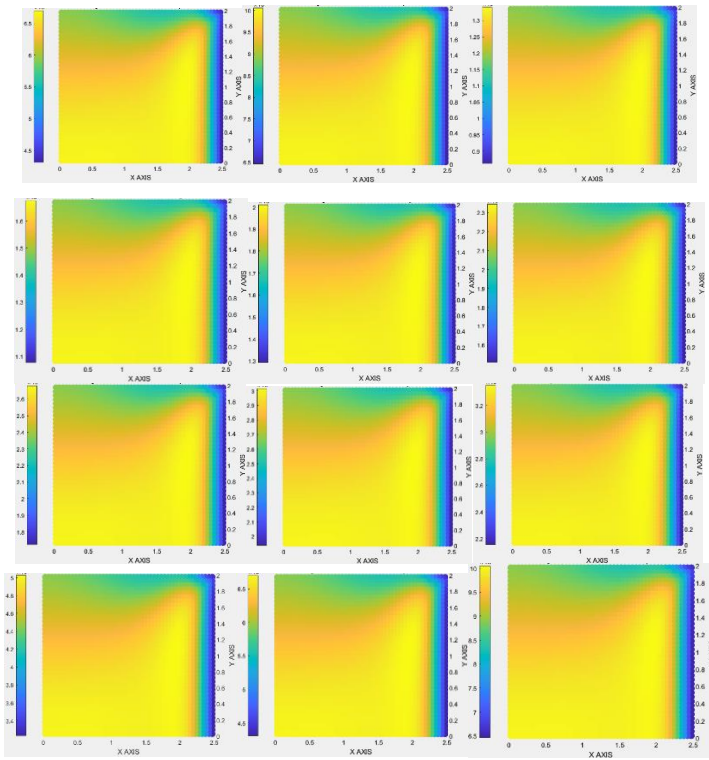


Figure 85: Dielectric Impermeability for different load modulus in Material Orientation A Doped Load Case X, left to right 100Kpa, 150Kpa, 200KPa, 250KPa, 300KPa, 350KPa, 400KPa, 450KPa, 500KPa, 750KPa, 1000KPa, 1500KPa

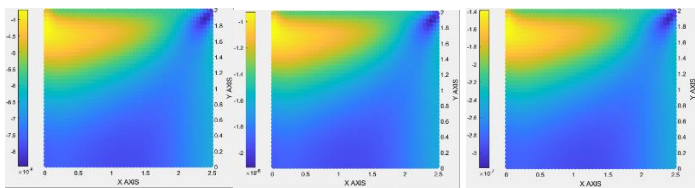


Figure 86: Dielectric Impermeability for different load modulus in Material Orientation A Doped Load Case Y, left to right 100KPa, 400KPa, 1500KPa

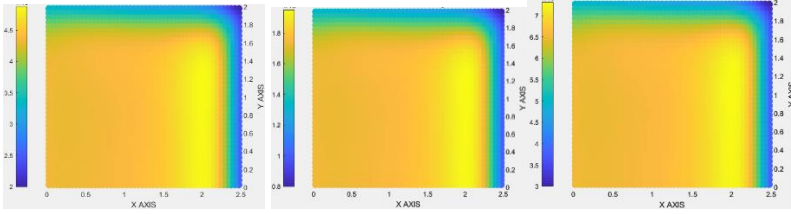


Figure 87: Dielectric Impermeability for different load modulus in Material Orientation A Doped Load Case XY, left to right 100KPa, 400KPa, 1500KPa

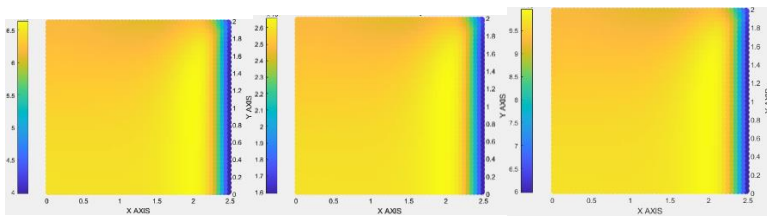


Figure 88: Dielectric Impermeability for different load modulus in Material Orientation E Doped Load Case X, left to right 100KPa, 400KPa, 1500KPa

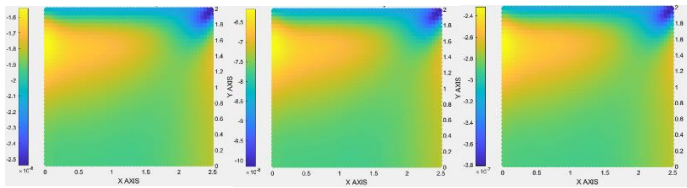


Figure 89: Dielectric Impermeability for different load modulus in Material Orientation E Doped Load Case Y, left to right 100KPa, 400KPa, 1500KPa

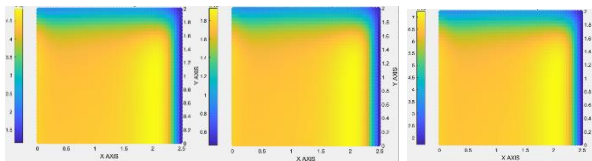


Figure 90: Dielectric Impermeability for different load modulus in Material Orientation E Doped Load Case XY, left to right 100KPa, 400KPa, 1500KPa

4.5. Variation in Refractive Index Comparison

The below images represent the variation in the Refractive Index on the middle plane for models with 0.05mm mesh sizes with different load modulus. The goal was to analyze how the variations of the refractive index would change due to the variation of load type, load modulus and crystal orientation.

The images below show that for both the pure and the doped crystal the effects of it can be seen in variations in both the refractive index in all the three axis N1X, N1Y, N1Z.

N1x

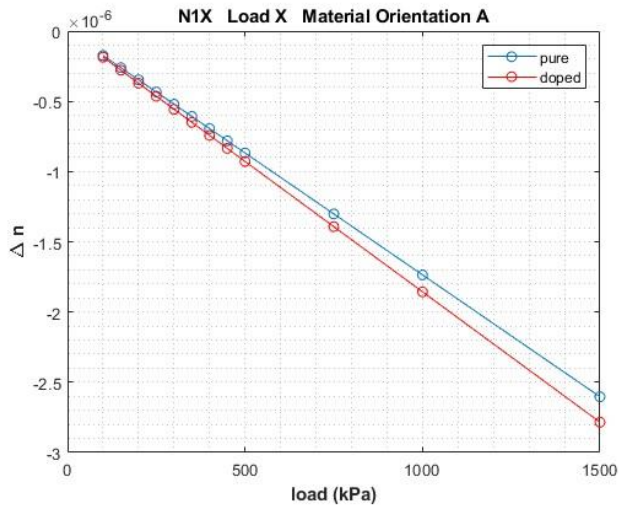


Figure 91: Variation of Refractive Index N1x Load X Material Orientation A.

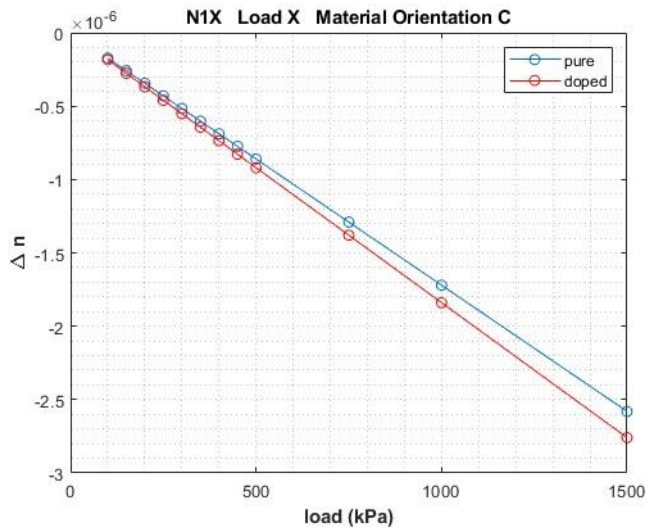


Figure 92: Variation of Refractive Index Δn Load X Material Orientation C

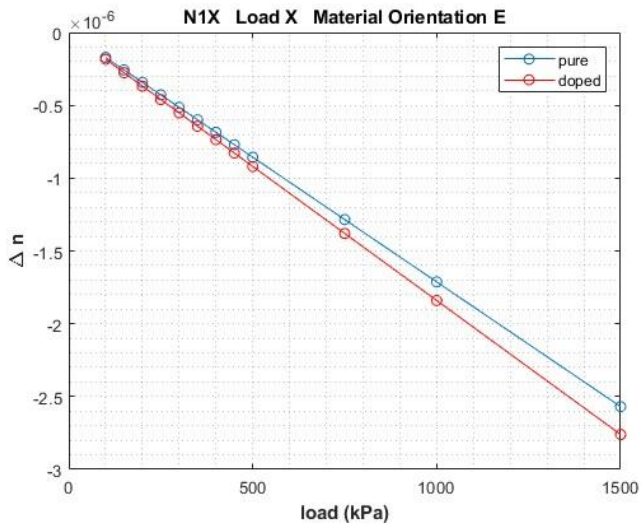


Figure 93: Variation of Refractive Index Δn Load X Material Orientation E

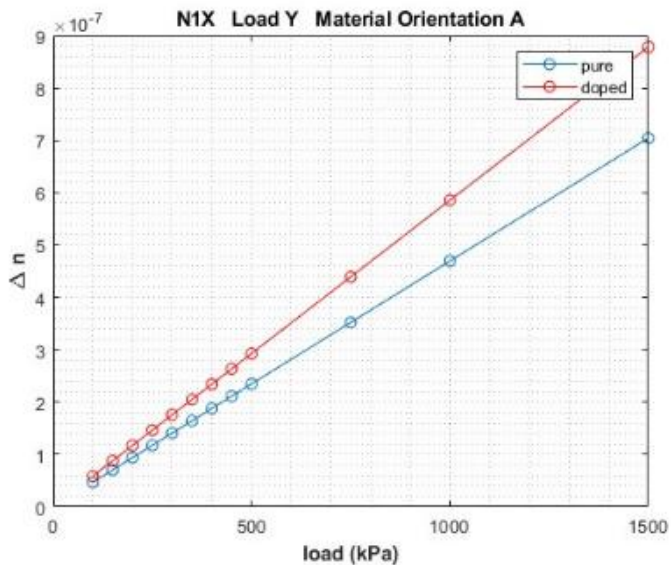


Figure 94: Variation of Refractive Index N1x Load Y Material Orientation A.

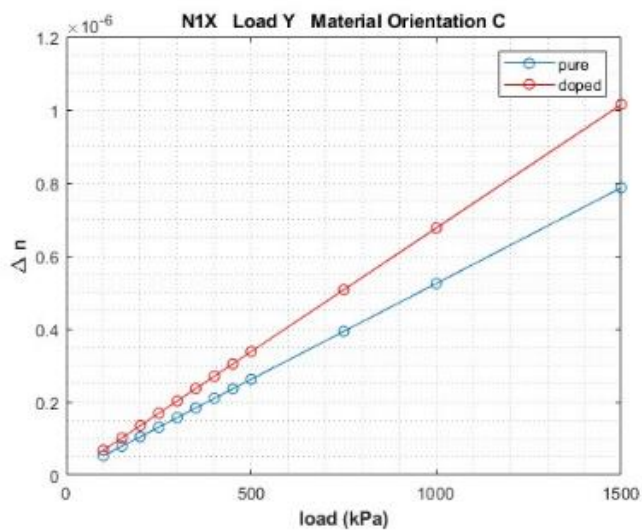


Figure 95: Variation of Refractive Index N1x Load Y Material Orientation C.

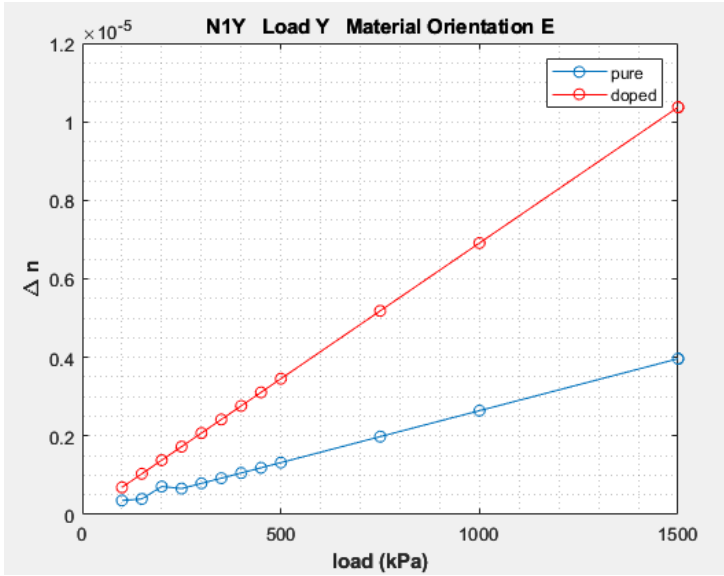


Figure 96: Variation of Refractive Index $N1x$ Load Y Material Orientation E.

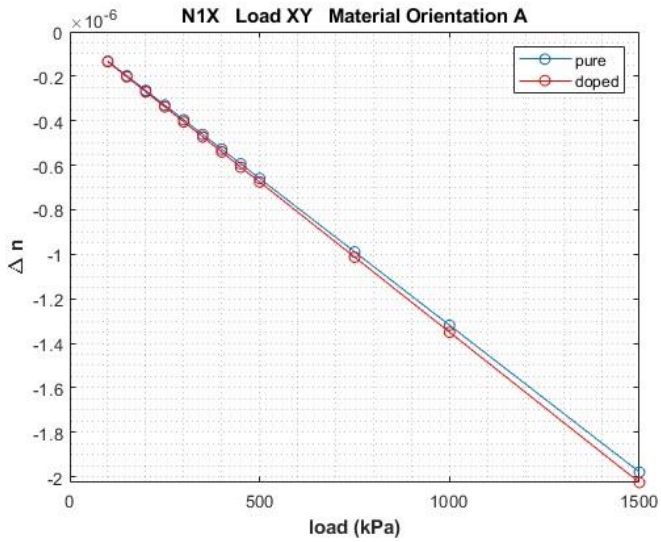


Figure 97: Variation of Refractive Index $N1x$ Load XY Material Orientation A

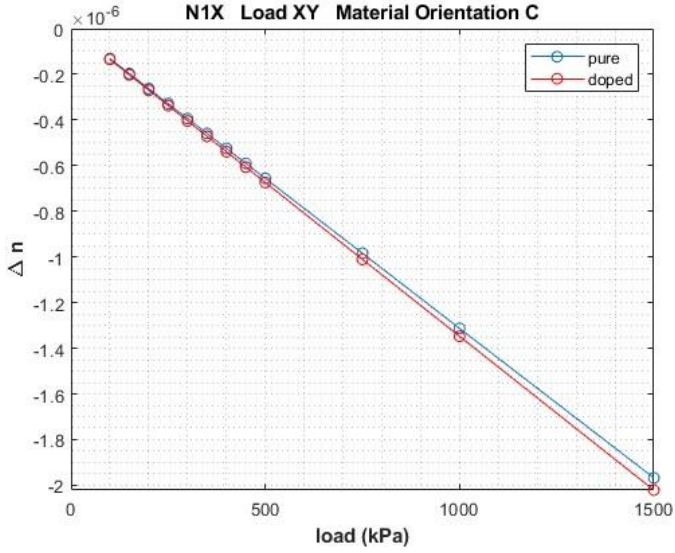


Figure 98: Variation of Refractive Index $N1x$ Load XY Material Orientation C

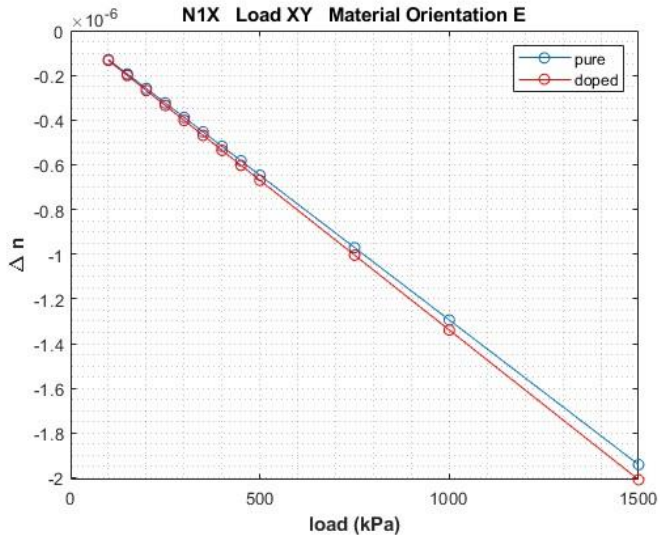


Figure 99: Variation of Refractive Index $N1x$ Load XY Material Orientation E.

N1y

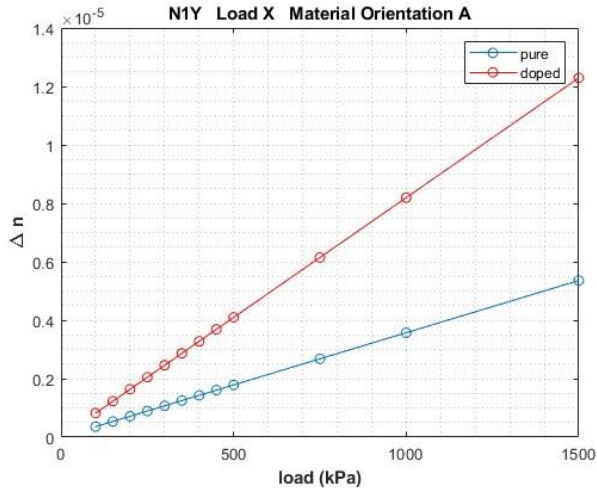


Figure 100: Variation of Refractive Index N1y Load X Material Orientation A.

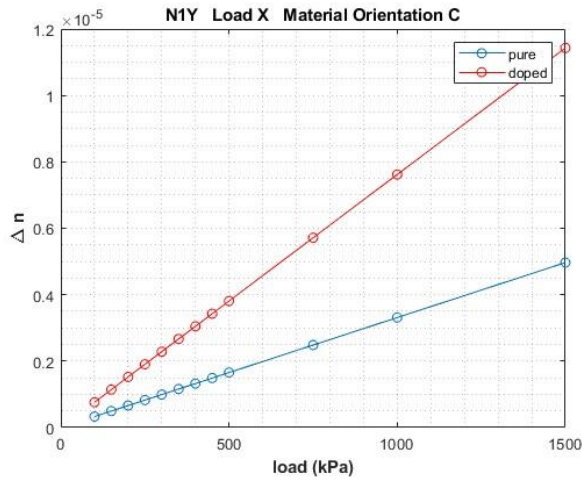


Figure 101: Variation of Refractive Index N1y Load X Material Orientation C.

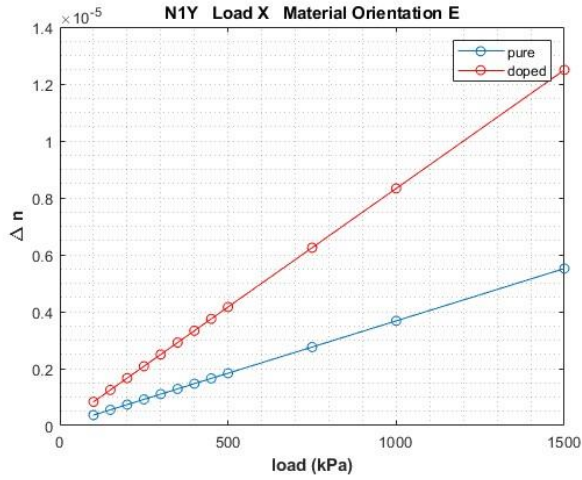


Figure 102: Variation of Refractive Index N1y Load X Material Orientation E

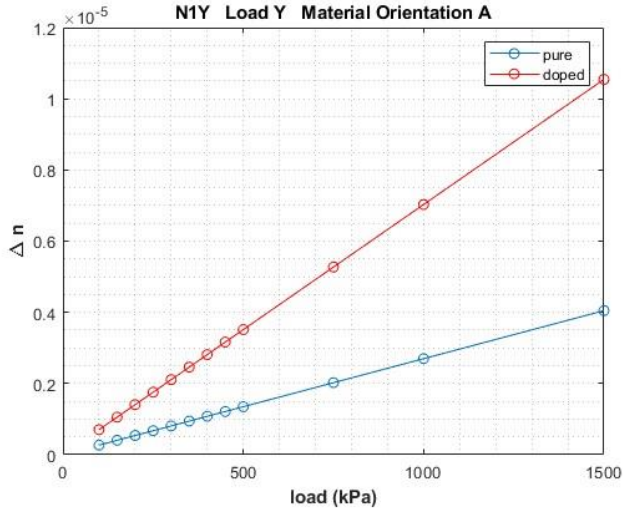


Figure 103: Variation of Refractive Index N1y Load Y Material Orientation A.

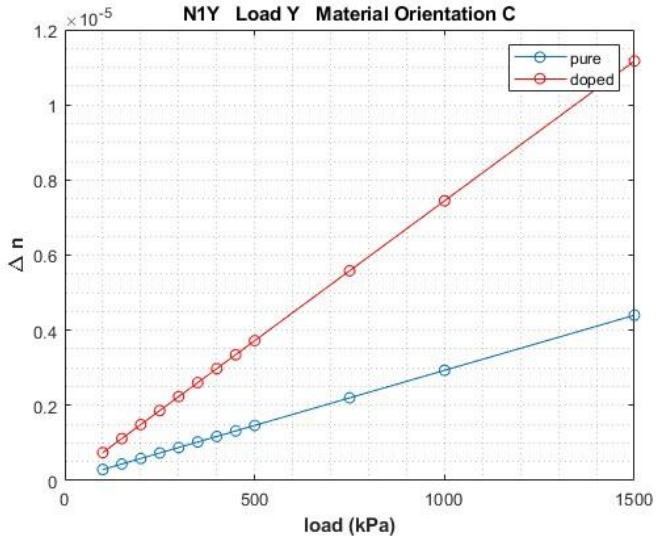


Figure 104: Variation of Refractive Index N1y Load Y Material Orientation C

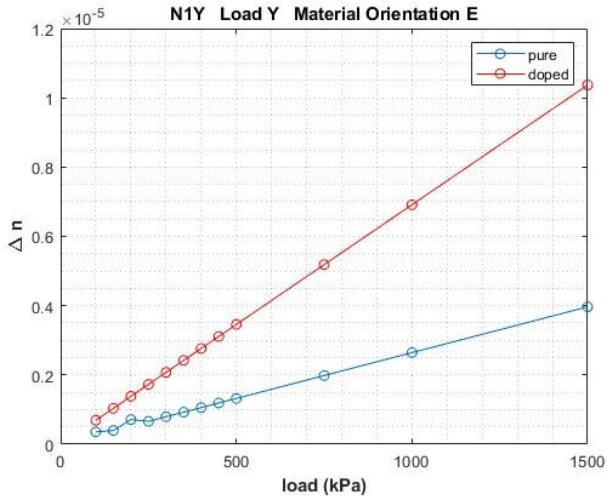


Figure 105: Variation of Refractive Index N1y Load Y Material Orientation E

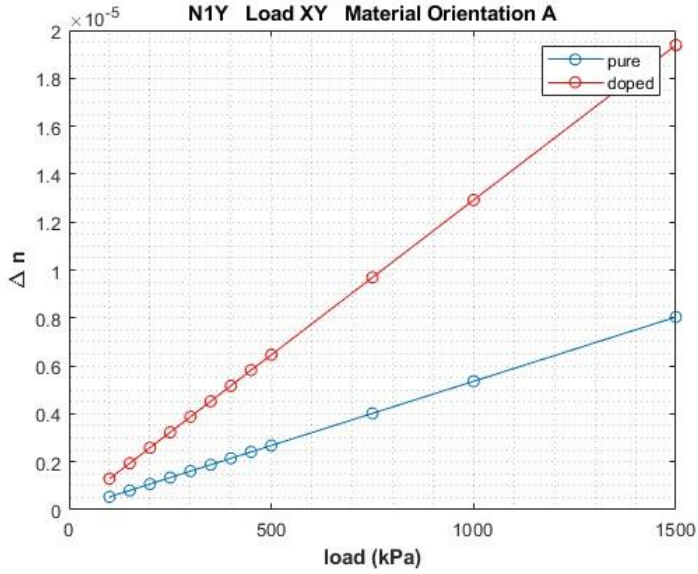


Figure 106: Variation of Refractive Index N1y Load XY Material Orientation A

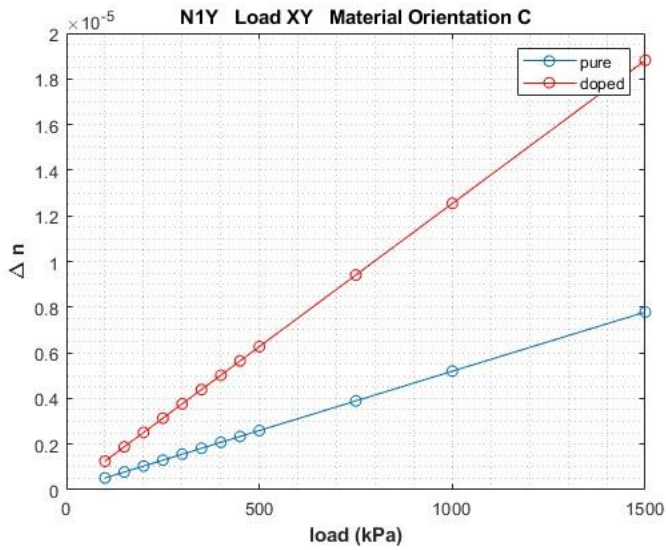


Figure 107: Variation of Refractive Index N1y Load XY Material Orientation C.

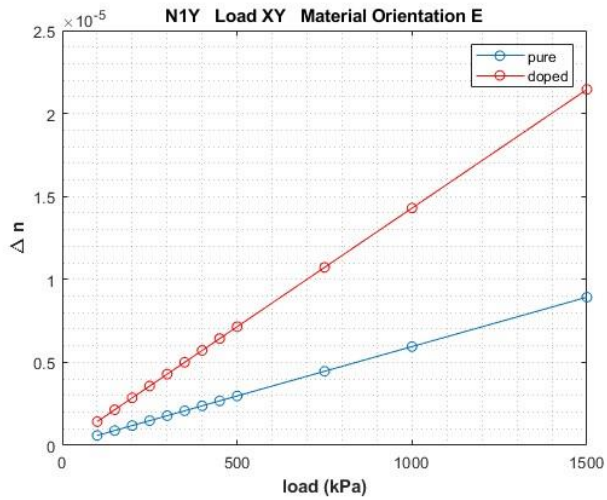


Figure 108: Variation of Refractive Index N1y Load XY Material Orientation E

N1z

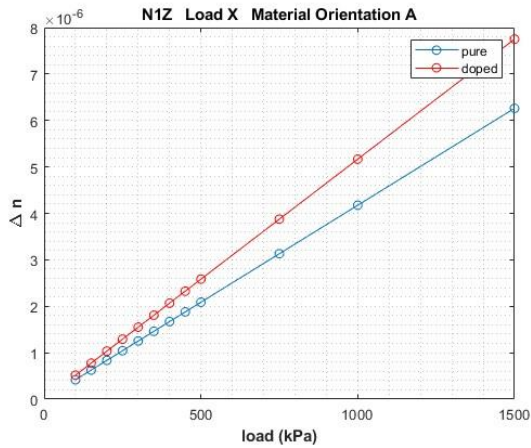


Figure 109: Variation of Refractive Index N1z Load X Material Orientation A

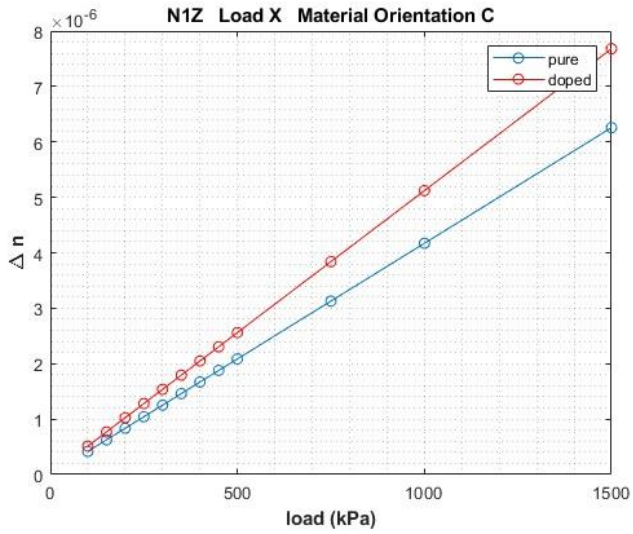


Figure 110: Variation of Refractive Index N1z Load X Material Orientation C

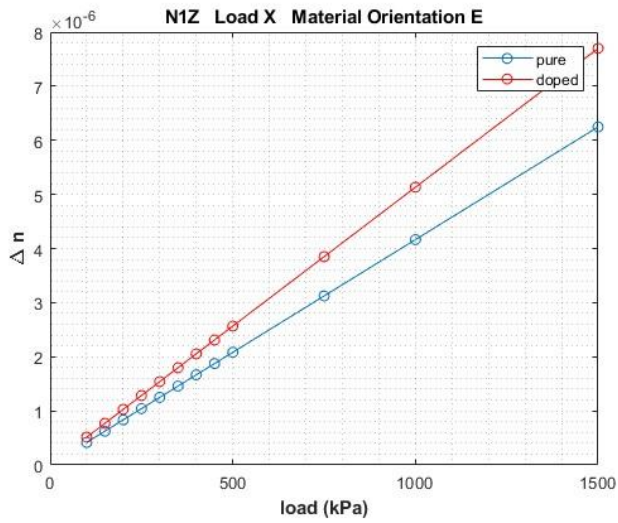


Figure 111: Variation of Refractive Index N1z Load X Material Orientation E

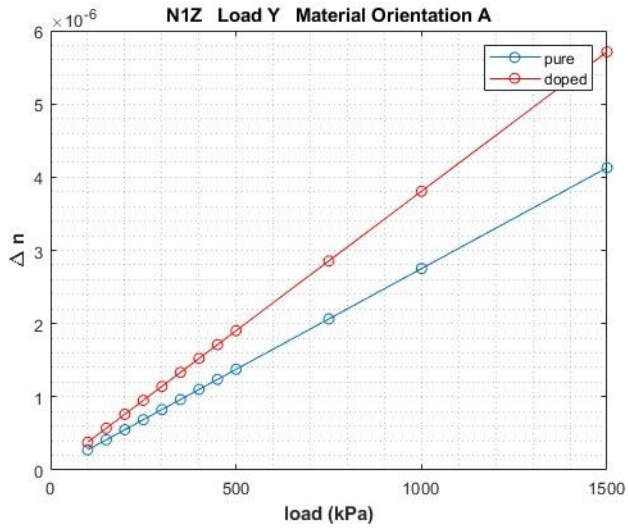


Figure 112: Variation of Refractive Index Δn versus load (kPa) for Material Orientation A

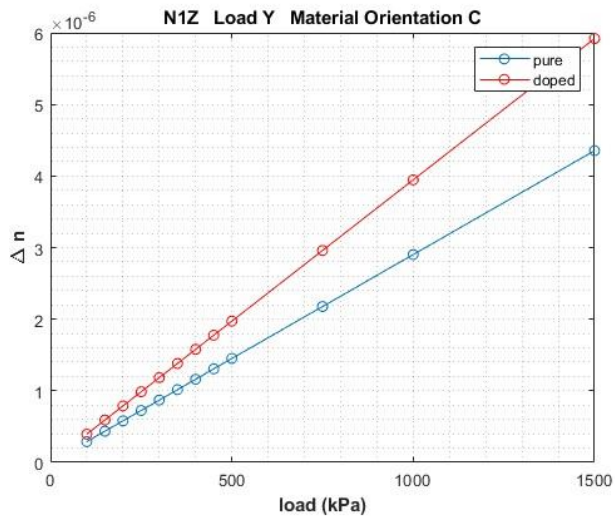


Figure 113: Variation of Refractive Index Δn versus load (kPa) for Material Orientation C

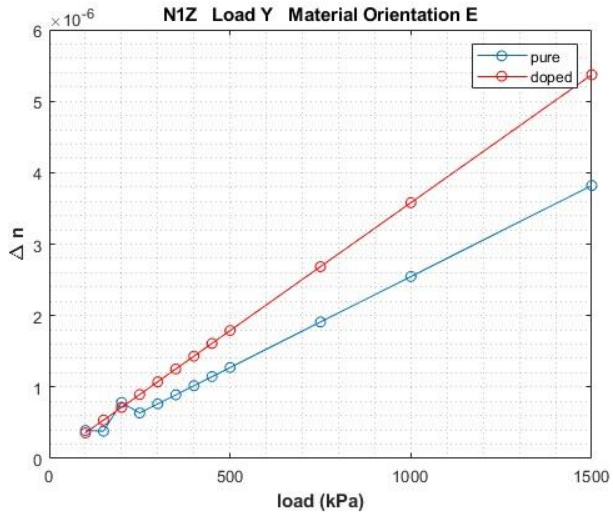


Figure 114: Variation of Refractive Index N1z Load Y Material Orientation E

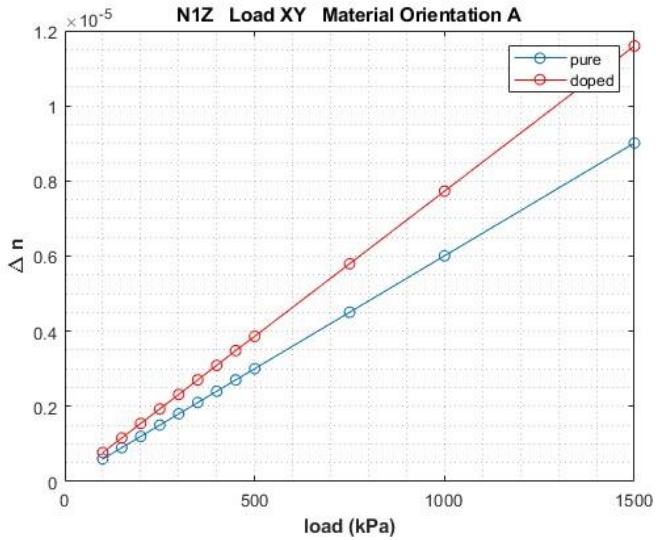


Figure 115: Variation of Refractive Index N1z Load XY Material Orientation A.

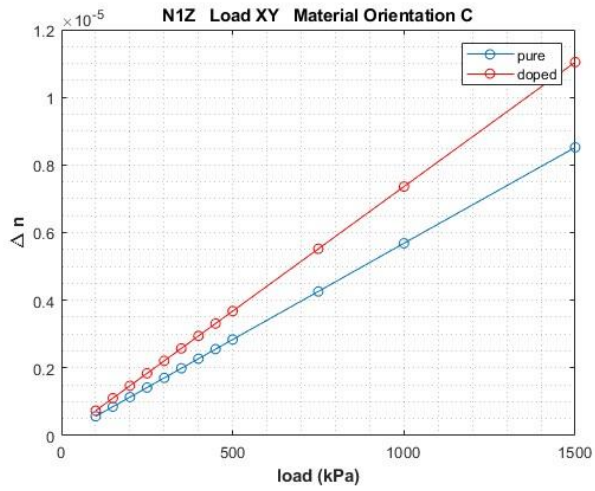


Figure 116: Variation of Refractive Index N1z Load XY Material Orientation C

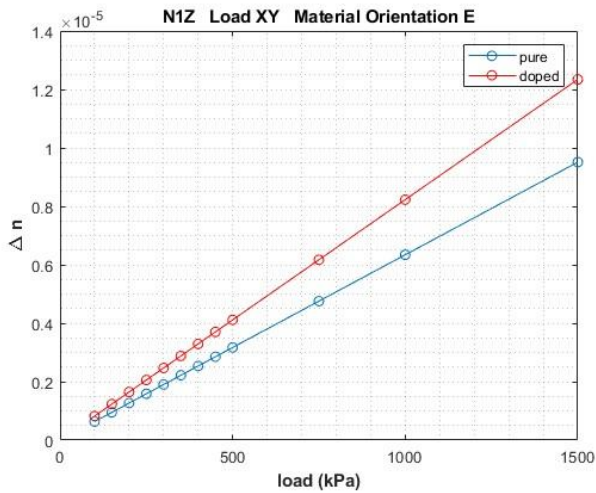


Figure 117: Variation of Refractive Index N1z Load XY Material Orientation E

4.5.1. Different load modulus

For N_{1x} it is possible to see that the load modulus plays a major role in the variation of index for both the pure and the doped crystal. In some cases, the magnitude of increase or decrease was deeply influenced by its variation.

For N_{1y} and N_{1z} it is possible to see that the load modulus also plays a major role in the variation of the refractive index for both the pure and the doped crystal. As the load increases the index varies increasing as well for all the cases.

4.5.2. Different load type

For N_{1x} it is possible to see that the load type plays a major role in the variation of the refractive index for both the pure and the doped crystal. In some cases generating an increase of the index and in others generating a decrease.

For N_{1y} and N_{1z} it is possible to see that the load type variation strongly influences the degree of variation of the refractive index for both the pure and the doped crystal. For all of the cases analyzed there is an increase in the index but the magnitude of how the increment happens differs from load type to load type.

4.5.3. Different material orientation

For N_{1x} , N_{1y} and N_{1z} it is possible to see that the material orientation influences the variation of the index for both the pure and the doped crystal but this influence is only clearer to be seen by analyzing the graphics for the biggest loads. In some cases the degree of variation of the index being smaller or bigger for some material orientations.

5. Conclusions and Suggestion of further works

In this work after analyzing the data it is possible to see that there is a pattern in variation of the refractive index for the variables of Load Case, Material Orientation and Load Modulus. Each of them presents a different result on the behavior of the index for both the pure and the doped crystal.

A variation in the load modulus varies proportionally the refractive index, a variation in the material orientation varies slightly the index as well. For the variation in Load Case, it generates a significant change in the degree that the index varies and also for some cases it generates an inversion of its values defining an increase in the index with load or a decrease with it.

However this was a first work on the area and some more investigation should be done outside the scope of this work to increase the knowledge in the field and have an even more defined behavior of the material. As examples of topics to develop more are: different load modulus, different planes to be analyzed, finer meshes.

As other values of loads to be applied the main hint was to search mostly in the values over 1500KPa where it was possible to see more clearly some of the effects of the variables. Different geometries to replicate the system could also be used in new research, the Cylinder geometry as Prakash and Girigimmalayanapalya (2021) did in their work is another geometry that would result in different tensions that is very interesting to be analyzed.

The study of variation of the refractive in the other planes and the combination of them all could also be an interesting study to be done in the future allowing the calculations of it in multiple planes and the equivalent one.

The analysis of an even finer mesh selection and its effect could also be of interest for future research, since this study had a license limitation there was a doubt about the possibility to increase even more the precision. There are a few indications that this could be an interesting topic since the footprint of the laser applications are from 5 to 50 μm and the mesh size was in the upper limit of that and also the tendency explored in this work of the finer meshes increasing precision.

References

- Bitarafan, Mohammad H., and Ray G. DeCorby. "On-chip high-finesse Fabry-Perot microcavities for optical sensing and quantum information." *Sensors* 17.8 (2017): 1748.
- Börgesson, L. "Abaqus." *Developments in geotechnical engineering*. Vol. 79. Elsevier, 1996. 565-570.
- Bui, Yvonne N. *How to write a master's thesis*. Sage Publications, 2013.
- Chang, T. Y., and S. M. Wang. *Evaluation of a Nonlinear Finite Element Program-ABAQUS*. AKRON UNIV OH DEPT OF CIVIL ENGINEERING, 1983.
- Craiciu, Ioana, et al. "Nanophotonic quantum storage at telecommunication wavelength." *Physical Review Applied* 12.2 (2019): 024062.
- Creswell, John W., and Cheryl N. Poth. *Qualitative inquiry and research design: Choosing among five approaches*. Sage publications, 2016.
- Dold, Gavin, et al. "High-cooperativity coupling of a rare-earth spin ensemble to a superconducting resonator using yttrium orthosilicate as a substrate." *Physical Review Applied* 11.5 (2019): 054082.
- Dutt, Aman. "Effect of mesh size on finite element analysis of beam." *International Journal of Mechanical Engineering* 2.12 (2015): 8-10.
- Feather, William G., Hojun Lim, and Marko Knezevic. "A numerical study into element type and mesh resolution for crystal plasticity finite element modeling of explicit grain structures." *Computational Mechanics* 67 (2021): 33-55.
- Fu, Huhui, et al. "Peasecod-Like Hollow Upconversion Nanocrystals with Excellent Optical Thermometric Performance." *Advanced Science* 7.14 (2020): 2000731.
- Fung, Y. C. "Elasticity of soft tissues in simple elongation." *American Journal of Physiology-Legacy Content* 213.6 (1967): 1532-1544.
- Gardner, Joel D., Athulan Vijayaraghavan, and David A. Dornfeld. "Comparative study of finite element simulation software." (2005).
- Ghosh, Pushpal, Suparna Sadhu, and Amitava Patra. "Preparation and photoluminescence properties of Y 2 SiO 5: Eu 3+ nanocrystals." *Physical Chemistry Chemical Physics* 8.28 (2006): 3342-3348.

-
- Giannakeas, Ilias N., Z. Sharif-Khodaei, and M. H. Aliabadi. "Assessment of the performance of different element types for guided wave simulations in abaqus." AIP Conference Proceedings. Vol. 2309. No. 1. AIP Publishing LLC, 2020.
 - Hampel, Andrea, et al. "Finite-element modelling of glacial isostatic adjustment (GIA): Use of elastic foundations at material boundaries versus the geometrically non-linear formulation." Computers & geosciences 122 (2019): 1-14.
 - Hibbitt, H., B. Karlsson, and P. J. D. S. S. C. P. Sorensen. "Abaqus analysis user's manual version 6.10." Dassault Systèmes Simulia Corp.: Providence, RI, USA (2011).
 - Horgan, C. O., J. G. Murphy, and G. Saccomandi. "The complex mechanical response of anisotropic materials in simple experiments." International Journal of Non-Linear Mechanics 106 (2018): 274-279.
 - Khennane, Amar. Introduction to finite element analysis using MATLAB® and abaqus. CRC Press, 2013.
 - Kitamura, Yuta, et al. "Birefringence simulation of annealed ingot of magnesium fluoride single crystal." Journal of crystal growth 311.15 (2009): 3954-3962.
 - Konijnenberg, A. P., A. J. L. Adam, and Paul Urbach. BSc Optics. TU Delft Open, 2021.
 - Kumbasar, B. Bartan. "The Effects of Symmetry Boundary Condition, Mass Scale and Impactor Size for Edge Impact Simulations on ABAQUS." (2022).
 - Li, C., Ch Wyon, and Richard Moncorge. "Spectroscopic properties and fluorescence dynamics of Er/sup 3+/and Yb/sup 3+/in Y/sub 2/SiO/sub 5." IEEE journal of quantum electronics 28.4 (1992): 1209-1221.
 - Liu, Y., et al. "Orientation effects in nanoindentation of single crystal copper." International Journal of Plasticity 24.11 (2008): 1990-2015.
 - Luo, Yixiu, et al. "Theoretical predictions on elastic stiffness and intrinsic thermal conductivities of yttrium silicates." Journal of the American Ceramic Society 97.3 (2014): 945-951.
 - Mandel, Jean. "Généralisation de la théorie de plasticité de WT Koiter." International Journal of Solids and structures 1.3 (1965): 273-295.

-
- Mason, W. P. "Properties of monoclinic crystals." *Physical Review* 70.9-10 (1946): 705.
 - Matlab, Starting. "Matlab." The MathWorks, Natick, MA (2012).
 - Mirzai, Amin, et al. "First-principle investigation of doping effects on mechanical and thermodynamic properties of Y₂SiO₅." *Mechanics of Materials* 154 (2021): 103739.
 - Narasimhamurty, Tamma Satya. *Photoelastic and electro-optic properties of crystals*. Springer Science & Business Media, 2012.
 - Nye, John Frederick. *Physical properties of crystals: their representation by tensors and matrices*. Oxford university press, 1985.
 - Okereke, Michael, et al. "Boundary conditions." *Finite Element Applications: A Practical Guide to the FEM Process* (2018): 243-297.
 - Oñate, Eugenio, and Gabriel Bugeda. "A study of mesh optimality criteria in adaptive finite element analysis." *Engineering computations* 10.4 (1993): 307-321.
 - Pak, Dongmin, et al. "Long-range cooperative resonances in rare-earth ion arrays inside photonic resonators." *Communications Physics* 5.1 (2022): 89.
 - Pavel, N., T. Dascalu, and V. Lupei. "Variable reflectivity mirror unstable resonator with deformable mirror thermal compensation." *Optics communications* 123.1-3 (1996): 115-120.
 - Prakash, Punith, and Sudarshan Girigimmalayanapalya Shivanna. "FE Simulations of Mounting of an Anisotropic Work Piece Material to Reduce the Effects of Vibration." (2021).
 - Prior, A. M. "Applications of implicit and explicit finite element techniques to metal forming." *Journal of Materials Processing Technology* 45.1-4 (1994): 649-656.
 - Reda, H., et al. "The role of anisotropy on the static and wave propagation characteristics of two-dimensional architected materials under finite strains." *Materials & Design* 147 (2018): 134-145.
 - Saha, Sujata, Paramita Saha Chowdhury, and Amitava Patra. "Luminescence of Ce³⁺ in Y₂SiO₅ nanocrystals: Role of crystal structure and crystal size." *The Journal of Physical Chemistry B* 109.7 (2005): 2699-2702.

-
- Scientific Materials "Y₂SiO₅ yttrium-orthosilicate" accessed in 31/05/2023
Link: https://www.scientificmaterials.com/products/ys_o_Y2SiO5_yttrium-orthosilicate.php
 - Shih, Randy. Introduction to finite element analysis using solidworks simulation 2014. SDC publications, 2014.
 - Steffen, Rebekka. "The influence of glacial isostatic adjustment on intraplate seismicity in northeastern Canada." (2013).
 - Sun, J. S., K. H. Lee, and H. P. Lee. "Comparison of implicit and explicit finite element methods for dynamic problems." Journal of materials processing technology 105.1-2 (2000): 110-118.
 - Sun, Ziqi, et al. "Mechanical properties and damage tolerance of Y₂SiO₅." Journal of the European Ceramic Society 28.15 (2008): 2895-2901.
 - Sun, Ziqi, Meishuan Li, and Yanchun Zhou. "Thermal properties of single-phase Y₂SiO₅." Journal of the European Ceramic Society 29.4 (2009): 551-557.
 - Systèmes, Dassault. "ABAQUS, Analysis User's Manual, Version 6.10-1." Dassault Systèmes, Simulia Corp., Providence, RI,(2010): accessed January 24 2023 .
 - Systèmes, Dassault. "ABAQUS, Analysis User's Manual, Version 6.6." Dassault Systèmes, Simulia Corp., Providence, RI,(2009): accessed February 2023 . Link: classes.engineering.wustl.edu/2009/spring/mase5513/abaqus/docs/v6.6/books/usb/default.htm?startat=pt05ch17s02abm02.html
 - Tănăsioiu, Bogdan, Aurelia Tănăsioiu, and Ion Copaci. "Study on the elastic elements that equip the bogies of freight railway cars." Proceedings of the 3rd WSEAS international conference on Finite differences-finite elements-finite volumes-boundary elements. 2010.
 - Thorpe, Michael J., et al. "Frequency stabilization to 6×10^{-16} via spectral-hole burning." Nature Photonics 5.11 (2011): 688-693.
 - Zamani, Vahid. (2017). Re: NLgeom off/on in Abaqus?. Retrieved from: https://www.researchgate.net/post/NLgeom_off_on_in_Abaqus/59ea39c196b7e4167f2e2789/citation/download.
-

Appendix A – List of Nomenclature Abbreviations and Acronyms

FEM - Finite Elements Modeling

FE - Finite Element

Y₂SiO₅ - Yttrium Orthosilicate

CAE - Computer Aided Engineering

FEA - Finite Elements Analysis

Ce - Cesium

Eu - Europium

Lu - Lutetium

Lab - Laboratory

CAD - Computer Aided Drawing / Computer Aided Design

CAE - Computer Aided Engineering

3D - Three Dimensional

BC - Boundary Condition

LC - Load Case

RP - Reference Point

Er - Erbium.

Appendix B - Matlab Code

The Matlab Code for taking the data from the output database from Abaqus and calculate the photoelastic parameter in Matlab.

```
digits(32)
%
% SizeX = input( "enter the size in X (2.5 or 5): ");
% SizeY = input( "enter the size in Y (2 or 4): ");
% SizeZ = input( "enter the size in Z (1): ");
%
% MeshSize = input( "enter the mesh size: "); %0.1;
SizeX =2.5;
SizeY =2;
SizeZ =1;
MeshSize=0.05
%X
if SizeX/MeshSize-fix(SizeX/MeshSize)>0
NmeshX = fix(SizeX/MeshSize)+1;
else
NmeshX = SizeX/MeshSize;
end
%Y
if SizeY/MeshSize-fix(SizeY/MeshSize)>0
NmeshY = fix(SizeY/MeshSize)+1;
else
NmeshY = SizeY/MeshSize;
end
%Z
```

```

if SizeZ/MeshSize-fix(SizeZ/MeshSize)>0
NmeshZ = fix(SizeZ/MeshSize)+1;
else
NmeshZ = SizeZ/MeshSize;
end
NelementsPlane = NmeshY*NmeshX
Nelements = NmeshY*NmeshX*NmeshZ
Planes = NmeshZ
%Z = input( "enter the number of the plane you want:
");
Z=10
temp= zeros(NmeshX);
%adaptation of the data
rowData2 = [table2array(PureMesh0)]; % MatOriA
%rowData2 (1:3,2:4) %to test if the correct table was
selected
number_of_nodes_per_element = 8;
Nnodes= number_of_nodes_per_element * Nelements;
indice_count = 0;
for i = 1:8:Nnodes
indice_count = indice_count+1;
temp_value_s11 = zeros(1,number_of_nodes_per_element);
temp_value_s22 = zeros(1,number_of_nodes_per_element);
temp_value_s33 = zeros(1,number_of_nodes_per_element);
temp_value_s12 = zeros(1,number_of_nodes_per_element);
temp_value_s13 = zeros(1,number_of_nodes_per_element);
temp_value_s23 = zeros(1,number_of_nodes_per_element);
for k = 0:7
temp_value_s11(k+1) = rowData2(i+k,3); %get all the
value of each element

```

```

temp_value_s22(k+1) = rawData2(i+k,4); %get all the
value of each element
temp_value_s33(k+1) = rawData2(i+k,5); %get all the
value of each element
temp_value_s12(k+1) = rawData2(i+k,6); %get all the
value of each element
temp_value_s13(k+1) = rawData2(i+k,7); %get all the
value of each element
temp_value_s23(k+1) = rawData2(i+k,8); %get all the
value of each element
end

matrix_average_element(indice_count,1) = indice_count;
%tell the element on the column
average_for_one_element_s11 = mean2(temp_value_s11);
matrix_average_element(indice_count,2) =
average_for_one_element_s11;
average_for_one_element_s22 = mean2(temp_value_s22);
matrix_average_element(indice_count,3) =
average_for_one_element_s22;
average_for_one_element_s33 = mean2(temp_value_s33);
matrix_average_element(indice_count,4) =
average_for_one_element_s33;
average_for_one_element_s12 = mean2(temp_value_s12);
matrix_average_element(indice_count,5) =
average_for_one_element_s12;
average_for_one_element_s13 = mean2(temp_value_s13);
matrix_average_element(indice_count,6) =
average_for_one_element_s13;
average_for_one_element_s23 = mean2(temp_value_s23);
matrix_average_element(indice_count,7) =
average_for_one_element_s23;
end

rawData = [matrix_average_element];
% Selection of Rows

```

```

s = 0;
new = [];
Rows = [];
while s < ((NmeshX-1)*NmeshY*NmeshZ)+(Z *NmeshY)
for i = 1:NmeshX
%disp(i);
Rows = ((i-1)*NmeshY*NmeshZ)+((Z-1) *NmeshY )+1:((i-1)*NmeshY*NmeshZ)+(Z *NmeshY);
s = ((i-1)*NmeshY*NmeshZ)+(Z *NmeshY);
% SelectedElements = [SelectedElements Rows]
if i==1
new=Rows;
else
% in case you want to convert the new to a 2D array,
one has to
% replace dim=2, with dim=1!!!!
new= cat(2,new,Rows);
end
%concatenate all elements
% SelectedElements= [Rows]
end
end
% Position o each element
PositionX = 2.45;
PositionY = 1.95;
PositionZ = 0.95;
%PositionMatrix = [];
Position = [];
PositionMatrix = [];
for x = 1:NmeshX
for z = 1:NmeshZ

```

```

for Y = 1:NmeshY
PositionY = (MeshSize/2) + NmeshY*MeshSize -
(Y*MeshSize);
PositionZ = (MeshSize/2)+ NmeshZ*MeshSize -
(z*MeshSize);
PositionX = (MeshSize/2)+NmeshX*MeshSize -
(x*MeshSize);
Position = [PositionX PositionY PositionZ];
PositionMatrix = cat(1,PositionMatrix,Position);
end
end
end
A = [];
FinalData = [];
AdjustedStresses = 10^6*rawData; %Convert the values to
Pa
for i = 1:Nelements
for j = 1:NelementsPlane
if i == new (1,j)
%n = n+1
A =
cat(2,AdjustedStresses(i,2:7),PositionMatrix(i,1:3));
FinalData= cat(1,FinalData,A);
%rawData(i,3:8) PositionMatrix(i,3)
end
end
end
%-----
%
%
% % Calculating Von Mises Stress
% VonMises = [];

```

```

% W = [];
% for i = 1:NelementsPlane
% % A = ((1/sqrt(2))*sqrt((((FinalData(i,1)-
FinalData(i,2))^2)+((FinalData(i,2)-
FinalData(i,3))^2)+((FinalData(i,3)-
FinalData(i,1))^2)+(6*(FinalData(i,4)^2+FinalData(i,5)^
2+FinalData(i,6)^2))))
%
% B = ((FinalData(i,1)-FinalData(i,2))^2);
%
% C = ((FinalData(i,2)-FinalData(i,3))^2);
%
% D = ((FinalData(i,3)-FinalData(i,1))^2);
%
% E =
(6*((FinalData(i,4)^2)+(FinalData(i,5)^2)+(FinalData(i,
6)^2)));
%
% A = ((1/sqrt(2))*sqrt((B+C+D+E)));
%
% VonMises = cat(1,VonMises,A);
%
% end
%
% PositionElementsPlane = [];
% for i = 1:NelementsPlane
%
% W = FinalData(i,7:9);
%
% PositionElementsPlane =
cat(1,PositionElementsPlane,W);
%

```

```

% end
% VonMises2 = cat(2,VonMises,PositionElementsPlane);
%Ploting Von Mises Stress
% X_axis = VonMises2(:,2);
% Y_axis = VonMises2(:,3);
% Z_axis = VonMises2(:,4);
% VM_axis = VonMises2(:,1);
% Surf =
scatter3(X_axis,Y_axis,Z_axis,100,VM_axis,'filled')
% ax = gca; %indicates the use of current axis
%
% view(90,90) %indicates the angle of vizualization
% camroll(90) %rotates in Z axis 90 degrees
%
%
% xlabel('X AXIS');
% ylabel('Y AXIS');
% zlabel('Z AXIS');
% cb = colorbar; % create and label the colorbar
% colormap('jet'); %colors from blue to red
% cb.Label.String = 'Von Mises Stress';
% cb.Limits= [0.06546,0.1071];
%-----
%PhotoElastic Constant
%Doped
%ConstantPE = [ -6.34e-13 1.921e-12 1.39e-12 0 -1.231e-
12 0; 1.95e-13 1.581e-12 8.15e-13 0 -1.31e-13 0; 4.78e-
13 1.611e-12 4.4e-13 0 4.889e-13 0; 0 0 0 3.2e-14 0 -
2.68e-13; -4.42e-13 -2.81e-13 2.69e-13 0 -5.72e-13 0; 0
0 0 2.5e-14 0 -1.526e-12]
%Pure

```

```

ConstantPE = 10^(-12)*[ -0.603 0.88 1.184 0 -1.223 0;
0.164 0.551 0.557 0 -0.131 0; 0.337 0.725 0.313 0 0.365
0; 0 0 0 -0.353 0 -0.037; -0.504 -0.073 0.459 0 -0.594
0; 0 0 0 0.117 0 -1.476];

PhotoElast = [];

aaa = FinalData(:,1:6);
for i = 1:NelementsPlane
R = FinalData(i,1:6)*ConstantPE; %inverti a ordem da
multiplicacao
PhotoElast = cat(1,PhotoElast,R);
end

PositionElementsPlane = [];
for i = 1:NelementsPlane
W = FinalData(i,7:9);
PositionElementsPlane = cat(1,PositionElementsPlane,W);
end

PhotoElast2 = [];
PhotoElast2 = cat(2,PhotoElast,PositionElementsPlane);
% calculate average and other stuff in photo elastic
data
%
% Z1=0;
% Z2=0;
% Z3=0;
% Z4=0;
% Z5=0;
% Z6=0;
% Sum_PE1 = [];
% Sum_PE2 = [];
% Sum_PE3 = [];
% Sum_PE4 = [];
% Sum_PE5 = [];

```

```

% Sum_PE6 = [];
%
% for i = 1:NelementsPlane
% Sum_PE1 = PhotoElast2(i,1);
% Sum_PE2 = PhotoElast2(i,2);
% Sum_PE3 = PhotoElast2(i,3);
% Sum_PE4 = PhotoElast2(i,4);
% Sum_PE5 = PhotoElast2(i,5);
% Sum_PE6 = PhotoElast2(i,6);
%
%
% Z1 = Z1 + Sum_PE1;
% Z2 = Z2 + Sum_PE2;
% Z3 = Z3 + Sum_PE3;
% Z4 = Z4 + Sum_PE4;
% Z5 = Z5 + Sum_PE5;
% Z6 = Z6 + Sum_PE6;
%
% end
%
%
% Average_PE1= Z1/NelementsPlane
% Average_PE2= Z2/NelementsPlane
% Average_PE3= Z3/NelementsPlane
% Average_PE4= Z4/NelementsPlane
% Average_PE5= Z5/NelementsPlane
% Average_PE6= Z6/NelementsPlane
% Average_PeAll=
(Average_PE1+Average_PE2+Average_PE3+Average_PE4+Averag
e_PE5+Average_PE6)/6

```

`%Pure;Doped`

`Order=[1500 1000 750 500 450 400 350 300 250 200 150
100]`

`N1X_LoadX_MatA=[N1X_LoadX_MatOriA_Pure1500KPa,
N1X_LoadX_MatOriA_Pure1000KPa,
N1X_LoadX_MatOriA_Pure750KPa,
N1X_LoadX_MatOriA_Pure500KPa,
N1X_LoadX_MatOriA_Pure450KPa,
N1X_LoadX_MatOriA_Pure400KPa,
N1X_LoadX_MatOriA_Pure350KPa,
N1X_LoadX_MatOriA_Pure300KPa,
N1X_LoadX_MatOriA_Pure250KPa,
N1X_LoadX_MatOriA_Pure200KPa,
N1X_LoadX_MatOriA_Pure150KPa,
N1X_LoadX_MatOriA_Pure100KPa;
N1X_LoadX_MatOriA_Doped1500KPa,
N1X_LoadX_MatOriA_Doped1000KPa,
N1X_LoadX_MatOriA_Doped750KPa,
N1X_LoadX_MatOriA_Doped500KPa,
N1X_LoadX_MatOriA_Doped450KPa,
N1X_LoadX_MatOriA_Doped400KPa,
N1X_LoadX_MatOriA_Doped350KPa,
N1X_LoadX_MatOriA_Doped300KPa,
N1X_LoadX_MatOriA_Doped250KPa,
N1X_LoadX_MatOriA_Doped200KPa,
N1X_LoadX_MatOriA_Doped150KPa,
N1X_LoadX_MatOriA_Doped100KPa];`

`N1X_LoadX_MatC=[N1X_LoadX_MatOriC_Pure1500KPa,
N1X_LoadX_MatOriC_Pure1000KPa,
N1X_LoadX_MatOriC_Pure750KPa,
N1X_LoadX_MatOriC_Pure500KPa,
N1X_LoadX_MatOriC_Pure450KPa,
N1X_LoadX_MatOriC_Pure400KPa,
N1X_LoadX_MatOriC_Pure350KPa,
N1X_LoadX_MatOriC_Pure300KPa,
N1X_LoadX_MatOriC_Pure250KPa,
N1X_LoadX_MatOriC_Pure200KPa,
N1X_LoadX_MatOriC_Pure150KPa,
N1X_LoadX_MatOriC_Pure100KPa;
N1X_LoadX_MatOriC_Doped1500KPa,
N1X_LoadX_MatOriC_Doped1000KPa,
N1X_LoadX_MatOriC_Doped750KPa,`

N1X_LoadX_MatOriC_Doped500KPa,
N1X_LoadX_MatOriC_Doped450KPa,
N1X_LoadX_MatOriC_Doped400KPa,
N1X_LoadX_MatOriC_Doped350KPa,
N1X_LoadX_MatOriC_Doped300KPa,
N1X_LoadX_MatOriC_Doped250KPa,
N1X_LoadX_MatOriC_Doped200KPa,
N1X_LoadX_MatOriC_Doped150KPa,
N1X_LoadX_MatOriC_Doped100KPa];

N1X_LoadX_MatE=[N1X_LoadX_MatOriE_Pure1500KPa,
N1X_LoadX_MatOriE_Pure1000KPa,
N1X_LoadX_MatOriE_Pure750KPa,
N1X_LoadX_MatOriE_Pure500KPa,
N1X_LoadX_MatOriE_Pure450KPa,
N1X_LoadX_MatOriE_Pure400KPa,
N1X_LoadX_MatOriE_Pure350KPa,
N1X_LoadX_MatOriE_Pure300KPa,
N1X_LoadX_MatOriE_Pure250KPa,
N1X_LoadX_MatOriE_Pure200KPa,
N1X_LoadX_MatOriE_Pure150KPa,
N1X_LoadX_MatOriE_Pure100KPa;
N1X_LoadX_MatOriE_Doped1500KPa,
N1X_LoadX_MatOriE_Doped1000KPa,
N1X_LoadX_MatOriE_Doped750KPa,
N1X_LoadX_MatOriE_Doped500KPa,
N1X_LoadX_MatOriE_Doped450KPa,
N1X_LoadX_MatOriE_Doped400KPa,
N1X_LoadX_MatOriE_Doped350KPa,
N1X_LoadX_MatOriE_Doped300KPa,
N1X_LoadX_MatOriE_Doped250KPa,
N1X_LoadX_MatOriE_Doped200KPa,
N1X_LoadX_MatOriE_Doped150KPa,
N1X_LoadX_MatOriE_Doped100KPa];

N1X_LoadXY_MatA=[N1X_LoadXY_MatOriA_Pure1500KPa,
N1X_LoadXY_MatOriA_Pure1000KPa,
N1X_LoadXY_MatOriA_Pure750KPa,
N1X_LoadXY_MatOriA_Pure500KPa,
N1X_LoadXY_MatOriA_Pure450KPa,
N1X_LoadXY_MatOriA_Pure400KPa,
N1X_LoadXY_MatOriA_Pure350KPa,
N1X_LoadXY_MatOriA_Pure300KPa,
N1X_LoadXY_MatOriA_Pure250KPa,
N1X_LoadXY_MatOriA_Pure200KPa,
N1X_LoadXY_MatOriA_Pure150KPa,

```
N1X_LoadXY_MatOriA_Pure100KPa;  
N1X_LoadXY_MatOriA_Doped1500KPa,  
N1X_LoadXY_MatOriA_Doped1000KPa,  
N1X_LoadXY_MatOriA_Doped750KPa,  
N1X_LoadXY_MatOriA_Doped500KPa,  
N1X_LoadXY_MatOriA_Doped451KPa,  
N1X_LoadXY_MatOriA_Doped400KPa,  
N1X_LoadXY_MatOriA_Doped350KPa,  
N1X_LoadXY_MatOriA_Doped300KPa,  
N1X_LoadXY_MatOriA_Doped250KPa,  
N1X_LoadXY_MatOriA_Doped200KPa,  
N1X_LoadXY_MatOriA_Doped150KPa,  
N1X_LoadXY_MatOriA_Doped100KPa];  
  
N1X_LoadXY_MatC=[ N1X_LoadXY_MatOriC_Pure1500KPa,  
N1X_LoadXY_MatOriC_Pure1001KPa,  
N1X_LoadXY_MatOriC_Pure750KPa,  
N1X_LoadXY_MatOriC_Pure500KPa,  
N1X_LoadXY_MatOriC_Pure450KPa,  
N1X_LoadXY_MatOriC_Pure400KPa,  
N1X_LoadXY_MatOriC_Pure350KPa,  
N1X_LoadXY_MatOriC_Pure300KPa,  
N1X_LoadXY_MatOriC_Pure250KPa,  
N1X_LoadXY_MatOriC_Pure200KPa,  
N1X_LoadXY_MatOriC_Pure150KPa,  
N1X_LoadXY_MatOriC_Pure100KPa;  
N1X_LoadXY_MatOriC_Doped1500KPa,  
N1X_LoadXY_MatOriC_Doped1000KPa,  
N1X_LoadXY_MatOriC_Doped750KPa,  
N1X_LoadXY_MatOriC_Doped500KPa,  
N1X_LoadXY_MatOriC_Doped450KPa,  
N1X_LoadXY_MatOriC_Doped400KPa,  
N1X_LoadXY_MatOriC_Doped350KPa,  
N1X_LoadXY_MatOriC_Doped300KPa,  
N1X_LoadXY_MatOriC_Doped250KPa,  
N1X_LoadXY_MatOriC_Doped200KPa,  
N1X_LoadXY_MatOriC_Doped150KPa,  
N1X_LoadXY_MatOriC_Doped100KPa];  
  
N1X_LoadXY_MatE=[ N1X_LoadXY_MatOriE_Pure1500KPa,  
N1X_LoadXY_MatOriE_Pure1000KPa,  
N1X_LoadXY_MatOriE_Pure750KPa,  
N1X_LoadXY_MatOriE_Pure500KPa,  
N1X_LoadXY_MatOriE_Pure450KPa,  
N1X_LoadXY_MatOriE_Pure400KPa,  
N1X_LoadXY_MatOriE_Pure350KPa,
```

```
N1X_LoadXY_MatOriE_Pure300KPa,  
N1X_LoadXY_MatOriE_Pure250KPa,  
N1X_LoadXY_MatOriE_Pure200KPa,  
N1X_LoadXY_MatOriE_Pure150KPa,  
N1X_LoadXY_MatOriE_Pure100KPa;  
N1X_LoadXY_MatOriE_Doped1500KPa,  
N1X_LoadXY_MatOriE_Doped1000KPa,  
N1X_LoadXY_MatOriE_Doped750KPa,  
N1X_LoadXY_MatOriE_Doped500KPa,  
N1X_LoadXY_MatOriE_Doped450KPa,  
N1X_LoadXY_MatOriE_Doped400KPa,  
N1X_LoadXY_MatOriE_Doped350KPa,  
N1X_LoadXY_MatOriE_Doped300KPa,  
N1X_LoadXY_MatOriE_Doped250KPa,  
N1X_LoadXY_MatOriE_Doped200KPa,  
N1X_LoadXY_MatOriE_Doped150KPa,  
N1X_LoadXY_MatOriE_Doped100KPa];  
  
N1X_LoadY_MatA=[ N1X_LoadY_MatOriA_Pure1500KPa,  
N1X_LoadY_MatOriA_Pure1000KPa,  
N1X_LoadY_MatOriA_Pure750KPa,  
N1X_LoadY_MatOriA_Pure500KPa,  
N1X_LoadY_MatOriA_Pure450KPa,  
N1X_LoadY_MatOriA_Pure400KPa,  
N1X_LoadY_MatOriA_Pure350KPa,  
N1X_LoadY_MatOriA_Pure300KPa,  
N1X_LoadY_MatOriA_Pure250KPa,  
N1X_LoadY_MatOriA_Pure200KPa,  
N1X_LoadY_MatOriA_Pure150KPa,  
N1X_LoadY_MatOriA_Pure100KPa;  
N1X_LoadY_MatOriA_Doped1500KPa,  
N1X_LoadY_MatOriA_Doped1000KPa,  
N1X_LoadY_MatOriA_Doped750KPa,  
N1X_LoadY_MatOriA_Doped500KPa,  
N1X_LoadY_MatOriA_Doped450KPa,  
N1X_LoadY_MatOriA_Doped400KPa,  
N1X_LoadY_MatOriA_Doped350KPa,  
N1X_LoadY_MatOriA_Doped300KPa,  
N1X_LoadY_MatOriA_Doped250KPa,  
N1X_LoadY_MatOriA_Doped200KPa,  
N1X_LoadY_MatOriA_Doped150KPa,  
N1X_LoadY_MatOriA_Doped100KPa];  
  
N1X_LoadY_MatC=[ N1X_LoadY_MatOriC_Pure1500KPa,  
N1X_LoadY_MatOriC_Pure1000KPa,  
N1X_LoadY_MatOriC_Pure750KPa,
```

```
N1X_LoadY_MatOriC_Pure500KPa,  
N1X_LoadY_MatOriC_Pure450KPa,  
N1X_LoadY_MatOriC_Pure400KPa,  
N1X_LoadY_MatOriC_Pure350KPa,  
N1X_LoadY_MatOriC_Pure300KPa,  
N1X_LoadY_MatOriC_Pure250KPa,  
N1X_LoadY_MatOriC_Pure200KPa,  
N1X_LoadY_MatOriC_Pure150KPa,  
N1X_LoadY_MatOriC_Pure100KPa;  
N1X_LoadY_MatOriC_Doped1500KPa,  
N1X_LoadY_MatOriC_Doped1000KPa,  
N1X_LoadY_MatOriC_Doped750KPa,  
N1X_LoadY_MatOriC_Doped500KPa,  
N1X_LoadY_MatOriC_Doped450KPa,  
N1X_LoadY_MatOriC_Doped400KPa,  
N1X_LoadY_MatOriC_Doped350KPa,  
N1X_LoadY_MatOriC_Doped300KPa,  
N1X_LoadY_MatOriC_Doped250KPa,  
N1X_LoadY_MatOriC_Doped200KPa,  
N1X_LoadY_MatOriC_Doped150KPa,  
N1X_LoadY_MatOriC_Doped100KPa];  
  
N1X_LoadY_MatE=[ N1X_LoadY_MatOriE_Pure1500KPa,  
N1X_LoadY_MatOriE_Pure1000KPa,  
N1X_LoadY_MatOriE_Pure750KPa,  
N1X_LoadY_MatOriE_Pure500KPa,  
N1X_LoadY_MatOriE_Pure450KPa,  
N1X_LoadY_MatOriE_Pure400KPa,  
N1X_LoadY_MatOriE_Pure350KPa,  
N1X_LoadY_MatOriE_Pure300KPa,  
N1X_LoadY_MatOriE_Pure250KPa,  
N1X_LoadY_MatOriE_Pure200KPa,  
N1X_LoadY_MatOriE_Pure150KPa,  
N1X_LoadY_MatOriE_Pure100KPa;  
N1X_LoadY_MatOriE_Doped1500KPa,  
N1X_LoadY_MatOriE_Doped1000KPa,  
N1X_LoadY_MatOriE_Doped750KPa,  
N1X_LoadY_MatOriE_Doped500KPa,  
N1X_LoadY_MatOriE_Doped450KPa,  
N1X_LoadY_MatOriE_Doped400KPa,  
N1X_LoadY_MatOriE_Doped350KPa,  
N1X_LoadY_MatOriE_Doped300KPa,  
N1X_LoadY_MatOriE_Doped250KPa,  
N1X_LoadY_MatOriE_Doped200KPa,  
N1X_LoadY_MatOriE_Doped150KPa,  
N1X_LoadY_MatOriE_Doped100KPa];
```

%-----

```
N1Y_LoadX_MatA=[ N1Y_LoadX_MatOriA_Pure1500KPa,  
N1Y_LoadX_MatOriA_Pure1000KPa,  
N1Y_LoadX_MatOriA_Pure750KPa,  
N1Y_LoadX_MatOriA_Pure500KPa,  
N1Y_LoadX_MatOriA_Pure450KPa,  
N1Y_LoadX_MatOriA_Pure400KPa,  
N1Y_LoadX_MatOriA_Pure350KPa,  
N1Y_LoadX_MatOriA_Pure300KPa,  
N1Y_LoadX_MatOriA_Pure250KPa,  
N1Y_LoadX_MatOriA_Pure200KPa,  
N1Y_LoadX_MatOriA_Pure150KPa,  
N1Y_LoadX_MatOriA_Pure100KPa;  
N1Y_LoadX_MatOriA_Doped1500KPa,  
N1Y_LoadX_MatOriA_Doped1000KPa,  
N1Y_LoadX_MatOriA_Doped750KPa,  
N1Y_LoadX_MatOriA_Doped500KPa,  
N1Y_LoadX_MatOriA_Doped450KPa,  
N1Y_LoadX_MatOriA_Doped400KPa,  
N1Y_LoadX_MatOriA_Doped350KPa,  
N1Y_LoadX_MatOriA_Doped300KPa,  
N1Y_LoadX_MatOriA_Doped250KPa,  
N1Y_LoadX_MatOriA_Doped200KPa,  
N1Y_LoadX_MatOriA_Doped150KPa,  
N1Y_LoadX_MatOriA_Doped100KPa];
```

```
N1Y_LoadX_MatC=[ N1Y_LoadX_MatOriC_Pure1500KPa,  
N1Y_LoadX_MatOriC_Pure1000KPa,  
N1Y_LoadX_MatOriC_Pure750KPa,  
N1Y_LoadX_MatOriC_Pure500KPa,  
N1Y_LoadX_MatOriC_Pure450KPa,  
N1Y_LoadX_MatOriC_Pure400KPa,  
N1Y_LoadX_MatOriC_Pure350KPa,  
N1Y_LoadX_MatOriC_Pure300KPa,  
N1Y_LoadX_MatOriC_Pure250KPa,  
N1Y_LoadX_MatOriC_Pure200KPa,  
N1Y_LoadX_MatOriC_Pure150KPa,  
N1Y_LoadX_MatOriC_Pure100KPa;  
N1Y_LoadX_MatOriC_Doped1500KPa,  
N1Y_LoadX_MatOriC_Doped1000KPa,  
N1Y_LoadX_MatOriC_Doped750KPa,  
N1Y_LoadX_MatOriC_Doped500KPa,  
N1Y_LoadX_MatOriC_Doped450KPa,  
N1Y_LoadX_MatOriC_Doped400KPa,  
N1Y_LoadX_MatOriC_Doped350KPa,
```

```
N1Y_LoadX_MatOriC_Doped300KPa,  
N1Y_LoadX_MatOriC_Doped250KPa,  
N1Y_LoadX_MatOriC_Doped200KPa,  
N1Y_LoadX_MatOriC_Doped150KPa,  
N1Y_LoadX_MatOriC_Doped100KPa];  
  
N1Y_LoadX_MatE=[ N1Y_LoadX_MatOriE_Pure1500KPa,  
N1Y_LoadX_MatOriE_Pure1000KPa,  
N1Y_LoadX_MatOriE_Pure750KPa,  
N1Y_LoadX_MatOriE_Pure500KPa,  
N1Y_LoadX_MatOriE_Pure450KPa,  
N1Y_LoadX_MatOriE_Pure400KPa,  
N1Y_LoadX_MatOriE_Pure350KPa,  
N1Y_LoadX_MatOriE_Pure300KPa,  
N1Y_LoadX_MatOriE_Pure250KPa,  
N1Y_LoadX_MatOriE_Pure200KPa,  
N1Y_LoadX_MatOriE_Pure150KPa,  
N1Y_LoadX_MatOriE_Pure100KPa;  
N1Y_LoadX_MatOriE_Doped1500KPa,  
N1Y_LoadX_MatOriE_Doped1000KPa,  
N1Y_LoadX_MatOriE_Doped750KPa,  
N1Y_LoadX_MatOriE_Doped500KPa,  
N1Y_LoadX_MatOriE_Doped450KPa,  
N1Y_LoadX_MatOriE_Doped400KPa,  
N1Y_LoadX_MatOriE_Doped350KPa,  
N1Y_LoadX_MatOriE_Doped300KPa,  
N1Y_LoadX_MatOriE_Doped250KPa,  
N1Y_LoadX_MatOriE_Doped200KPa,  
N1Y_LoadX_MatOriE_Doped150KPa,  
N1Y_LoadX_MatOriE_Doped100KPa];  
  
N1Y_LoadXY_MatA=[ N1Y_LoadXY_MatOriA_Pure1500KPa,  
N1Y_LoadXY_MatOriA_Pure1000KPa,  
N1Y_LoadXY_MatOriA_Pure750KPa,  
N1Y_LoadXY_MatOriA_Pure500KPa,  
N1Y_LoadXY_MatOriA_Pure450KPa,  
N1Y_LoadXY_MatOriA_Pure400KPa,  
N1Y_LoadXY_MatOriA_Pure350KPa,  
N1Y_LoadXY_MatOriA_Pure300KPa,  
N1Y_LoadXY_MatOriA_Pure250KPa,  
N1Y_LoadXY_MatOriA_Pure200KPa,  
N1Y_LoadXY_MatOriA_Pure150KPa,  
N1Y_LoadXY_MatOriA_Pure100KPa;  
N1Y_LoadXY_MatOriA_Doped1500KPa,  
N1Y_LoadXY_MatOriA_Doped1000KPa,  
N1Y_LoadXY_MatOriA_Doped750KPa,
```

N1Y_LoadXY_MatOriA_Doped500KPa,
N1Y_LoadXY_MatOriA_Doped451KPa,
N1Y_LoadXY_MatOriA_Doped400KPa,
N1Y_LoadXY_MatOriA_Doped350KPa,
N1Y_LoadXY_MatOriA_Doped300KPa,
N1Y_LoadXY_MatOriA_Doped250KPa,
N1Y_LoadXY_MatOriA_Doped200KPa,
N1Y_LoadXY_MatOriA_Doped150KPa,
N1Y_LoadXY_MatOriA_Doped100KPa];

N1Y_LoadXY_MatC=[N1Y_LoadXY_MatOriC_Pure1500KPa,
N1Y_LoadXY_MatOriC_Pure1001KPa,
N1Y_LoadXY_MatOriC_Pure750KPa,
N1Y_LoadXY_MatOriC_Pure500KPa,
N1Y_LoadXY_MatOriC_Pure450KPa,
N1Y_LoadXY_MatOriC_Pure400KPa,
N1Y_LoadXY_MatOriC_Pure350KPa,
N1Y_LoadXY_MatOriC_Pure300KPa,
N1Y_LoadXY_MatOriC_Pure250KPa,
N1Y_LoadXY_MatOriC_Pure200KPa,
N1Y_LoadXY_MatOriC_Pure150KPa,
N1Y_LoadXY_MatOriC_Pure100KPa;
N1Y_LoadXY_MatOriC_Doped1500KPa,
N1Y_LoadXY_MatOriC_Doped1000KPa,
N1Y_LoadXY_MatOriC_Doped750KPa,
N1Y_LoadXY_MatOriC_Doped500KPa,
N1Y_LoadXY_MatOriC_Doped450KPa,
N1Y_LoadXY_MatOriC_Doped400KPa,
N1Y_LoadXY_MatOriC_Doped350KPa,
N1Y_LoadXY_MatOriC_Doped300KPa,
N1Y_LoadXY_MatOriC_Doped250KPa,
N1Y_LoadXY_MatOriC_Doped200KPa,
N1Y_LoadXY_MatOriC_Doped150KPa,
N1Y_LoadXY_MatOriC_Doped100KPa];

N1Y_LoadXY_MatE=[N1Y_LoadXY_MatOriE_Pure1500KPa,
N1Y_LoadXY_MatOriE_Pure1000KPa,
N1Y_LoadXY_MatOriE_Pure750KPa,
N1Y_LoadXY_MatOriE_Pure500KPa,
N1Y_LoadXY_MatOriE_Pure450KPa,
N1Y_LoadXY_MatOriE_Pure400KPa,
N1Y_LoadXY_MatOriE_Pure350KPa,
N1Y_LoadXY_MatOriE_Pure300KPa,
N1Y_LoadXY_MatOriE_Pure250KPa,
N1Y_LoadXY_MatOriE_Pure200KPa,
N1Y_LoadXY_MatOriE_Pure150KPa,

```
N1Y_LoadXY_MatOriE_Pure100KPa;  
N1Y_LoadXY_MatOriE_Doped1500KPa,  
N1Y_LoadXY_MatOriE_Doped1000KPa,  
N1Y_LoadXY_MatOriE_Doped750KPa,  
N1Y_LoadXY_MatOriE_Doped500KPa,  
N1Y_LoadXY_MatOriE_Doped450KPa,  
N1Y_LoadXY_MatOriE_Doped400KPa,  
N1Y_LoadXY_MatOriE_Doped350KPa,  
N1Y_LoadXY_MatOriE_Doped300KPa,  
N1Y_LoadXY_MatOriE_Doped250KPa,  
N1Y_LoadXY_MatOriE_Doped200KPa,  
N1Y_LoadXY_MatOriE_Doped150KPa,  
N1Y_LoadXY_MatOriE_Doped100KPa];  
  
N1Y_LoadY_MatA=[ N1Y_LoadY_MatOriA_Pure1500KPa,  
N1Y_LoadY_MatOriA_Pure1000KPa,  
N1Y_LoadY_MatOriA_Pure750KPa,  
N1Y_LoadY_MatOriA_Pure500KPa,  
N1Y_LoadY_MatOriA_Pure450KPa,  
N1Y_LoadY_MatOriA_Pure400KPa,  
N1Y_LoadY_MatOriA_Pure350KPa,  
N1Y_LoadY_MatOriA_Pure300KPa,  
N1Y_LoadY_MatOriA_Pure250KPa,  
N1Y_LoadY_MatOriA_Pure200KPa,  
N1Y_LoadY_MatOriA_Pure150KPa,  
N1Y_LoadY_MatOriA_Pure100KPa;  
N1Y_LoadY_MatOriA_Doped1500KPa,  
N1Y_LoadY_MatOriA_Doped1000KPa,  
N1Y_LoadY_MatOriA_Doped750KPa,  
N1Y_LoadY_MatOriA_Doped500KPa,  
N1Y_LoadY_MatOriA_Doped450KPa,  
N1Y_LoadY_MatOriA_Doped400KPa,  
N1Y_LoadY_MatOriA_Doped350KPa,  
N1Y_LoadY_MatOriA_Doped300KPa,  
N1Y_LoadY_MatOriA_Doped250KPa,  
N1Y_LoadY_MatOriA_Doped200KPa,  
N1Y_LoadY_MatOriA_Doped150KPa,  
N1Y_LoadY_MatOriA_Doped100KPa];  
  
N1Y_LoadY_MatC=[ N1Y_LoadY_MatOriC_Pure1500KPa,  
N1Y_LoadY_MatOriC_Pure1000KPa,  
N1Y_LoadY_MatOriC_Pure750KPa,  
N1Y_LoadY_MatOriC_Pure500KPa,  
N1Y_LoadY_MatOriC_Pure450KPa,  
N1Y_LoadY_MatOriC_Pure400KPa,  
N1Y_LoadY_MatOriC_Pure350KPa,
```

```

N1Y_LoadY_MatOriC_Pure300KPa,
N1Y_LoadY_MatOriC_Pure250KPa,
N1Y_LoadY_MatOriC_Pure200KPa,
N1Y_LoadY_MatOriC_Pure150KPa,
N1Y_LoadY_MatOriC_Pure100KPa;
N1Y_LoadY_MatOriC_Doped1500KPa,
N1Y_LoadY_MatOriC_Doped1000KPa,
N1Y_LoadY_MatOriC_Doped750KPa,
N1Y_LoadY_MatOriC_Doped500KPa,
N1Y_LoadY_MatOriC_Doped450KPa,
N1Y_LoadY_MatOriC_Doped400KPa,
N1Y_LoadY_MatOriC_Doped350KPa,
N1Y_LoadY_MatOriC_Doped300KPa,
N1Y_LoadY_MatOriC_Doped250KPa,
N1Y_LoadY_MatOriC_Doped200KPa,
N1Y_LoadY_MatOriC_Doped150KPa,
N1Y_LoadY_MatOriC_Doped100KPa];

N1Y_LoadY_MatE=[ N1Y_LoadY_MatOriE_Pure1500KPa,
N1Y_LoadY_MatOriE_Pure1000KPa,
N1Y_LoadY_MatOriE_Pure750KPa,
N1Y_LoadY_MatOriE_Pure500KPa,
N1Y_LoadY_MatOriE_Pure450KPa,
N1Y_LoadY_MatOriE_Pure400KPa,
N1Y_LoadY_MatOriE_Pure350KPa,
N1Y_LoadY_MatOriE_Pure300KPa,
N1Y_LoadY_MatOriE_Pure250KPa,
N1Y_LoadY_MatOriE_Pure200KPa,
N1Y_LoadY_MatOriE_Pure150KPa,
N1Y_LoadY_MatOriE_Pure100KPa;
N1Y_LoadY_MatOriE_Doped1500KPa,
N1Y_LoadY_MatOriE_Doped1000KPa,
N1Y_LoadY_MatOriE_Doped750KPa,
N1Y_LoadY_MatOriE_Doped500KPa,
N1Y_LoadY_MatOriE_Doped450KPa,
N1Y_LoadY_MatOriE_Doped400KPa,
N1Y_LoadY_MatOriE_Doped350KPa,
N1Y_LoadY_MatOriE_Doped300KPa,
N1Y_LoadY_MatOriE_Doped250KPa,
N1Y_LoadY_MatOriE_Doped200KPa,
N1Y_LoadY_MatOriE_Doped150KPa,
N1Y_LoadY_MatOriE_Doped100KPa];

%-----

N1Z_LoadX_MatA=[ N1Z_LoadX_MatOriA_Pure1500KPa,
N1Z_LoadX_MatOriA_Pure1000KPa,

```

N1Z_LoadX_MatOriA_Pure750KPa,
N1Z_LoadX_MatOriA_Pure500KPa,
N1Z_LoadX_MatOriA_Pure450KPa,
N1Z_LoadX_MatOriA_Pure400KPa,
N1Z_LoadX_MatOriA_Pure350KPa,
N1Z_LoadX_MatOriA_Pure300KPa,
N1Z_LoadX_MatOriA_Pure250KPa,
N1Z_LoadX_MatOriA_Pure200KPa,
N1Z_LoadX_MatOriA_Pure150KPa,
N1Z_LoadX_MatOriA_Pure100KPa;
N1Z_LoadX_MatOriA_Doped1500KPa,
N1Z_LoadX_MatOriA_Doped1000KPa,
N1Z_LoadX_MatOriA_Doped750KPa,
N1Z_LoadX_MatOriA_Doped500KPa,
N1Z_LoadX_MatOriA_Doped450KPa,
N1Z_LoadX_MatOriA_Doped400KPa,
N1Z_LoadX_MatOriA_Doped350KPa,
N1Z_LoadX_MatOriA_Doped300KPa,
N1Z_LoadX_MatOriA_Doped250KPa,
N1Z_LoadX_MatOriA_Doped200KPa,
N1Z_LoadX_MatOriA_Doped150KPa,
N1Z_LoadX_MatOriA_Doped100KPa];

N1Z_LoadX_MatC=[N1Z_LoadX_MatOriC_Pure1500KPa,
N1Z_LoadX_MatOriC_Pure1000KPa,
N1Z_LoadX_MatOriC_Pure750KPa,
N1Z_LoadX_MatOriC_Pure500KPa,
N1Z_LoadX_MatOriC_Pure450KPa,
N1Z_LoadX_MatOriC_Pure400KPa,
N1Z_LoadX_MatOriC_Pure350KPa,
N1Z_LoadX_MatOriC_Pure300KPa,
N1Z_LoadX_MatOriC_Pure250KPa,
N1Z_LoadX_MatOriC_Pure200KPa,
N1Z_LoadX_MatOriC_Pure150KPa,
N1Z_LoadX_MatOriC_Pure100KPa;
N1Z_LoadX_MatOriC_Doped1500KPa,
N1Z_LoadX_MatOriC_Doped1000KPa,
N1Z_LoadX_MatOriC_Doped750KPa,
N1Z_LoadX_MatOriC_Doped500KPa,
N1Z_LoadX_MatOriC_Doped450KPa,
N1Z_LoadX_MatOriC_Doped400KPa,
N1Z_LoadX_MatOriC_Doped350KPa,
N1Z_LoadX_MatOriC_Doped300KPa,
N1Z_LoadX_MatOriC_Doped250KPa,
N1Z_LoadX_MatOriC_Doped200KPa,

```
N1Z_LoadX_MatOriC_Doped150KPa,  
N1Z_LoadX_MatOriC_Doped100KPa];  
  
N1Z_LoadX_MatE=[ N1Z_LoadX_MatOriE_Pure1500KPa,  
N1Z_LoadX_MatOriE_Pure1000KPa,  
N1Z_LoadX_MatOriE_Pure750KPa,  
N1Z_LoadX_MatOriE_Pure500KPa,  
N1Z_LoadX_MatOriE_Pure450KPa,  
N1Z_LoadX_MatOriE_Pure400KPa,  
N1Z_LoadX_MatOriE_Pure350KPa,  
N1Z_LoadX_MatOriE_Pure300KPa,  
N1Z_LoadX_MatOriE_Pure250KPa,  
N1Z_LoadX_MatOriE_Pure200KPa,  
N1Z_LoadX_MatOriE_Pure150KPa,  
N1Z_LoadX_MatOriE_Pure100KPa;  
N1Z_LoadX_MatOriE_Doped1500KPa,  
N1Z_LoadX_MatOriE_Doped1000KPa,  
N1Z_LoadX_MatOriE_Doped750KPa,  
N1Z_LoadX_MatOriE_Doped500KPa,  
N1Z_LoadX_MatOriE_Doped450KPa,  
N1Z_LoadX_MatOriE_Doped400KPa,  
N1Z_LoadX_MatOriE_Doped350KPa,  
N1Z_LoadX_MatOriE_Doped300KPa,  
N1Z_LoadX_MatOriE_Doped250KPa,  
N1Z_LoadX_MatOriE_Doped200KPa,  
N1Z_LoadX_MatOriE_Doped150KPa,  
N1Z_LoadX_MatOriE_Doped100KPa];  
  
N1Z_LoadXY_MatA=[ N1Z_LoadXY_MatOriA_Pure1500KPa,  
N1Z_LoadXY_MatOriA_Pure1000KPa,  
N1Z_LoadXY_MatOriA_Pure750KPa,  
N1Z_LoadXY_MatOriA_Pure500KPa,  
N1Z_LoadXY_MatOriA_Pure450KPa,  
N1Z_LoadXY_MatOriA_Pure400KPa,  
N1Z_LoadXY_MatOriA_Pure350KPa,  
N1Z_LoadXY_MatOriA_Pure300KPa,  
N1Z_LoadXY_MatOriA_Pure250KPa,  
N1Z_LoadXY_MatOriA_Pure200KPa,  
N1Z_LoadXY_MatOriA_Pure150KPa,  
N1Z_LoadXY_MatOriA_Pure100KPa ;  
N1Z_LoadXY_MatOriA_Doped1500KPa,  
N1Z_LoadXY_MatOriA_Doped1000KPa,  
N1Z_LoadXY_MatOriA_Doped750KPa,  
N1Z_LoadXY_MatOriA_Doped500KPa,  
N1Z_LoadXY_MatOriA_Doped451KPa,  
N1Z_LoadXY_MatOriA_Doped400KPa,
```

N1Z_LoadXY_MatOriA_Doped350KPa,
N1Z_LoadXY_MatOriA_Doped300KPa,
N1Z_LoadXY_MatOriA_Doped250KPa,
N1Z_LoadXY_MatOriA_Doped200KPa,
N1Z_LoadXY_MatOriA_Doped150KPa,
N1Z_LoadXY_MatOriA_Doped100KPa];

N1Z_LoadXY_MatC=[N1Z_LoadXY_MatOriC_Pure1500KPa,
N1Z_LoadXY_MatOriC_Pure1001KPa,
N1Z_LoadXY_MatOriC_Pure750KPa,
N1Z_LoadXY_MatOriC_Pure500KPa,
N1Z_LoadXY_MatOriC_Pure450KPa,
N1Z_LoadXY_MatOriC_Pure400KPa,
N1Z_LoadXY_MatOriC_Pure350KPa,
N1Z_LoadXY_MatOriC_Pure300KPa,
N1Z_LoadXY_MatOriC_Pure250KPa,
N1Z_LoadXY_MatOriC_Pure200KPa,
N1Z_LoadXY_MatOriC_Pure150KPa,
N1Z_LoadXY_MatOriC_Pure100KPa ;
N1Z_LoadXY_MatOriC_Doped1500KPa,
N1Z_LoadXY_MatOriC_Doped1000KPa,
N1Z_LoadXY_MatOriC_Doped750KPa,
N1Z_LoadXY_MatOriC_Doped500KPa,
N1Z_LoadXY_MatOriC_Doped450KPa,
N1Z_LoadXY_MatOriC_Doped400KPa,
N1Z_LoadXY_MatOriC_Doped350KPa,
N1Z_LoadXY_MatOriC_Doped300KPa,
N1Z_LoadXY_MatOriC_Doped250KPa,
N1Z_LoadXY_MatOriC_Doped200KPa,
N1Z_LoadXY_MatOriC_Doped150KPa,
N1Z_LoadXY_MatOriC_Doped100KPa];

N1Z_LoadXY_MatE=[N1Z_LoadXY_MatOriE_Pure1500KPa,
N1Z_LoadXY_MatOriE_Pure1000KPa,
N1Z_LoadXY_MatOriE_Pure750KPa,
N1Z_LoadXY_MatOriE_Pure500KPa,
N1Z_LoadXY_MatOriE_Pure450KPa,
N1Z_LoadXY_MatOriE_Pure400KPa,
N1Z_LoadXY_MatOriE_Pure350KPa,
N1Z_LoadXY_MatOriE_Pure300KPa,
N1Z_LoadXY_MatOriE_Pure250KPa,
N1Z_LoadXY_MatOriE_Pure200KPa,
N1Z_LoadXY_MatOriE_Pure150KPa,
N1Z_LoadXY_MatOriE_Pure100KPa ;
N1Z_LoadXY_MatOriE_Doped1500KPa,
N1Z_LoadXY_MatOriE_Doped1000KPa,

```
N1Z_LoadXY_MatOriE_Doped750KPa,  
N1Z_LoadXY_MatOriE_Doped500KPa,  
N1Z_LoadXY_MatOriE_Doped450KPa,  
N1Z_LoadXY_MatOriE_Doped400KPa,  
N1Z_LoadXY_MatOriE_Doped350KPa,  
N1Z_LoadXY_MatOriE_Doped300KPa,  
N1Z_LoadXY_MatOriE_Doped250KPa,  
N1Z_LoadXY_MatOriE_Doped200KPa,  
N1Z_LoadXY_MatOriE_Doped150KPa,  
N1Z_LoadXY_MatOriE_Doped100KPa ];  
  
N1Z_LoadY_MatA=[ N1Z_LoadY_MatOriA_Pure1500KPa,  
N1Z_LoadY_MatOriA_Pure1000KPa,  
N1Z_LoadY_MatOriA_Pure750KPa,  
N1Z_LoadY_MatOriA_Pure500KPa,  
N1Z_LoadY_MatOriA_Pure450KPa,  
N1Z_LoadY_MatOriA_Pure400KPa,  
N1Z_LoadY_MatOriA_Pure350KPa,  
N1Z_LoadY_MatOriA_Pure300KPa,  
N1Z_LoadY_MatOriA_Pure250KPa,  
N1Z_LoadY_MatOriA_Pure200KPa,  
N1Z_LoadY_MatOriA_Pure150KPa,  
N1Z_LoadY_MatOriA_Pure100KPa;  
N1Z_LoadY_MatOriA_Doped1500KPa,  
N1Z_LoadY_MatOriA_Doped1000KPa,  
N1Z_LoadY_MatOriA_Doped750KPa,  
N1Z_LoadY_MatOriA_Doped500KPa,  
N1Z_LoadY_MatOriA_Doped450KPa,  
N1Z_LoadY_MatOriA_Doped400KPa,  
N1Z_LoadY_MatOriA_Doped350KPa,  
N1Z_LoadY_MatOriA_Doped300KPa,  
N1Z_LoadY_MatOriA_Doped250KPa,  
N1Z_LoadY_MatOriA_Doped200KPa,  
N1Z_LoadY_MatOriA_Doped150KPa,  
N1Z_LoadY_MatOriA_Doped100KPa ];  
  
N1Z_LoadY_MatC=[ N1Z_LoadY_MatOriC_Pure1500KPa,  
N1Z_LoadY_MatOriC_Pure1000KPa,  
N1Z_LoadY_MatOriC_Pure750KPa,  
N1Z_LoadY_MatOriC_Pure500KPa,  
N1Z_LoadY_MatOriC_Pure450KPa,  
N1Z_LoadY_MatOriC_Pure400KPa,  
N1Z_LoadY_MatOriC_Pure350KPa,  
N1Z_LoadY_MatOriC_Pure300KPa,  
N1Z_LoadY_MatOriC_Pure250KPa,  
N1Z_LoadY_MatOriC_Pure200KPa,
```

```
N1Z_LoadY_MatOriC_Pure150KPa,  
N1Z_LoadY_MatOriC_Pure100KPa;  
N1Z_LoadY_MatOriC_Doped1500KPa,  
N1Z_LoadY_MatOriC_Doped1000KPa,  
N1Z_LoadY_MatOriC_Doped750KPa,  
N1Z_LoadY_MatOriC_Doped500KPa,  
N1Z_LoadY_MatOriC_Doped450KPa,  
N1Z_LoadY_MatOriC_Doped400KPa,  
N1Z_LoadY_MatOriC_Doped350KPa,  
N1Z_LoadY_MatOriC_Doped300KPa,  
N1Z_LoadY_MatOriC_Doped250KPa,  
N1Z_LoadY_MatOriC_Doped200KPa,  
N1Z_LoadY_MatOriC_Doped150KPa,  
N1Z_LoadY_MatOriC_Doped100KPa];
```

```
N1Z_LoadY_MatE=[ N1Z_LoadY_MatOriE_Pure1500KPa,  
N1Z_LoadY_MatOriE_Pure1000KPa,  
N1Z_LoadY_MatOriE_Pure750KPa,  
N1Z_LoadY_MatOriE_Pure500KPa,  
N1Z_LoadY_MatOriE_Pure450KPa,  
N1Z_LoadY_MatOriE_Pure400KPa,  
N1Z_LoadY_MatOriE_Pure350KPa,  
N1Z_LoadY_MatOriE_Pure300KPa,  
N1Z_LoadY_MatOriE_Pure250KPa,  
N1Z_LoadY_MatOriE_Pure200KPa,  
N1Z_LoadY_MatOriE_Pure150KPa,  
N1Z_LoadY_MatOriE_Pure100KPa;  
N1Z_LoadY_MatOriE_Doped1500KPa,  
N1Z_LoadY_MatOriE_Doped1000KPa,  
N1Z_LoadY_MatOriE_Doped750KPa,  
N1Z_LoadY_MatOriE_Doped500KPa,  
N1Z_LoadY_MatOriE_Doped450KPa,  
N1Z_LoadY_MatOriE_Doped400KPa,  
N1Z_LoadY_MatOriE_Doped350KPa,  
N1Z_LoadY_MatOriE_Doped300KPa,  
N1Z_LoadY_MatOriE_Doped250KPa,  
N1Z_LoadY_MatOriE_Doped200KPa,  
N1Z_LoadY_MatOriE_Doped150KPa,  
N1Z_LoadY_MatOriE_Doped100KPa];
```

```
%-----
```

```
DeltaB_LoadX_MatA=[ DeltaB_LoadXMatOriA_Pure1500KPa,  
DeltaB_LoadXMatOriA_Pure1000KPa,  
DeltaB_LoadXMatOriA_Pure750KPa,  
DeltaB_LoadXMatOriA_Pure500KPa,  
DeltaB_LoadXMatOriA_Pure450KPa,
```

DeltaB_LoadXMatOriA_Pure400KPa,
DeltaB_LoadXMatOriA_Pure350KPa,
DeltaB_LoadXMatOriA_Pure300KPa,
DeltaB_LoadXMatOriA_Pure250KPa,
DeltaB_LoadXMatOriA_Pure200KPa,
DeltaB_LoadXMatOriA_Pure150KPa,
DeltaB_LoadXMatOriA_Pure100KPa,
DeltaB_LoadXMatOriA_Doped1500KPa,
DeltaB_LoadXMatOriA_Doped1000KPa,
DeltaB_LoadXMatOriA_Doped750KPa,
DeltaB_LoadXMatOriA_Doped500KPa,
DeltaB_LoadXMatOriA_Doped450KPa,
DeltaB_LoadXMatOriA_Doped400KPa,
DeltaB_LoadXMatOriA_Doped350KPa,
DeltaB_LoadXMatOriA_Doped300KPa,
DeltaB_LoadXMatOriA_Doped250KPa,
DeltaB_LoadXMatOriA_Doped200KPa,
DeltaB_LoadXMatOriA_Doped150KPa,
DeltaB_LoadXMatOriA_Doped100KPa];

DeltaB_LoadX_MatC=[DeltaB_LoadXMatOriC_Pure1500KPa,
DeltaB_LoadXMatOriC_Pure1000KPa,
DeltaB_LoadXMatOriC_Pure750KPa,
DeltaB_LoadXMatOriC_Pure500KPa,
DeltaB_LoadXMatOriC_Pure450KPa,
DeltaB_LoadXMatOriC_Pure400KPa,
DeltaB_LoadXMatOriC_Pure350KPa,
DeltaB_LoadXMatOriC_Pure300KPa,
DeltaB_LoadXMatOriC_Pure250KPa,
DeltaB_LoadXMatOriC_Pure200KPa,
DeltaB_LoadXMatOriC_Pure150KPa,
DeltaB_LoadXMatOriC_Pure100KPa,
DeltaB_LoadXMatOriC_Doped1500KPa,
DeltaB_LoadXMatOriC_Doped1000KPa,
DeltaB_LoadXMatOriC_Doped750KPa,
DeltaB_LoadXMatOriC_Doped500KPa,
DeltaB_LoadXMatOriC_Doped450KPa,
DeltaB_LoadXMatOriC_Doped400KPa,
DeltaB_LoadXMatOriC_Doped350KPa,
DeltaB_LoadXMatOriC_Doped300KPa,
DeltaB_LoadXMatOriC_Doped250KPa,
DeltaB_LoadXMatOriC_Doped200KPa,
DeltaB_LoadXMatOriC_Doped150KPa,
DeltaB_LoadXMatOriC_Doped100KPa];

```
DeltaB_LoadX_MatE=[ DeltaB_LoadXMatOriE_Pure1500KPa,  
DeltaB_LoadXMatOriE_Pure1000KPa,  
DeltaB_LoadXMatOriE_Pure750KPa,  
DeltaB_LoadXMatOriE_Pure500KPa,  
DeltaB_LoadXMatOriE_Pure450KPa,  
DeltaB_LoadXMatOriE_Pure400KPa,  
DeltaB_LoadXMatOriE_Pure350KPa,  
DeltaB_LoadXMatOriE_Pure300KPa,  
DeltaB_LoadXMatOriE_Pure250KPa,  
DeltaB_LoadXMatOriE_Pure200KPa,  
DeltaB_LoadXMatOriE_Pure150KPa,  
DeltaB_LoadXMatOriE_Pure100KPa,  
DeltaB_LoadXMatOriE_Doped1500KPa,  
DeltaB_LoadXMatOriE_Doped1000KPa,  
DeltaB_LoadXMatOriE_Doped750KPa,  
DeltaB_LoadXMatOriE_Doped500KPa,  
DeltaB_LoadXMatOriE_Doped450KPa,  
DeltaB_LoadXMatOriE_Doped400KPa,  
DeltaB_LoadXMatOriE_Doped350KPa,  
DeltaB_LoadXMatOriE_Doped300KPa,  
DeltaB_LoadXMatOriE_Doped250KPa,  
DeltaB_LoadXMatOriE_Doped200KPa,  
DeltaB_LoadXMatOriE_Doped150KPa,  
DeltaB_LoadXMatOriE_Doped100KPa];
```

```
DeltaB_LoadXY_MatA=[ DeltaB_LoadXYMatOriA_Pure1500KPa,  
DeltaB_LoadXYMatOriA_Pure1000KPa,  
DeltaB_LoadXYMatOriA_Pure750KPa,  
DeltaB_LoadXYMatOriA_Pure500KPa,  
DeltaB_LoadXYMatOriA_Pure450KPa,  
DeltaB_LoadXYMatOriA_Pure400KPa,  
DeltaB_LoadXYMatOriA_Pure350KPa,  
DeltaB_LoadXYMatOriA_Pure300KPa,  
DeltaB_LoadXYMatOriA_Pure250KPa,  
DeltaB_LoadXYMatOriA_Pure200KPa,  
DeltaB_LoadXYMatOriA_Pure150KPa,  
DeltaB_LoadXYMatOriA_Pure100KPa,  
DeltaB_LoadXYMatOriA_Doped1500KPa,  
DeltaB_LoadXYMatOriA_Doped1000KPa,  
DeltaB_LoadXYMatOriA_Doped750KPa,  
DeltaB_LoadXYMatOriA_Doped500KPa,  
DeltaB_LoadXYMatOriA_Doped451KPa,  
DeltaB_LoadXYMatOriA_Doped400KPa,  
DeltaB_LoadXYMatOriA_Doped350KPa,  
DeltaB_LoadXYMatOriA_Doped300KPa,  
DeltaB_LoadXYMatOriA_Doped250KPa,
```

DeltaB_LoadXYMatOriA_Doped200KPa,
DeltaB_LoadXYMatOriA_Doped150KPa,
DeltaB_LoadXYMatOriA_Doped100KPa];

DeltaB_LoadXY_MatC=[DeltaB_LoadXYMatOriC_Pure1500KPa,
DeltaB_LoadXYMatOriC_Pure1001KPa,
DeltaB_LoadXYMatOriC_Pure750KPa,
DeltaB_LoadXYMatOriC_Pure500KPa,
DeltaB_LoadXYMatOriC_Pure450KPa,
DeltaB_LoadXYMatOriC_Pure400KPa,
DeltaB_LoadXYMatOriC_Pure350KPa,
DeltaB_LoadXYMatOriC_Pure300KPa,
DeltaB_LoadXYMatOriC_Pure250KPa,
DeltaB_LoadXYMatOriC_Pure200KPa,
DeltaB_LoadXYMatOriC_Pure150KPa,
DeltaB_LoadXYMatOriC_Pure100KPa,
DeltaB_LoadXYMatOriC_Doped1500KPa,
DeltaB_LoadXYMatOriC_Doped1000KPa,
DeltaB_LoadXYMatOriC_Doped750KPa,
DeltaB_LoadXYMatOriC_Doped500KPa,
DeltaB_LoadXYMatOriC_Doped450KPa,
DeltaB_LoadXYMatOriC_Doped400KPa,
DeltaB_LoadXYMatOriC_Doped350KPa,
DeltaB_LoadXYMatOriC_Doped300KPa,
DeltaB_LoadXYMatOriC_Doped250KPa,
DeltaB_LoadXYMatOriC_Doped200KPa,
DeltaB_LoadXYMatOriC_Doped150KPa,
DeltaB_LoadXYMatOriC_Doped100KPa];

DeltaB_LoadXY_MatE=[DeltaB_LoadXYMatOriE_Pure1500KPa,
DeltaB_LoadXYMatOriE_Pure1000KPa,
DeltaB_LoadXYMatOriE_Pure750KPa,
DeltaB_LoadXYMatOriE_Pure500KPa,
DeltaB_LoadXYMatOriE_Pure450KPa,
DeltaB_LoadXYMatOriE_Pure400KPa,
DeltaB_LoadXYMatOriE_Pure350KPa,
DeltaB_LoadXYMatOriE_Pure300KPa,
DeltaB_LoadXYMatOriE_Pure250KPa,
DeltaB_LoadXYMatOriE_Pure200KPa,
DeltaB_LoadXYMatOriE_Pure150KPa,
DeltaB_LoadXYMatOriE_Pure100KPa,
DeltaB_LoadXYMatOriE_Doped1500KPa,
DeltaB_LoadXYMatOriE_Doped1000KPa,
DeltaB_LoadXYMatOriE_Doped750KPa,
DeltaB_LoadXYMatOriE_Doped500KPa,
DeltaB_LoadXYMatOriE_Doped450KPa,

DeltaB_LoadXYMatOriE_Doped400KPa,
DeltaB_LoadXYMatOriE_Doped350KPa,
DeltaB_LoadXYMatOriE_Doped300KPa,
DeltaB_LoadXYMatOriE_Doped250KPa,
DeltaB_LoadXYMatOriE_Doped200KPa,
DeltaB_LoadXYMatOriE_Doped150KPa,
DeltaB_LoadXYMatOriE_Doped100KPa];

DeltaB_LoadY_MatA=[DeltaB_LoadYMatOriA_Pure1500KPa,
DeltaB_LoadYMatOriA_Pure1000KPa,
DeltaB_LoadYMatOriA_Pure750KPa,
DeltaB_LoadYMatOriA_Pure500KPa,
DeltaB_LoadYMatOriA_Pure450KPa,
DeltaB_LoadYMatOriA_Pure400KPa,
DeltaB_LoadYMatOriA_Pure350KPa,
DeltaB_LoadYMatOriA_Pure300KPa,
DeltaB_LoadYMatOriA_Pure250KPa,
DeltaB_LoadYMatOriA_Pure200KPa,
DeltaB_LoadYMatOriA_Pure150KPa,
DeltaB_LoadYMatOriA_Pure100KPa,
DeltaB_LoadYMatOriA_Doped1500KPa,
DeltaB_LoadYMatOriA_Doped1000KPa,
DeltaB_LoadYMatOriA_Doped750KPa,
DeltaB_LoadYMatOriA_Doped500KPa,
DeltaB_LoadYMatOriA_Doped450KPa,
DeltaB_LoadYMatOriA_Doped400KPa,
DeltaB_LoadYMatOriA_Doped350KPa,
DeltaB_LoadYMatOriA_Doped300KPa,
DeltaB_LoadYMatOriA_Doped250KPa,
DeltaB_LoadYMatOriA_Doped200KPa,
DeltaB_LoadYMatOriA_Doped150KPa,
DeltaB_LoadYMatOriA_Doped100KPa];

DeltaB_LoadY_MatC=[DeltaB_LoadYMatOriC_Pure1500KPa,
DeltaB_LoadYMatOriC_Pure1000KPa,
DeltaB_LoadYMatOriC_Pure750KPa,
DeltaB_LoadYMatOriC_Pure500KPa,
DeltaB_LoadYMatOriC_Pure450KPa,
DeltaB_LoadYMatOriC_Pure400KPa,
DeltaB_LoadYMatOriC_Pure350KPa,
DeltaB_LoadYMatOriC_Pure300KPa,
DeltaB_LoadYMatOriC_Pure250KPa,
DeltaB_LoadYMatOriC_Pure200KPa,
DeltaB_LoadYMatOriC_Pure150KPa,
DeltaB_LoadYMatOriC_Pure100KPa,
DeltaB_LoadYMatOriC_Doped1500KPa,

```
DeltaB_LoadYMatOriC_Doped1000KPa,  
DeltaB_LoadYMatOriC_Doped750KPa,  
DeltaB_LoadYMatOriC_Doped500KPa,  
DeltaB_LoadYMatOriC_Doped450KPa,  
DeltaB_LoadYMatOriC_Doped400KPa,  
DeltaB_LoadYMatOriC_Doped350KPa,  
DeltaB_LoadYMatOriC_Doped300KPa,  
DeltaB_LoadYMatOriC_Doped250KPa,  
DeltaB_LoadYMatOriC_Doped200KPa,  
DeltaB_LoadYMatOriC_Doped150KPa,  
DeltaB_LoadYMatOriC_Doped100KPa];
```

```
DeltaB_LoadY_MatE=[ DeltaB_LoadYMatOriE_Pure1500KPa,  
DeltaB_LoadYMatOriE_Pure1000KPa,  
DeltaB_LoadYMatOriE_Pure750KPa,  
DeltaB_LoadYMatOriE_Pure500KPa,  
DeltaB_LoadYMatOriE_Pure450KPa,  
DeltaB_LoadYMatOriE_Pure400KPa,  
DeltaB_LoadYMatOriE_Pure350KPa,  
DeltaB_LoadYMatOriE_Pure300KPa,  
DeltaB_LoadYMatOriE_Pure250KPa,  
DeltaB_LoadYMatOriE_Pure200KPa,  
DeltaB_LoadYMatOriE_Pure150KPa,  
DeltaB_LoadYMatOriE_Pure100KPa,  
DeltaB_LoadYMatOriE_Doped1500KPa,  
DeltaB_LoadYMatOriE_Doped1000KPa,  
DeltaB_LoadYMatOriE_Doped750KPa,  
DeltaB_LoadYMatOriE_Doped500KPa,  
DeltaB_LoadYMatOriE_Doped450KPa,  
DeltaB_LoadYMatOriE_Doped400KPa,  
DeltaB_LoadYMatOriE_Doped350KPa,  
DeltaB_LoadYMatOriE_Doped300KPa,  
DeltaB_LoadYMatOriE_Doped250KPa,  
DeltaB_LoadYMatOriE_Doped200KPa,  
DeltaB_LoadYMatOriE_Doped150KPa,  
DeltaB_LoadYMatOriE_Doped100KPa];
```

```
%-----
```

```
save("DATA_PLOTTED.mat", "Order", "N1Z_LoadY_MatE",  
"N1Z_LoadY_MatC", "N1Z_LoadY_MatA", "N1Z_LoadXY_MatE",  
"N1Z_LoadXY_MatC", "N1Z_LoadXY_MatA", "N1Z_LoadX_MatE",  
"N1Z_LoadX_MatC", "N1Z_LoadX_MatA", "N1Y_LoadY_MatE",  
"N1Y_LoadY_MatC", "N1Y_LoadY_MatA", "N1Y_LoadXY_MatE",  
"N1Y_LoadXY_MatC", "N1Y_LoadXY_MatA", "N1Y_LoadX_MatE",  
"N1Y_LoadX_MatC", "N1Y_LoadX_MatA", "N1X_LoadY_MatE",  
"N1X_LoadY_MatC", "N1X_LoadY_MatA", "N1X_LoadXY_MatE",
```

```

"N1X_LoadXY_MatC", "N1X_LoadXY_MatA", "N1X_LoadX_MatE",
"N1X_LoadX_MatC", "N1X_LoadX_MatA",
"DeltaB_LoadY_MatE", "DeltaB_LoadY_MatC",
"DeltaB_LoadY_MatA", "DeltaB_LoadXY_MatE",
"DeltaB_LoadXY_MatC", "DeltaB_LoadXY_MatA",
"DeltaB_LoadX_MatE", "DeltaB_LoadX_MatC",
"DeltaB_LoadX_MatA")

% here is the analysis for the applied pressure on the
n
n0_x_pure = 1.7577;
n0_y_pure = 1.7621;
n0_z_pure = 1.7789;

% the refractive index of doped crystal at 0 kpa
n0_x_doped = 1.7691;
n0_y_doped = 1.7692;
n0_z_doped = 1.7892;
load = flip(Order);
Delta_n_pure = flip(N1X_LoadX_MatC(1,:)) - n0_x_pure;
Delta_n_doped = flip(N1X_LoadX_MatC(2,:)) - n0_x_doped;

% tile plot begins here
t = tiledlayout(2,1);
t.TileSpacing = 'tight';
t.Padding = 'compact';
nexttile
%pure
plot(load, Delta_n_pure, '-o')
title('Pure N1X Load X Material Orientation C')
%set(gca,'xtick',[])
ylabel('\Delta n',FontWeight='bold')
legend('pure')
grid minor
% doped

```

```

nexttile
plot(load, Delta_n_doped, 'r -o')
legend('doped')
xlabel('load (kPa)', FontWeight='bold')
ylabel('\Delta n', FontWeight='bold')
grid minor
title('Doped N1X Load X Material Orientation C')
figure(2)
plot(load, Delta_n_pure, '-o', load, Delta_n_doped, 'r -
o')
legend('pure', 'doped')
xlabel('load (kPa)', FontWeight='bold')
ylabel('\Delta n', FontWeight='bold')
grid minor
title('N1X Load X Material Orientation C')
% frequency analysis part
c = 299792458; % m/s
L = 0.001; %mm
f0 = c/(2*n0_x_pure*L);
n1x_pure = flip(N1X_LoadX_MatC(1,:));
f = c./(2.*n1x_pure.*L);
delta_f = (f-f0)/(10^3); % unit in kHz
figure(3)
plot(load, delta_f, 'b -o')
grid minor
xlabel('Load (kPa)', FontWeight='bold')
ylabel('Frequency Shift (kHz)', FontWeight='bold')
title('N1X Load X Material Orientation C')
%% yy
n0_y_pure = 1.7621;

```

```

% the refractive index of doped crystal at 0 kpa
n0_y_doped = 1.7692;
load = flip(Order);
Delta_n_pure = flip(N1Y_LoadX_MatC(1,:)) - n0_y_pure;
Delta_n_doped = flip(N1Y_LoadX_MatC(2,:)) - n0_y_doped;
% tile plot begins here
t = tiledlayout(2,1);
t.TileSpacing = 'tight';
t.Padding = 'compact';
nexttile
plot(load, Delta_n_pure, '-o')
ylabel('\Delta n', FontWeight='bold')
legend('pure')
grid minor
title('Pure N1Y Load X Material Orientation C')
% doped
nexttile
plot(load, Delta_n_doped, 'r -o')
legend('doped')
xlabel('load (kPa)', FontWeight='bold')
ylabel('\Delta n', FontWeight='bold')
title('Doped N1Y Load X Material Orientation C')
grid minor
figure(2)
plot(load, Delta_n_pure, '-o', load, Delta_n_doped, 'r -
o')
legend('pure', 'doped')
xlabel('load (kPa)', FontWeight='bold')
ylabel('\Delta n', FontWeight='bold')
grid minor

```

```

title('N1Y Load X Material Orientation C')
% frequency analysis part
c = 299792458; % m/s
L = 0.001; %mm
f0 = c/(2*n0_y_pure*L);
n1x_pure = flip(N1Y_LoadX_MatC(1,:));
f = c./(2.*n1x_pure.*L);
delta_f = (f-f0)/(10^3); % unit in kHz
figure(3)
plot(load, delta_f, 'b -o')
grid minor
xlabel('Load (kPa)', FontWeight='bold')
ylabel('Frequency Shift (kHz)', FontWeight='bold')
title('N1Y Load X Material Orientation C')
%% zz
n0_y_pure = 1.7621;
% the refractive index of doped crystal at 0 kpa
n0_y_doped = 1.7692;
load = flip(Order);
Delta_n_pure = flip(N1Z_LoadX_MatC(1,:)) - n0_z_pure;
Delta_n_doped = flip(N1Z_LoadX_MatC(2,:)) - n0_z_doped;
% tile plot begins here
t = tiledlayout(2,1);
t.TileSpacing = 'tight';
t.Padding = 'compact';
nexttile
plot(load, Delta_n_pure, '-o')
ylabel('\Delta n', FontWeight='bold')
legend('pure')
title('Pure N1Z Load X Material Orientation C')

```

```

grid minor
% doped
nexttile
plot(load, Delta_n_doped, 'r -o')
legend('doped')
xlabel('load (kPa)', FontWeight='bold')
ylabel('\Delta n', FontWeight='bold')
title('Doped N1Z Load X Material Orientation C')
grid minor
figure(2)
plot(load, Delta_n_pure, '-o', load, Delta_n_doped, 'r -
o')
legend('pure', 'doped')
xlabel('load (kPa)', FontWeight='bold')
ylabel('\Delta n', FontWeight='bold')
grid minor
title('N1Z Load X Material Orientation C')
% frequency analysis part
c = 299792458; % m/s
L = 0.001; %mm
f0 = c/(2*n0_z_pure*L);
n1x_pure = flip(N1Z_LoadX_MatC(1,:))
f = c./(2.*n1x_pure.*L);
delta_f = (f-f0)/(10^3); % unit in kHz
figure(3)
plot(load, delta_f, 'b -o')
grid minor
xlabel('Load (kPa)', FontWeight='bold')
ylabel('Frequency Shift (kHz)', FontWeight='bold')
title('N1Z Load X Material Orientation C')

```
